

國立臺灣大學電機資訊學院電信工程學研究所

博士論文

Graduate Institute of Communication Engineering  
College of Electrical Engineering & Computer Science  
National Taiwan University  
Doctoral Dissertation

背覆導體共面波導饋入開槽天線之設計

Design of Slot Antennas Fed by Conductor-Backed  
Coplanar Waveguide



I-Ching Lan

指導教授：許博文 博士

Advisor: Dr. Powen Hsu

中華民國 97 年 6 月

June, 2008



# 國立臺灣大學博士學位論文

## 口試委員會審定書

### 背覆導體共面波導饋入開槽天線之設計 Design of Slot Antennas Fed by Conductor-Backed Coplanar Waveguide

本論文係藍逸青君 (F92942005) 在國立臺灣大學電信工程學研究所完成之博士學位論文，於民國九十七年六月十四日承下列考試委員審查通過及口試及格，特此證明

口試委員：

許博文

(簽名)

張道治 (指導教授)

莊晴光

張知難

陳士元

鄭士康

沈世中

系主任、所長

王暉

(簽名)



# 誌謝

本論文的完成，首先得感謝許博文教授長期的指導與栽培。我常覺得自己很幸運，擁有每個研究生夢寐以求的、最高的自由度。五年的研究生生涯，我總能自由挑選並全心全意投入自己熱愛的研究主題而毫無顧慮，這都得感謝老師全力的支持以及完全的信任。研究的道路上，或顯或隱，更常可發現老師細心的安排。

其次我要感謝學長陳士元教授，自我是個專題生起，學長就以師長的態度引領我熟悉天線這個領域、不辭辛勞解答我無數次的請益；擔任教職後，依然保持學長的親切與熱心。感謝口試委員張道治教授、莊晴光教授、張知難教授、鄭士康教授，以及鍾世忠教授，委員們的寶貴意見使本論文更臻完備。感謝胡振國教授在我求學路上多次的推薦。



感謝王儷憲助教在大學部電磁波實驗時的指導與諸多討論，促使我對微波領域產生更高的興趣。感謝季重儀先生傾囊相授的寶貴實驗技巧，以及維護電波組實驗設備的良苦用心。感謝陳一仁、曾昭雄、劉安錫、賴明佑、孫瑞伯、鄧卜華、吳昭篁、趙世峰等學長在諸方面的指導。感謝電波組92級的所有夥伴們，同窗兩年真是愉快又難忘的回憶。尤其是同門派的一哥柏翔、賴博宗民、蔡兄書孔；共同在博班打拼的宗男、士程；還有千哥大千、大蛇士傑，以及我的火雞好友建勳。

感謝許派的眾同學與學弟們：忠侯、昱緯、襄臨、君朋、奇軒、祐傑、如弘、舷剛、兆祥、秉孝、彥儒、人傑、佑霖，很榮幸能與各位齊力在天線研究上努力。

感謝電波組的美女助理群：辣媽淑貞、惠美、宜芳、葦珊，有你們的照顧真幸福。

感謝電信所辦公室的趙姐文瑛、欣梅、惠玲，謝謝你們長期的幫忙。

感謝爸爸、媽媽、哥哥、姐姐、姐夫，你們無盡的愛是我一生最強韌又柔軟的倚靠，我所以為我，皆來自於你們的愛。感謝阿公，讓您載在腳踏車後座兜風上學的回憶仍常縈繞我心頭。感謝佳雲，未來的路我們還要一起走，如同一路走來那般美麗與甜蜜。最後，感謝上天與大地。



逸青 2008.7.21

# 摘要

本論文提出了創新的背覆導體共面波導饋入之開槽天線，其中包括了三種耦合雙開槽天線以及兩種平行板開槽陣列天線。首先介紹的是背覆導體共面波導在開槽偶極天線這個不連續環境下產生的洩漏效應，然後藉由利用此洩漏波並適當設計開槽偶極天線與另一平直開槽天線的耦合，天線整體的輻射表現得以增進。接著提出的是開槽偶極天線與一弧形開槽天線的耦合結構，此一設計的天線尺寸比前一個設計來得小巧。緊接其後的是一個藉由截斷接地面與介質基板達成微小化的設計，其中截斷處的邊際電場扮演了耦合開槽天線在前述兩個設計中的角色，而天線整體表現也相似。

論文下半部轉而處理均勻的背覆導體共面波導傳輸線產生的平行板模態洩漏效應，並提出了兩種利用此洩漏波激發的平行板開槽陣列天線。為了達成線性極化，分別設計了一個縱向陣列天線與一個橫向陣列天線，並詳敘其設計流程。而前者優於後者之處也將在文中彰顯。這種型式的結構擁有在背覆導體共面波導基礎下設計大型陣列天線的潛力。





# Abstract

Novel slot antennas fed by the conductor-backed coplanar waveguide are proposed in this dissertation. These include three kinds of the coupled twin slots and two versions of the parallel-plate slot array. First the leakage effect at the slot dipole discontinuity of the parallel-plate slot array. First the leakage effect at the slot dipole discontinuity of the conductor-backed coplanar waveguide is introduced. Then the slot dipole coupled with a straight slot is properly designed to utilize the leakage wave for enhanced radiation performance. Next, the slot dipole coupled with an arc-slot is presented, which is more compact than the previous design. After that, the miniaturized design with truncated ground planes and dielectric substrate is presented. The fringing fields at the truncation play the role of the coupling slot in the previous two designs. The overall performance is found to be comparable to its predecessors.

The second half of this dissertation deals with the parallel-plate mode leakage from the uniform conductor-backed coplanar waveguide. Two parallel-plate slot arrays that are excited by this leakage wave are presented. To obtain linear polarizations, a longitudinal and a transverse slot array are designed and the procedures are detailed. The superiority of the former over the latter will also become obvious in the context. This type of structure has the potential for large array design based on the conductor-backed coplanar waveguide.



# Contents

口試委員會審定書	i
誌謝	iii
摘要	v
Abstract	vii
Contents	ix
List of Tables	xii
List of Figures	xiii
<b>Chapter 1 Introduction</b>	<b>1</b>
1.1 Motivation.....	1
1.2 Literature Survey .....	1
1.3 Contribution .....	9
1.4 Chapter Outlines .....	10
<b>Chapter 2 Coupled Twin Slots Fed by Conductor-Backed Coplanar Waveguide</b>	<b>14</b>
2.1 The Straight-Slot Case.....	14
2.1.1 Introduction .....	14
2.1.2 Antenna Structure and Design.....	16
2.1.3 Experimental Results.....	19



2.1.4 Design Procedure.....	21
2.1.5 Summary.....	21
2.2 The Arc-Slot Case .....	22
2.2.1 Introduction .....	22
2.2.2 Antenna Structure.....	23
2.2.3 Simulation and Measurement Results .....	24
2.2.4 Design Procedure.....	26
2.2.5 Summary.....	26
2.3 The Miniaturized Case .....	27
2.3.1 Introduction .....	27
2.3.2 Antenna Operation.....	28
2.3.3 Simulation and Measurement .....	29
2.3.4 Design Procedure.....	30
2.3.5 Summary.....	30
2.4 Comparison.....	32



**Chapter 3 Parallel-Plate Slot Array Fed by Conductor-Backed Coplanar**

**Waveguide 57**

3.1 The Longitudinal Case .....	57
---------------------------------	----

3.1.1 Introduction .....	58
--------------------------	----

3.1.2 Antenna Structure.....	59
3.1.3 Analysis .....	61
3.1.4 Array Design and Measurement.....	66
3.1.5 Design Procedure.....	69
3.1.6 Summary.....	70
3.2 The Transverse Case.....	71
3.2.1 Introduction .....	71
3.2.2 Antenna Structure.....	71
3.2.3 Simulation and Measurement Results .....	72
3.2.4 Design Procedure.....	74
3.2.5 Summary.....	75
<b>Chapter 4 Conclusion</b>	<b>100</b>
<b>Appendix A Explanation of the Leakage Occurrence</b>	<b>103</b>
<b>Reference</b>	<b>106</b>
<b>Publication List of I-Ching Lan</b>	<b>125</b>



# List of Tables

## Chapter 2

Table I	Summary of the measurement results of the three designs of the coupled twin slots.....	56
---------	--	----

## Chapter 3

Table II	Summary of the H-plane main beam positions and antenna gains of the 5x6 array without termination .....	94
Table III	Summary of the E-plane main beam positions.....	99



# List of Figures

## Chapter 1

Fig. 1. 1 Structure of the coplanar waveguide (CPW)..... 12

Fig. 1. 2 Structure of the conductor-backed coplanar waveguide (CBCPW)..... 13

## Chapter 2

Fig. 2. 1 Simulated surface current density distributions of (a) a single slot dipole, (b) twin slots with the first slot dipole  $\sim 1\lambda$  long, and (c) twin slots with the first slot dipole  $\sim 2\lambda$  long. All cases are fed by the CBCPW with the same dimension. .... 34

Fig. 2. 2 Geometry and photograph of the proposed CBCPW-fed slot dipole coupled with a straight slot. .... 35

Fig. 2. 3 Simulated results for normalized  $L_2$  versus  $L_1$  with a broadside main beam at 5 GHz.  $S_1 = 1.5$  mm,  $L_f = 15$  mm,  $d = 13.1$  mm,  $W = 2.5$  mm,  $G = 0.8$  mm,  $h = 1.6$  mm,  $\epsilon_r = 4.2$ , and  $\tan\delta = 0.02$ . .... 36

Fig. 2. 4 Simulated (a) radiation and antenna efficiencies and (b) antenna gain versus  $L_1$  at 5 GHz.  $S_1 = 1.5$  mm,  $L_f = 15$  mm,  $d = 13.1$  mm,  $W = 2.5$  mm,  $G = 0.8$  mm,  $h = 1.6$  mm,  $\epsilon_r = 4.2$ , and  $\tan\delta = 0.02$ . .... 38

Fig. 2. 5	Simulated and measured input return losses and gains of the proposed antenna with $L_1 = 60$ mm, $L_2 = 59$ mm, $S_1 = 1.5$ mm, $S_2 = 2.7$ mm, $d = 13.1$ mm, $L_f = 15$ mm, $W = 2.5$ mm, $G = 0.8$ mm, $h = 1.6$ mm, $\epsilon_r = 4.2$ , and $\tan\delta = 0.02$ .	39
Fig. 2. 6	Simulated and measured radiation patterns of the proposed antenna at 5 GHz. (a) E-plane (y-z plane). (b) H-plane (x-z plane).	41
Fig. 2. 7	(a) Geometry of the proposed CBCPW-fed slot dipole coupled with an arc-slot. (b) Equivalent magnetic current on the radiating slots. (c) Photograph.	43
Fig. 2. 8	Simulations of (a) radiation efficiency and (b) antenna gain. $S_d = 1$ mm, $S_a = 1.5$ mm, $S_m = 1$ mm, $L_d = 18.5$ mm, $L_m = 4$ mm, and $d = 15.65$ mm.	45
Fig. 2. 9	Simulated and measured input return losses.	46
Fig. 2. 10	Simulated and measured antenna gains.	47
Fig. 2. 11	Measured radiation patterns at 5.02 GHz. (a) E-plane; (b) H-plane.	48
Fig. 2. 12	Measured radiation patterns at 4.9 GHz. (a) E-plane; (b) H-plane.	49
Fig. 2. 13	Measured radiation patterns at 5.2 GHz. (a) E-plane; (b) H-plane.	50
Fig. 2. 14	Geometry and photograph of the proposed CBCPW-fed finite ground slot dipole antenna.	51
Fig. 2. 15	Measured and simulated input return losses of the proposed antenna.	52



Fig. 2. 16	Normalized measured (a) E-plane and (b) H-plane radiation patterns at 5.0 GHz.....	53
------------	--	----

Fig. 2. 17	Normalized measured E-plane co-polarization patterns at (a) 4.8 GHz, (b) 4.9 GHz, and (c) 5.1 GHz.....	55
------------	--	----

### Chapter 3

Fig. 3. 1	Geometry of the proposed antenna with a 3 x 6 longitudinal slot array. ....	76
-----------	---	----

Fig. 3. 2	Relationship between the leakage wave and the relative phases of the fields on the slots.....	77
-----------	---	----

Fig. 3. 3	Normalized leakage power from (a) different lengths of the CBCPW-line and (b) different sections within a line with a total length of 250 mm. ....	79
-----------	--	----

Fig. 3. 4	Normalized radiated power of a slot pair versus $d_s$ at 5.5 GHz. $l_s = 23$ mm and $w_s = 2$ mm. ....	80
-----------	--	----

Fig. 3. 5	Normalized radiated power of a slot pair versus slot length. $f = 5.5$ GHz, $w_s = 2$ mm, $d_s = 13$ mm, and $d_y = 31$ mm.....	81
-----------	---	----

Fig. 3. 6	Normalized radiated power versus $d_t$ for a 5 x 2 array at 5.5 GHz.....	82
-----------	--	----

Fig. 3. 7	Measured and simulated input return losses of the 5 x 2 array without termination.....	83
-----------	--	----

Fig. 3. 8	Measured and simulated H-plane patterns of the 5 x 2 array with and without termination at 5.5 GHz. Solid line: measurement without termination; dotted	
-----------	---	--

	line: measurement with termination; cross: simulation without termination; circle: simulation with termination.....	84
Fig. 3. 9	Measured and simulated E-plane patterns of the 5 x 2 array with and without termination at 5.5 GHz. Solid line: measurement without termination; dotted line: measurement with termination; cross: simulation without termination; circle: simulation with termination.....	85
Fig. 3. 10	Photograph of the 5 x 6 array.....	86
Fig. 3. 11	Measured and simulated input return losses of the 5 x 6 array without termination.....	87
Fig. 3. 12	Measured and simulated H-plane patterns of the 5 x 6 array without termination at 5.5 GHz.....	88
Fig. 3. 13	Measured and simulated E-plane patterns of the 5 x 6 array without termination at 5.5 GHz. ....	89
Fig. 3. 14	H-plane patterns of the 5 x 6 array without termination. (a) 5 GHz, (b) 5.25 GHz, (c) 5.75 GHz, and (d) 6 GHz.....	93
Fig. 3. 15	Geometry and photograph of the proposed transverse array.....	95
Fig. 3. 16	Measured and simulated input return losses. ....	96
Fig. 3. 17	Measured and simulated radiation patterns in the y-z plane.....	97
Fig. 3. 18	Radiation patterns in the E-plane at various frequencies. ....	98

## Appendix A

Fig. A. 1 Top view of a printed strip, showing the angle of leakage  $\theta$  into the surface wave of wave number  $k_s$  on the surrounding dielectric substrate layer..... 105



# Chapter 1

## Introduction

### 1.1 MOTIVATION

Surprises are no surprise to research works. For some researchers analyzing the modal problems of certain wave-guiding structures, the phenomenon of leaky wave radiations was discovered and evolved into a new category of powerful antennas. For some, like the author, attempting to include a conducting plane in the backside of slot antennas to obtain a unidirectional radiation pattern and perhaps higher antenna directivity and gain, the consequence is a disaster. The structure becomes overmoded and the antenna performances degrade drastically. This dissertation endeavors to seek for an elegant engineering method to improve the radiation performance of slot antennas backed by a conducting plane, especially with a coplanar waveguide feed.

### 1.2 LITERATURE SURVEY

Proposed in 1969 [1], the coplanar waveguide (CPW) has become increasingly

popular nowadays because of several advantages it offers over the conventional microstrip line, such as the uniplanar structure, low radiation loss, low dispersion, ease of fabrication, and the ability of being easily integrated with active and passive devices without the need of via holes [2]. The structure of the CPW is shown in Fig. 1.1, where the gray area represents the metal plane and the white portion is the dielectric substrate. The parameters  $W$  and  $S$  are, respectively, the strip and slot widths of the CPW, whereas  $h$  and  $\epsilon_r$  are the height and the dielectric constant of the substrate, respectively.

In practical situations there are often conducting planes backing the substrate either intentionally to improve the mechanical strength and the heat-sinking capability, to render the radiation pattern unidirectional in the antenna applications, or accidentally due to the existence of nearby metal objects. Besides, in multilayered structures, while the isolation on the same layer can be achieved by placing vias, the isolation between layers is usually realized by placing conducting planes between layers [3]. The structure now becomes the conductor-backed coplanar waveguide (CBCPW), and the structure is shown in Fig. 1.2. Some examples of using the CBCPW as a feed-line can be found in [4] – [16]. Special purposes or applications such as transitions [17] – [19], measurements of complex permittivity and permeability [20], [21], or even sensors [22] also exist.

The CBCPW is an overmoded, leaky guiding structure. In addition to the CPW

mode, the top and bottom conducting planes also support the parallel-plate mode. The originally bound CPW mode now leaks power in the form of the parallel-plate mode along a particular angle relative to the main CPW line. Since the transverse electromagnetic (TEM) wave in the parallel-plate waveguide region does not have a cut-off frequency, there will always be some power leakage in the lateral direction for all frequencies [23]. In addition, the parallel-plate mode has the same symmetry as the CPW mode and therefore cannot be suppressed by air bridges [24]. The physical idea of the leakage phenomenon was clearly explained in [25] and is adapted in Appendix A.

Early studies on the CBCPW can be traced back to the 1980s. In 1982 Shih and Itoh [26] treated the CBCPW as a mixture of a microstrip line and a coplanar waveguide and computed the dispersion relations as well as the characteristic impedance of the CBCPW. However, as pointed out by Shigesawa et al. [27], the analysis was not complete because it was done before the leakage was recognized to occur and therefore it missed the leakage effect altogether. In [27] the leakage effects on both conductor-backed slot lines and conductor-backed coplanar waveguides, with finite or infinite lateral extent of conductors, were introduced, and theoretical and experimental results of the phase and attenuation constants were compared. Chou et al. [23] explained why the attenuation constant of the CBCPW increases with frequency until it reaches a peak, after which it starts to decrease. The dimensions of the strip and slot widths

become electrically large at higher frequencies such that the fields concentrate below the center conductor of the CPW and get weaker in the slot region. Thus weaker fields are excited in the parallel-plate region. So the normalized phase constant approaches  $\sqrt{\epsilon_r}$  and the attenuation constant decreases at higher frequencies. In other words, the CBCPW with larger values of the center strip width and the slot widths behaves more like a microstrip line rather than a coplanar waveguide. Other studies on the basic properties of the CBCPW appear in [28] and [29], which stated that the leakage rate of the CBCPW increases with reducing substrate height, same conclusion as in [30], [31]. The CBCPW in a metallic enclosure was discussed in [32]. Analysis of the asymmetric CBCPW can be found in [33], [34].

One of the main problems of an overmoded wave-guiding structure is the mode conversion at discontinuities. Jackson [31], [35] discussed both the gap end and the short end discontinuities in the finite-width conductor-backed coplanar waveguide. Three modes are significant in the setup, namely the coplanar waveguide (CPW) mode, the coplanar microstrip (CPM) mode, and the microstrip (MS) mode. It was found that more power is coupled from the CPW mode to the CPM and the MS modes at the gap end discontinuity than at the short end one, and the coupled power decreases when either the substrate height is increased or the guide cross-sectional area is reduced. Another problem of the CBCPW is the coupling between devices and crosstalk.

Coupling may be due to direct leakage, substrate resonances, or both [36]. Coupling between slotlines through a conductor backing was explained in [37], where Hirota and Itoh showed that the coupling was not due to the proximity effect but through the conductor backing.

Resonance of the CPW side conducting planes is another issue [38] – [47]. Excited by the leakage wave, the side conducting planes of the CPW behave like the resonator [38], [39], [44], so the energy is confined under the side planes and the transmission line performs awfully. Thorough investigations of this resonance phenomenon can be found in [39], where the resonant frequencies were predicted by both the patch-resonator model and the MSL (microstrip-like) model. Also found was that various side plane patterns did not suppress the resonance. Haydl [40] drew similar conclusions that the resonant frequencies of the CBCPW side planes are predictable by the patch antenna theory.

To deal with the leakage problem of the CBCPW and various side effects, several methods have been proposed. First, via holes that short the top and bottom conducting planes were used to suppress the parallel-plate modes [9], [12], [14], [18], [44], [45], [48] – [59]. Among these works, [44] is of particular importance, in which Haydl systematically investigated the effects of the via positions on the leakage suppression. It was found that placing the vias near the excitation region of the parallel-plate mode,



which is the gap region of the CBCPW, was superior to both random placements and shorting the periphery of the ground planes, which just shifted the resonant frequencies of the ground planes. Transmission characteristics of the CBCPW with via holes can also be found in [60]. The effect of the lateral walls, which closely spaced via holes resemble, on the propagation characteristics of the finite-width conductor-backed coplanar waveguide (FW-CBCPW) were presented in [61]. However, the use of via holes contradicts one main advantage of the CPW technology that via holes are not necessary for grounding [36]. Besides, placing via holes close to the CBCPW also affects the impedance [12].

The second approach is the non-leaky coplanar (NLC) waveguide proposed by Liu et al. [62], although this idea had already been practiced implicitly by other researchers [63] – [66]. The concept is to make the CPW mode slower than the dominant parallel-plate TEM mode by incorporating an additional dielectric layer, which has higher dielectric constant, with two possible configurations, i.e., either above or beneath the top metal layer the CPW ground resides. Usage and discussions of the NLC waveguide can be found in [67] – [74]. Although the transmission line itself is made no longer leaky by this method, coupling to the parallel-plate modes still occurs at discontinuities [24]. The structure also becomes more complicated and expensive due to the additional dielectric layer.

There are some other techniques developed to prevent the propagation of the parallel-plate mode, such as the uniplanar compact photonic-bandgap (UC-PBG) structure [75] – [77], the patterned backside metallization [36], the backside grooving [78], and the use of finite width dielectric guide with much higher dielectric constant that results in the total reflection of the leakage wave [58]. While the third and the fourth methods are obviously formidable due to the difficult dielectric processing, the second method still suffers when a conducting plane lies beneath the patterned metallization, not uncommon in power amplifier MMICs which have to be placed on a heat sink [42], and the first method involves the additional design of the bandgap structure.



The above are solutions specific to the transmission line scope. As for antenna applications, some different approaches have also been developed. The most noticeable is the phase cancellation technique, originally proposed in the 1980s to deal with the surface wave problems of printed dipoles [79] as well as slots on electrically thick dielectric substrates [80] – [84]. This technique uses twin broadside slots half a guided wavelength apart to cancel the undesired propagating power. Successful implementations of this technique for conductor-backed slots can be found in [85] – [90]. For these excellent works, the complexities always come from the feeding structures, since both slots are fed directly and separately. The number of dielectric

layers used, the number of feed points, or the accompanying bulky feeding circuits are major problems.

The second type is the aperture coupled patch antennas [4] – [6] that have the CPW feed-line and the coupling aperture on opposite sides of the substrate and an additional dielectric layer with the patch above. Although the patch antenna works fine, there are potential dangers because the leakage problem of the feed-line is not taken care of. Besides, two dielectric layers are needed, which may not be acceptable in certain applications.

The final one is the coplanar patch antenna (CPA) which looks like a CPW-fed slot loop antenna with conductor backing [91] – [106]. So far this is, in the author's opinion, the most elegant design of CBCPW-fed antennas due to its structural simplicity. Only one dielectric layer is used and via holes are not needed. Besides the characteristics of the antenna are similar to those of the conventional patch antenna so the design is straightforward. However, viewing the CPA as the microstrip patch antenna lacks completeness because the parallel-plate mode leakage indeed exists in the side ground regions, as evidenced by Fig. 7 of [103], which is obviously not true for the microstrip patch antenna that has no side grounds at all. In this dissertation we will use our proposed CBCPW-fed coupled twin slots to provide another point of view.

## 1.3 CONTRIBUTION

This dissertation is devoted to the analysis and design of two novel types of antennas, both fed by the CBCPW. The first type is the coupled twin slots with three variants, including the slot dipole coupled with a straight slot, the slot dipole coupled with an arc-slot, and the miniaturized version. They utilize the leakage power generated at the discontinuity where the feed-line meets the slot dipole to excite an additional slot (or the fringing fields in the miniaturized case), thus forming a radiation-efficient coupled pair. These coupled twin slots are one of the simplest, if not the simplest, forms of antennas fed by the CBCPW to date.

The second type is the parallel-plate slot array. The parallel-plate mode leakage from the feeding CBCPW is intercepted by the slots on the side ground planes. Depending on the directions of alignment of the slots with respect to the feed-line, a longitudinal array and a transverse array are designed. Wide impedance bandwidth, high directivity, high front-to-back ratio, and frequency-scanning of the main beam in one of the major plane cuts are the features of the proposed array.

The aforementioned two types are both designed with the CBCPW feed-line in its most basic form, i.e. with only one dielectric layer without any via holes. Besides, the height of the dielectric substrate doesn't need to be a quarter guided wavelengths as in

several references [85], [87], [88], [107].

## 1.4 CHAPTER OUTLINES

This dissertation is organized in the sequence described below.

In Chapter 2, three versions of the coupled twin slots fed by the CBCPW are presented in order. First of all, the leakage phenomenon that occurs at the discontinuity of the CBCPW-fed slot dipole is illustrated visually. Then the CBCPW-fed slot dipole coupled with a straight slot is designed, fabricated, and experimented. Second, the CBCPW-fed slot dipole coupled with an arc-slot slot is presented. Some cautions about CBCPW-fed slot antenna designs are also discussed. The simulation and measurement results are demonstrated. Finally the miniaturized version is presented. Simulation and measurement results about the performance of the reduced-size antenna are shown. The smoother radiation patterns that prove the ground diffractions are alleviated are also presented.

In Chapter 3, two parallel-plate slot arrays are presented in order. First, the novel parallel-plate longitudinal slot array fed by the CBCPW is proposed. Design considerations about the choices of the slot orientation, the feed-line dimension, the inter-element spacing, and the slot dimensions are explained in detail. The reflected

wave from the end of the feed-line is also taken into consideration to compensate for the power tapering along the radiating apertures. A 5 x 6 and two 5 x 2 arrays with and without the feed-line termination are simulated, fabricated and tested. Next, the parallel-plate transverse slot array is presented. An array with an off-broadside main beam is designed to illustrate the basic concept and the predictable main beam position. Then another array with a broadside main beam is designed to demonstrate the frequency-scanning property. Simulation and measurement results are presented.

Finally, conclusions are drawn in Chapter 4.



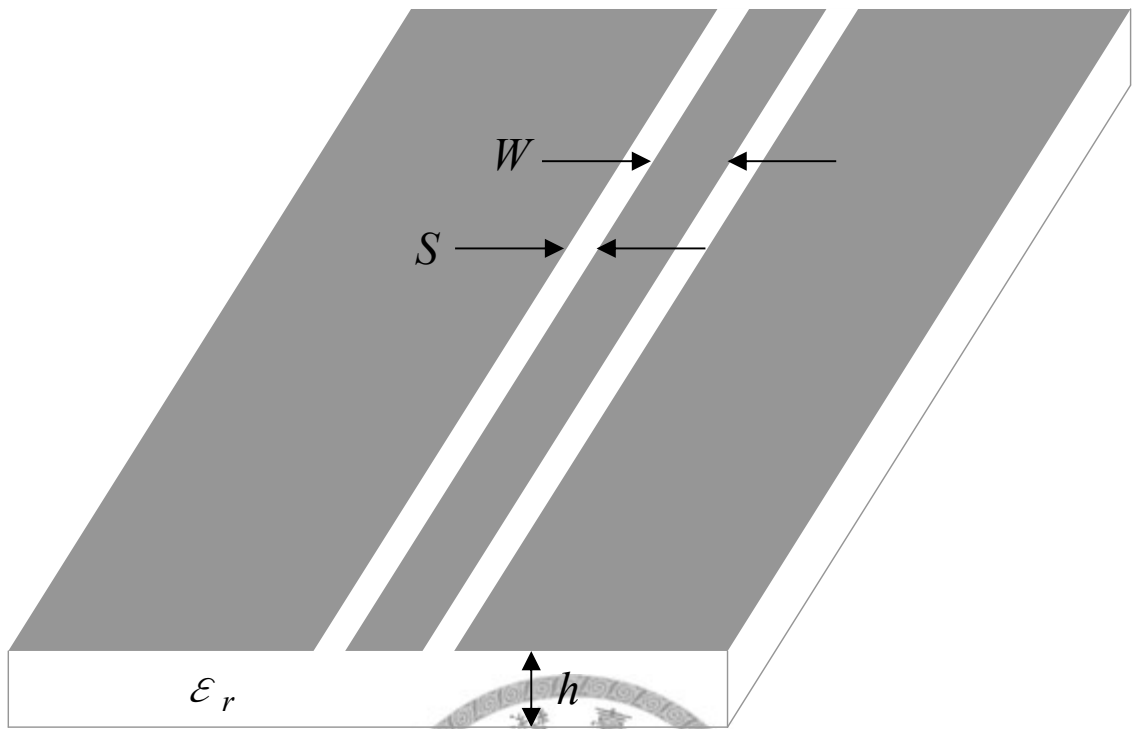
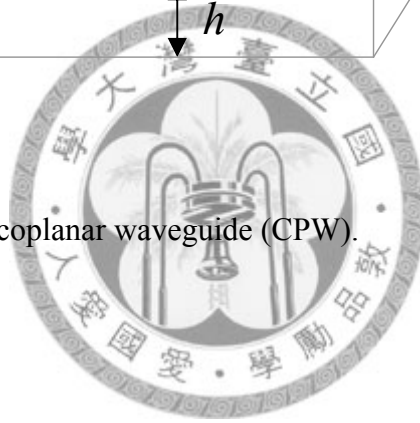


Fig. 1. 1 Structure of the coplanar waveguide (CPW).



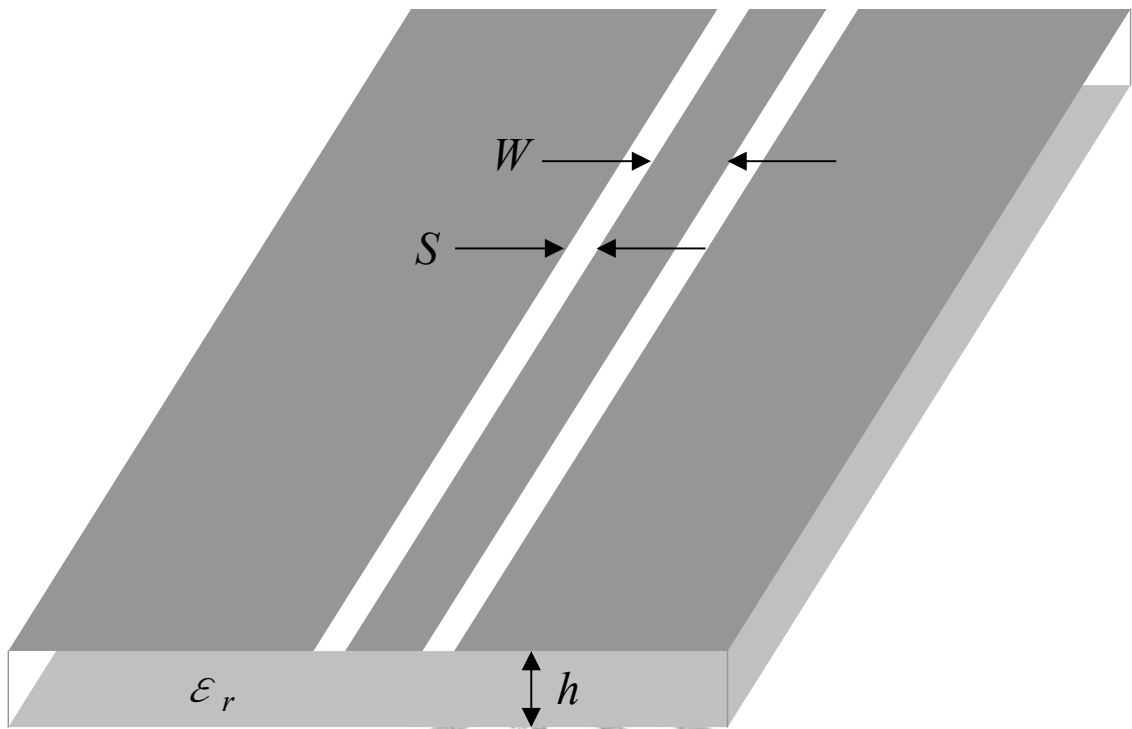


Fig. 1. 2 Structure of the conductor-backed coplanar waveguide (CBCPW).





# Chapter 2

## Coupled Twin Slots Fed by Conductor-Backed Coplanar Waveguide

### 2.1 THE STRAIGHT-SLOT CASE

The coupling mechanism of the twin slots fed by the conductor-backed coplanar waveguide is investigated. The goal is to improve the antenna efficiency by using the phase cancellation technique and at the same time keep the structure as simple as possible. The leakage phenomenon is illustrated visually and the effects of the antenna parameters are examined numerically for choosing the appropriate variables. Finally the proposed antenna is fabricated and tested, showing 69.8 % of antenna efficiency.

#### 2.1.1 INTRODUCTION

Coplanar-waveguide-fed slot antennas are attractive due to their uniplanar structures and the ease of fabrication [2]. To render the radiation from bidirectional to

unidirectional, conducting planes are usually placed at the back of the antennas. The performance, however, suffers because the conductor-backed coplanar waveguide (CBCPW) and the conductor-backed slot are both leaky structures due to the incursion of the parallel-plate mode leakage [27]. The parallel-plate TEM mode has zero cut-off frequency, so the leakage phenomenon occurs at all frequencies. One major trend toward solving the leakage problem of conductor-backed slots is the phase cancellation technique originally proposed in the 1980s to deal with the surface wave problem of dipoles [79] as well as slots on electrically thick dielectric substrates [80] using infinitesimal elements. This technique uses twin broadside slots half a guided wavelength apart to cancel the undesired propagating power. Successful implementations of this technique for conductor-backed slots can be found in [88] and [90], where the slot lengths are 0.84 and 0.95 wavelengths long in [88] and about one wavelength long in [90]. For these excellent works, the complexities always come from the feeding structures, since both slots are fed directly and separately. Two dielectric layers and feeding circuits are used in [88], whereas two dielectric layers and two feeding ports are required in [90].

In this chapter we propose a new feeding mechanism for the twin slots configuration, of which the first slot dipole is directly fed by the CBCPW, whereas the second slot is coupled by the parallel-plate mode leakage excited at the discontinuity of

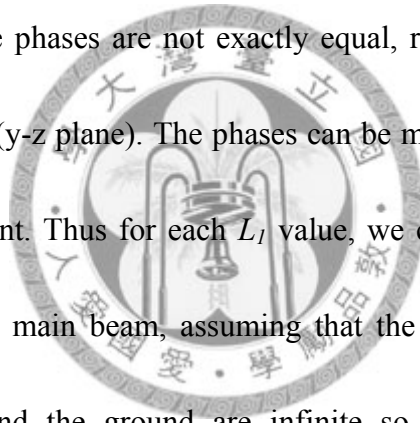
the first slot dipole. By means of this feeding method, the resulting geometry is single-layered with only one feed and without any additional feeding circuits or via holes. The simplicity and conciseness greatly enhance the usability of CBCPW-fed slot antennas for practical applications.

## 2.1.2 ANTENNA STRUCTURE AND DESIGN

The single slot dipole fed by the CBCPW acts more like a mode converter than an efficient antenna. It converts most of the power from the CBCPW mode to the parallel-plate mode, leaving the radiated power very small. The typical antenna gain is far below 0 dBi and the radiation efficiency below 10 %. Using the simulator HFSS from *Ansoft*, Fig. 2.1(a) illustrates this phenomenon, where the surface current density at the interface between the dielectric and the top metal layer is plotted. At the junction of the CBCPW feed-line and the slot dipole, the parallel-plate mode is strongly excited and propagates radially into the substrate region. In contrast, as Figs. 2.1(b) and (c) show, if an additional slot with suitable dimension is placed in front of the first slot dipole at a distance about half a guided wavelength of the parallel-plate mode according to the phase cancellation technique, the leakage is reduced significantly. Although the leakage suppression is not complete, the gain and the efficiency are greatly improved, as

will be shown shortly.

The geometry and the photograph of the proposed twin slots fed by the CBCPW are shown in Fig. 2.2. The gray area represents the metal portion and the white ones are the etched slots and the feed-line. The relative phases of the fields on the first and the second slots depend on the distance  $d$  as well as the lengths and widths of the slots,  $L_1$ ,  $L_2$ ,  $S_1$ , and  $S_2$ . When the distance  $d$  is half a guided wavelength of the parallel-plate mode according to the phase cancellation technique and the slots are of the same length, it is found that usually the phases are not exactly equal, resulting in an off-broadside main beam in the E-plane (y-z plane). The phases can be made equal if the slot lengths are allowed to be discrepant. Thus for each  $L_1$  value, we can find a corresponding  $L_2$  that results in a broadside main beam, assuming that the transverse dimensions (x-y plane) of the substrate and the ground are infinite so the influence of the edge diffractions on radiation patterns is temporarily ignored. The following simulations are carried out using the package software IE3D from *Zeland*. Fig. 2.3 illustrates the simulated results at 5 GHz, where the normalized  $L_2$  ( $L_2 / L_1$ ) is plotted versus  $L_1$ . The effect of different slot widths is also considered. From Fig. 2.3 we see that  $L_2$  might be greater than, equal to, or smaller than  $L_1$ , depending on the choices of  $L_1$  and the widths of the slots. Note that since the CBCPW is a leaky line, the length of the feed-line ( $L_f$ ) should not be too long. In our simulations the feed-line length is chosen to be 15 mm,



with the corresponding loss estimated to be 0.45 dB.

For each combination of  $L_1$  and  $L_2$  that results in a broadside main beam, the corresponding efficiencies and gains are calculated and shown in Fig. 2.4. Here the radiation efficiency is defined as the ratio between the radiated power and the input power, whereas the antenna efficiency as the ratio between the radiated power and the incident power. The difference between the incident power and the input power is the return loss at the input. Fig. 2.4(a) reveals that the radiation efficiency has local maximums when  $L_1$  is near integer multiples of  $\lambda$ , where  $\lambda$  is approximated by  $\lambda_0 / \sqrt{(\epsilon_r + 1)/2}$ , which is 37.2 mm at 5 GHz for the present case. However, the serious input mismatch makes the overall antenna efficiency below 50 % when  $L_1 \doteq \lambda$ . On the other hand, the highest antenna gain is achieved when  $S_2 = 2.7$  mm and  $L_1 = 78$  mm  $\doteq 2\lambda$ , as can be seen in Fig. 2.4(b). The corresponding antenna efficiency is 64.7 % but the input return loss is just about 10 dB. If a better input matching condition is required, smaller  $L_1$  values should be chosen such that the curves of the radiation and antenna efficiencies are closer to each other. In our experiment we choose  $L_1 = 60$  mm for a better input return loss and a slightly higher antenna efficiency, although the gain is smaller due to the smaller antenna size. Note that although it seems like increasing  $S_2$  results in higher efficiencies and gains, these performances soon begin to saturate and finally fall off. Therefore in our simulations higher  $S_2$  values are not pursued further.

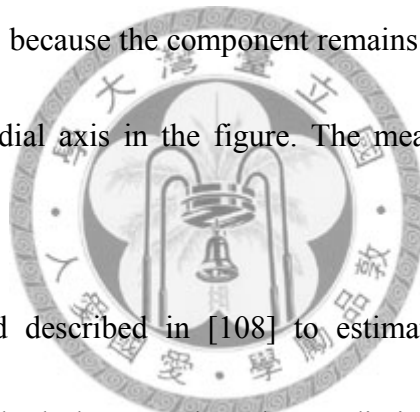
## 2.1.3 EXPERIMENTAL RESULTS

A twin slot fed by the CBCPW is fabricated and tested with the following parameters:  $L_1 = 60$  mm,  $L_2 = 59$  mm,  $S_1 = 1.5$  mm,  $S_2 = 2.7$  mm,  $d = 13.1$  mm,  $L_f = 15$  mm,  $W = 2.5$  mm, and  $G = 0.8$  mm. The FR4 substrate with  $h = 1.6$  mm,  $\epsilon_r = 4.2$ , and  $\tan\delta = 0.02$  is used in the fabrication. Note that for antenna applications, the substrate material with lower dielectric constant and loss tangent would be more preferable. However, in this work, the FR4 substrate was used merely because it is more accessible to us and much cheaper than other substrates. The dimensions of the substrate and the ground plane are 150 mm in the x-direction and 85 mm in the y-direction.

Fig. 2.5 plots the frequency response of the simulated and measured input return losses and gains. The measured input return loss is seen to have about 0.1-GHz frequency shift from the simulated one, whereas the simulated and measured gains are very close to each other. Considering that the simulation tool IE3D does not take the finite ground and the finite substrate into account and the mechanical tolerance of the fabrication process would unavoidably result in some discrepancy between the physical dimensions of the simulation model and the test piece, the results are quite satisfactory. At 5 GHz the measured return loss is 24.1 dB and the measured gain is 5.64 dBi. The

measured 10-dB return loss bandwidth is 5 %, extending from 4.88 GHz to 5.13 GHz.

Fig. 2.6 shows both the simulated and measured E- and H-plane radiation patterns at 5 GHz. Mild ripples are observed in the measured E-plane co-polarization pattern. This is caused by the edge diffractions of the finite ground plane, which is a common phenomenon in slot antenna E-planes. The measured cross-polarization levels are fairly low in the E-plane and a bit higher in the H-plane, but are still below -15 dB in all directions. Note in Fig. 2.6(a) that the simulated cross-polarized component in the E-plane is invisible. This is because the component remains lower than -40 dB, which is the lower bound of the radial axis in the figure. The measured front-to-back ratio is higher than 17 dB.



By using the method described in [108] to estimate the directivity from the half-power beamwidths of both the E- and H-plane radiation patterns, together with the measured gain data, the antenna efficiency is found to be 69.8 % at 5 GHz. As will be shown in the next section, the antenna efficiency of the CBCPW-fed slot dipole coupled with an arc-slot is calculated using the same method, and is found to be 50.6 %. Although the structure in the next section has the advantage of occupying a smaller area, the performance of the present structure is superior in terms of the antenna efficiency, the main concern of antennas fed by the leaky CBCPW.

## 2.1.4 DESIGN PROCEDURE

The design procedure can be summarized as follows.

1. Choose  $L_1 \doteq 1.5 \sim 1.6 \lambda$ .
2. For  $d$  being about half the guided wavelength of the parallel-plate TEM mode, find a  $L_2$  value that is close to  $L_1$  such that the coupled twin slots have a broadside main beam in the E-plane.
3. Make  $S_2$  large enough before the antenna efficiency and gain saturate.

## 2.1.5 SUMMARY



The CBCPW-fed coupled twin slots have been proposed and the properties demonstrated. The coupling mechanism and the effects of the antenna parameters have been studied and utilized to design a unidirectional antenna of 69.8 % antenna efficiency with a simple structure without any complicated feeding circuits. This type of antennas would be very attractive when the CBCPW feed is unavoidable and the whole structure must be kept simple.



## 2.2 THE ARC-SLOT CASE

A novel compact slot antenna fed by the conductor-backed coplanar waveguide (CBCPW) is proposed. The antenna is composed of a CBCPW-fed slot dipole and an additional arc-slot in front of the dipole. Compared to the CBCPW-fed slot dipole without the arc-slot, the antenna gain is improved significantly. The antenna occupies a small area and uses only one layer of dielectric substrate and a single feed without any via holes. The impedance bandwidth is 7.2 % and the highest in-band antenna gain is 3.4 dBi.



### 2.2.1 INTRODUCTION

In this section, we propose a new CBCPW-fed slot dipole antenna that incorporates an additional arc-slot to achieve the phase cancellation with only one layer of substrate and a single feed. The excitation of the arc-slot is through the coupling of the power leaked from the discontinuity of the feed-line, as described in the previous section. The feeding mechanism alleviates the burden of designing complicated power dividing circuits. This results in a simple geometry and a compact antenna size.

## 2.2.2 ANTENNA STRUCTURE

Figs. 2.7(a), (b), and (c) show the geometry of the antenna, the equivalent magnetic currents flowing on the radiating slots, and the photograph, respectively. The gray area represents the metal, whereas the white ones are the etched slots and the feed-line. As the input power travels down the feed-line and excites the slot dipole, part of the power propagates, in the parallel-plate region, toward and excites the arc-slot. When the distance  $d$  is about half the guided wavelength of the parallel-plate TEM mode, the field on the central region of the arc-slot and that on the slot dipole are in phase, which reinforces the effect of the phase cancellation. The length of the slot dipole ( $2 \times L_d$ ) is about  $\lambda$ , which is approximated by  $\lambda_0 / \sqrt{(\epsilon_r + 1)/2}$ . On the other hand, because the length of the arc-slot is fixed by its radius, two additional sections ( $L_m \times S_m$ ) are attached to extend the total arc-slot length to about  $1.5 * \lambda$ . As opposed to the conventional transmission lines, such as the coplanar waveguide, where the feed-line length basically merely alters the phase of the input reflection coefficient, it is not true for the CBCPW-fed antennas. Since the CBCPW is a leaky line, the input power is fed directly into the antenna as well as through the coupling of the leakage power. Therefore as the feed-line length is varied, so are the amount of the coupling and hence the characteristics of the antenna. This phenomenon is best illustrated by Fig. 2.8, where the

radiation efficiency and the antenna gain simulated by IE3D from *Zeland* are plotted. When the feed-line length is changed from 5 mm to 20 mm, the variation of the radiation efficiency is about 11 % at the design frequency of 5 GHz, whereas that of the gain is about 0.9 dB. Also note in these figures that the variations with frequency are not monotonic, which would be the case if there is only material loss. These two observations reveal the distinctive feature of the CBCPW and the caution that should be kept in mind when designing CBCPW-fed antennas.

### 2.2.3 SIMULATION AND MEASUREMENT RESULTS

The design is based on the FR4 substrate with dielectric constant  $\epsilon_r = 4.2$ , thickness  $h = 1.6$  mm, and loss tangent  $\tan\delta = 0.02$ . The central distance between the arc-slot and the dipole slot is  $d = 15.65$  mm, which is slightly larger than one half the guided wavelength of the parallel-plate mode at 5 GHz. The remaining parameters are as follows:  $S_d = 1$  mm,  $S_a = 1.5$  mm,  $S_m = 1$  mm,  $L_d = 18.5$  mm,  $L_m = 4$  mm, and  $L_f = 14$  mm. The strip and slot widths of the CPW feed-line are 2 mm and 0.5 mm, respectively, which correspond to a 50- $\Omega$  characteristic impedance. Throughout the design process, simulations are carried out using the package software IE3D from *Zeland*.

The return loss and gain are plotted in Figs. 2.9 and 2.10, respectively. The

simulated resonant frequency is 5.05 GHz, whereas the measured one is 5.02 GHz. The shift in resonant frequency is less than 0.6 %. The measured bandwidth is wider than the simulated one, which may be attributed to the large loss of the dielectric substrate used in the experiment. The measured return loss at 5.02 GHz is 16.25 dB and the 10-dB return loss bandwidth is 7.2 % extending from 4.86 to 5.22 GHz. The in-band measured gain ranges from 0.55 dBi to 3.4 dBi and is 2.89 dBi at 5.02 GHz. Compared to the CBCPW-fed slot dipole without the arc-slot, which has gain far below 0 dBi, the current design increases the gain significantly, while the antenna size still kept compact.

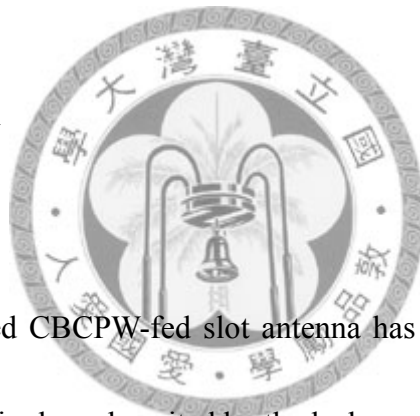
The measured radiation patterns at 5.02 GHz are shown in Fig. 2.11. The cross-polarization level in the E-plane (yz-plane) is below -20 dB except for the region near  $\theta = 90^\circ$ , which has higher levels due to the disturbance of the connecting cable in that direction. As for the H-plane (xz-plane), the cross-polarization level is higher than that in the E-plane, but still remains under -10 dB. Especially in the direction of the main beam, the level is down to below -30 dB. For comparison, the in-band patterns at 4.9 GHz and 5.2 GHz are shown in Figs. 2.12 and 2.13, respectively. As can be seen, the pattern is quite stable with respect to the frequency variations. By using the method described in [108] to estimate the directivity from the half-power beamwidths of both the E- and H-plane radiation patterns, together with the measured gain data, the antenna efficiency is found to be 50.6 % at 5.02 GHz.

## 2.2.4 DESIGN PROCEDURE

The design procedure can be summarized as follows.

1. Choose  $2 * L_d \doteq \lambda$ .
2. For  $d$  being about half the guided wavelength of the parallel-plate TEM mode, attach two sections to both ends of the arc-slot to extend the total length to about  $1.5 * \lambda$ .

## 2.2.5 SUMMARY



A novel gain-enhanced CBCPW-fed slot antenna has been proposed. An arc-slot placed in front of the slot dipole and excited by the leakage power from the CBCPW has been shown to significantly increase the gain of the slot dipole on the leaky conductor-backed structure. The measured impedance bandwidth is 7.2 %, the highest gain is 3.4 dBi in the band, and the radiation pattern is stable within the band. This antenna is useful when the compact CBCPW-fed antenna is needed.

## 2.3 THE MINIATURIZED CASE

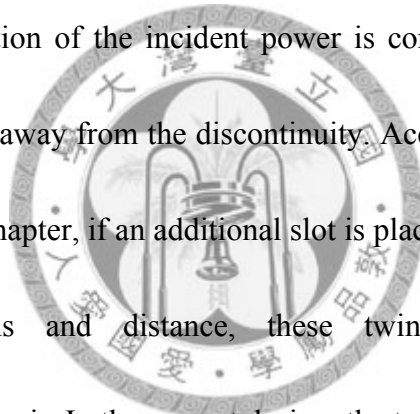
### 2.3.1 INTRODUCTION

Slot antennas fed by the conductor-backed coplanar waveguide (CBCPW) are created when there is a conducting plane, either intentionally or accidentally, lying beneath the coplanar waveguide (CPW) and the slot antenna. The conductor-backed coplanar waveguides and the conductor-backed slots are both leaky structures due to the incursion of the parallel-plate mode leakage [27]. Therefore the CBCPW-fed slot antennas usually radiate inefficiently. On the other hand, the E-plane radiation patterns of slot antennas [109], [110], similar to microstrip patches [111], usually suffer from the space-wave and surface-wave diffractions of the finite ground plane, resulting in ripples, dips, and distortions in the radiation patterns. While the problem of pattern distortion of microstrip patch antennas had been tackled in several papers [112] – [114], little had been reported for slot antennas. In this section, we propose a novel finite ground slot dipole antenna fed by the CBCPW, derived from the prototype of the CBCPW-fed coupled twin slots discussed in the first section of this chapter. By merging the finite ground diffractions with the radiating slot, the gain of the originally leaky CBCPW-fed slot dipole is increased and the radiation pattern is much smoother. The overall antenna

size is also reduced.

### 2.3.2 ANTENNA OPERATION

The antenna structure and the photograph are shown in Fig. 2.14. The gray and white areas represent the metal plates and the dielectric substrate, respectively. At the discontinuity where the CBCPW feed line meets the slot dipole (characterized by the size  $L_s \times W_s$ ), a great portion of the incident power is converted to the parallel-plate mode propagating radially away from the discontinuity. According to the investigations in the first section of this chapter, if an additional slot is placed in front of the slot dipole with suitable dimensions and distance, these twin elements will form a radiation-efficient coupled pair. In the current design, the top ground plane on which the slots are etched is truncated at the position of the additional slot such that it is replaced by the fringing field at the edge. The dielectric substrate and the bottom ground plane protrude a little for better impedance matching. The advantages the proposed structure offers are twofold. First the performance is similar to its prototype in the first section of this chapter but the current design occupies a smaller area. Second, the influence of the finite ground diffractions are overwhelmed by the fringing field radiations at the ground edge, as will be evident in the following figures that, compared to the conventional slot



antennas, the smoothness of the radiation patterns is improved and the ripple levels are much reduced.

### 2.3.3 SIMULATION AND MEASUREMENT

The antenna is designed and fabricated on the FR4 substrate with height  $h = 1.6$  mm,  $\epsilon_r = 4.35$ , and loss tangent  $\tan\delta = 0.02$ . The strip and slot widths of the 50- $\Omega$  CBCPW are  $S = 2.5$  mm and  $G = 0.8$  mm, respectively. The distance from the slot dipole to the ground edge is  $d = 15.5$  mm, which corresponds to about half a guided wavelength of the parallel-plate mode at the design frequency of 5 GHz. Remaining parameters are as follows:  $L_f = 16.5$  mm,  $L_s = 60.5$  mm,  $W_s = 2$  mm,  $L_g = 82$  mm, and  $W_g = 42.5$  mm. *Ansoft* HFSS was used as the simulation tool.

The measured and simulated input return losses are shown in Fig. 2.15. The measured 10-dB return loss bandwidth is 8.6 %, extending from 4.74 GHz to 5.17 GHz. The measured results agree well with the simulated ones. The E- and H-plane radiation patterns at 5 GHz are plotted in Figs. 2.16 (a) and (b), respectively. The antenna gain at this frequency is measured to be 6.4 dBi. The E-plane co-polarization patterns at 4.8, 4.9, and 5.1 GHz are also plotted in Fig. 2.17. Note that the off-broadside main beams in some of these patterns are due to the frequency scanning property rather than the

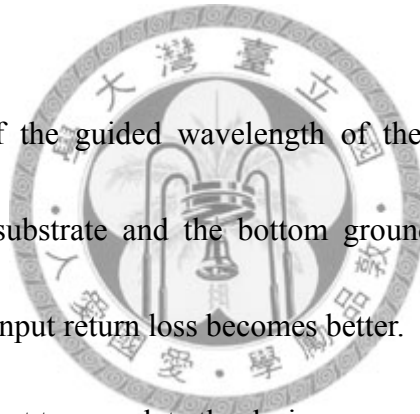


distortions caused by ground diffractions. The patterns are seen to be much smoother than those of conventional slot antennas. This indicates that the influence of the finite ground diffractions is indeed alleviated.

### 2.3.4 DESIGN PROCEDURE

The design procedure can be summarized as follows.

1. Choose  $L_s \doteq \lambda$ .
2. For  $d$  being about half the guided wavelength of the parallel-plate TEM mode, protrude the dielectric substrate and the bottom ground plane a little beyond the truncation such that the input return loss becomes better.
3. Fine-tune  $L_g$  as a last resort to complete the design.



### 2.3.5 SUMMARY

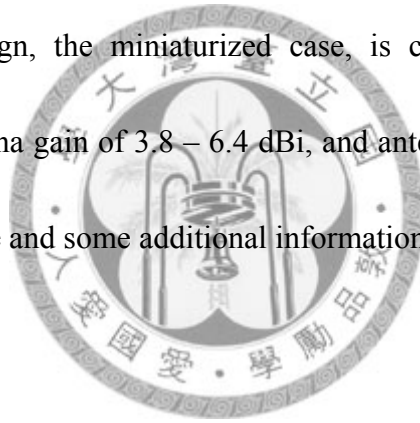
A novel CBCPW-fed finite ground slot dipole antenna has been proposed. Using the fringing fields at one of the ground edge, the proposed antenna has been shown to provide improved gains and smoother patterns over the conventional CBCPW-fed slot antennas. This antenna is well-suited for applications of slot antennas requiring

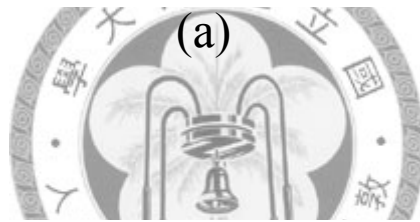
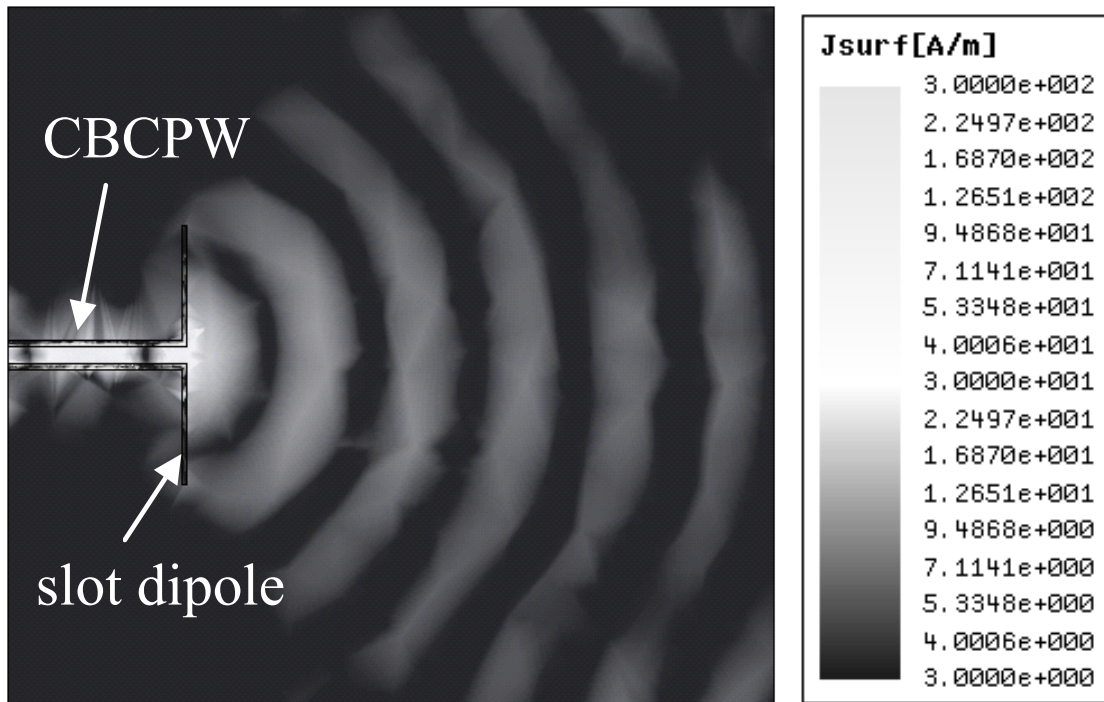
compactness and unidirectional radiation with back conducting planes.



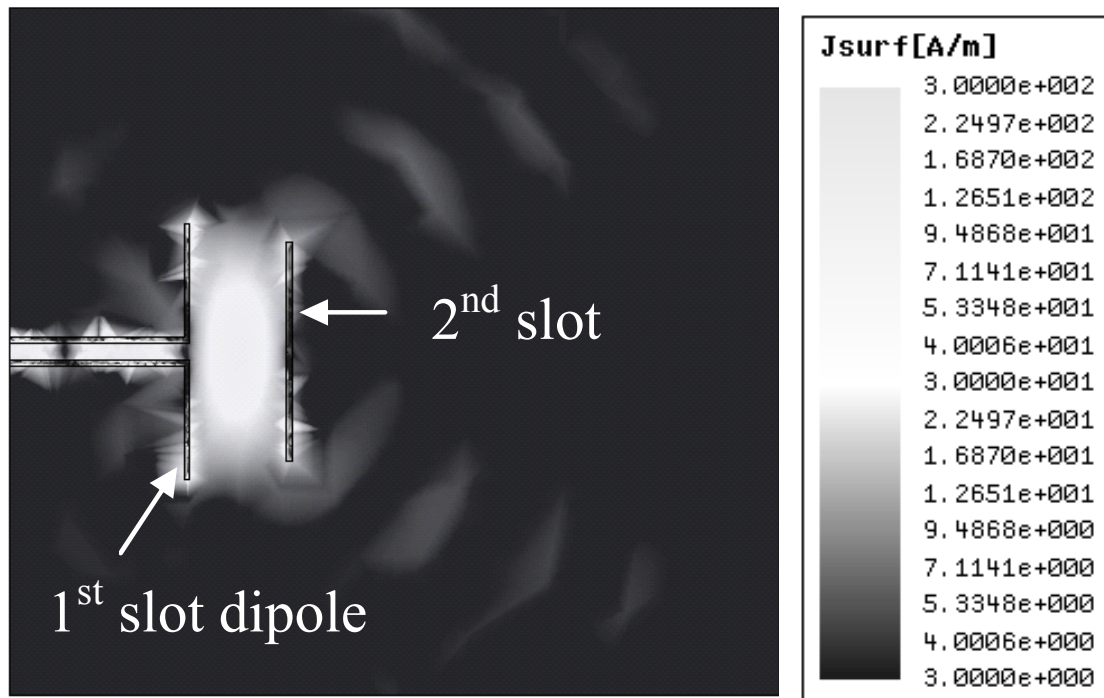
## 2.4 COMPARISON

Three versions of the coupled twin slots fed by the CBCPW have been proposed in this chapter. The first design, the straight slot case, features impedance bandwidth of 5 %, antenna gain of 4.92 – 6.37 dBi, and antenna efficiency of 69.8 % at the center frequency. The second design, the arc-slot case, has impedance bandwidth of 7.2 %, antenna gain of 0.55 – 3.40 dBi, and antenna efficiency of 50.6 % at the center frequency. The final design, the miniaturized case, is characterized by impedance bandwidth of 8.6 %, antenna gain of 3.8 – 6.4 dBi, and antenna efficiency of 84.4 % at the center frequency. These and some additional information are summarized in Table I.





(a)



(b)

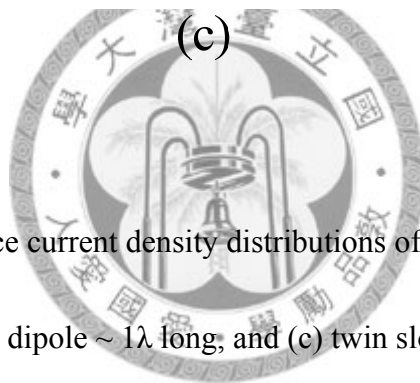
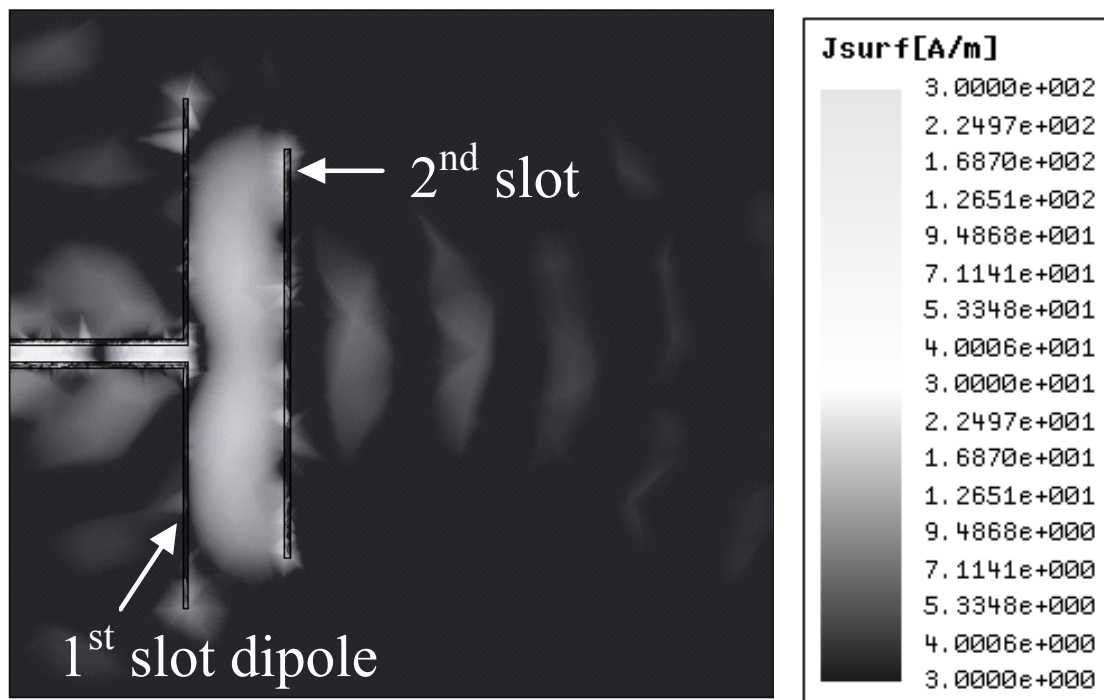


Fig. 2. 1 Simulated surface current density distributions of (a) a single slot dipole, (b) twin slots with the first slot dipole  $\sim 1\lambda$  long, and (c) twin slots with the first slot dipole  $\sim 2\lambda$  long. All cases are fed by the CBCPW with the same dimension.

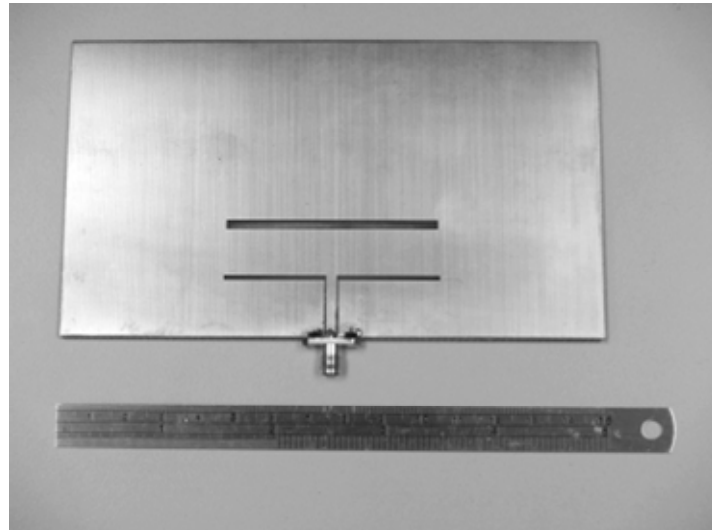
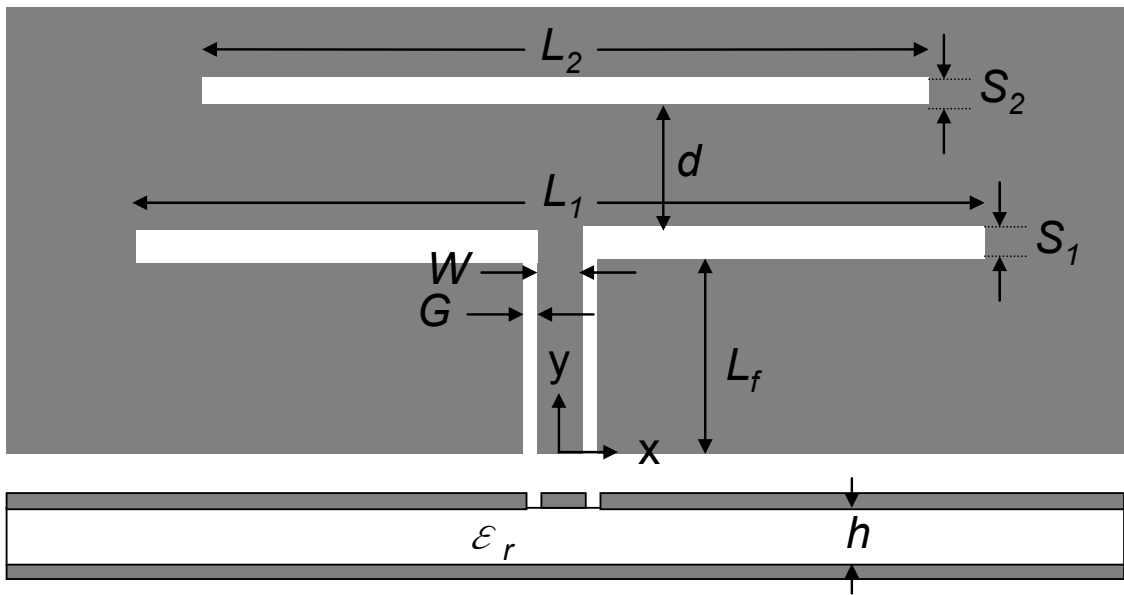


Fig. 2. 2 Geometry and photograph of the proposed CBCPW-fed slot dipole coupled with a straight slot.

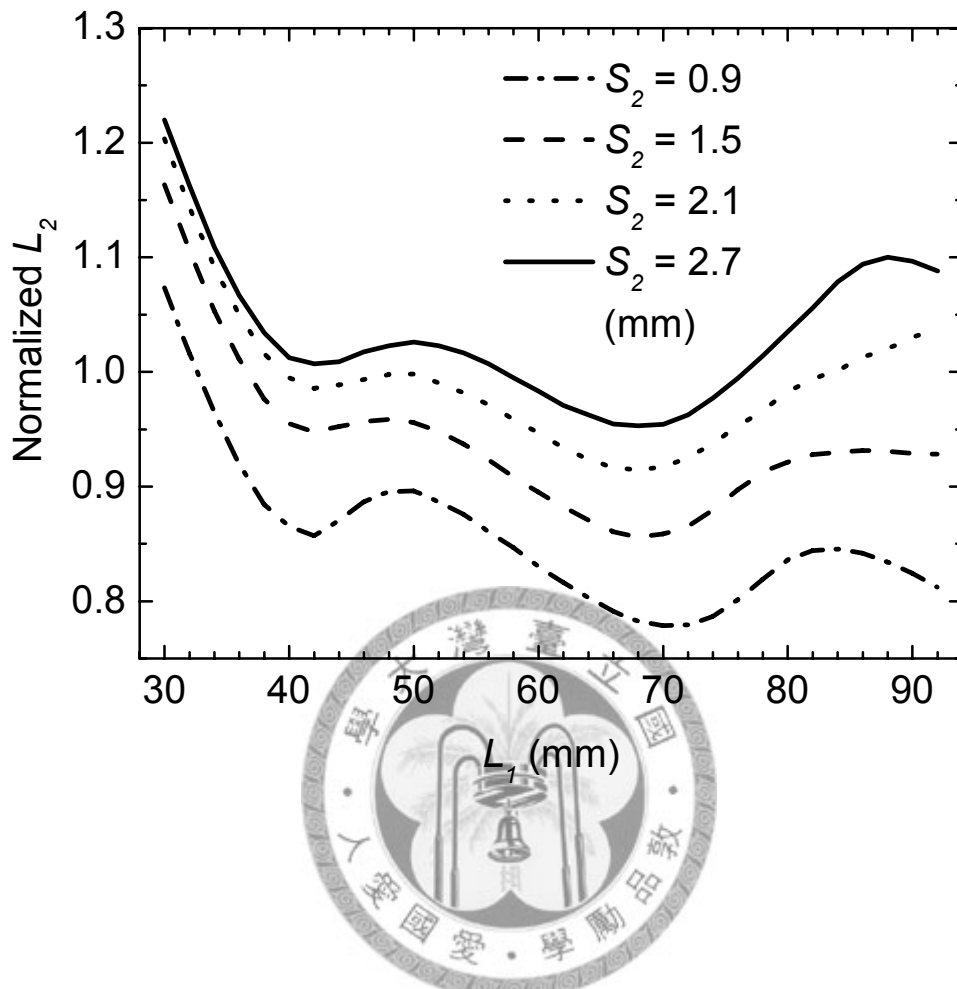
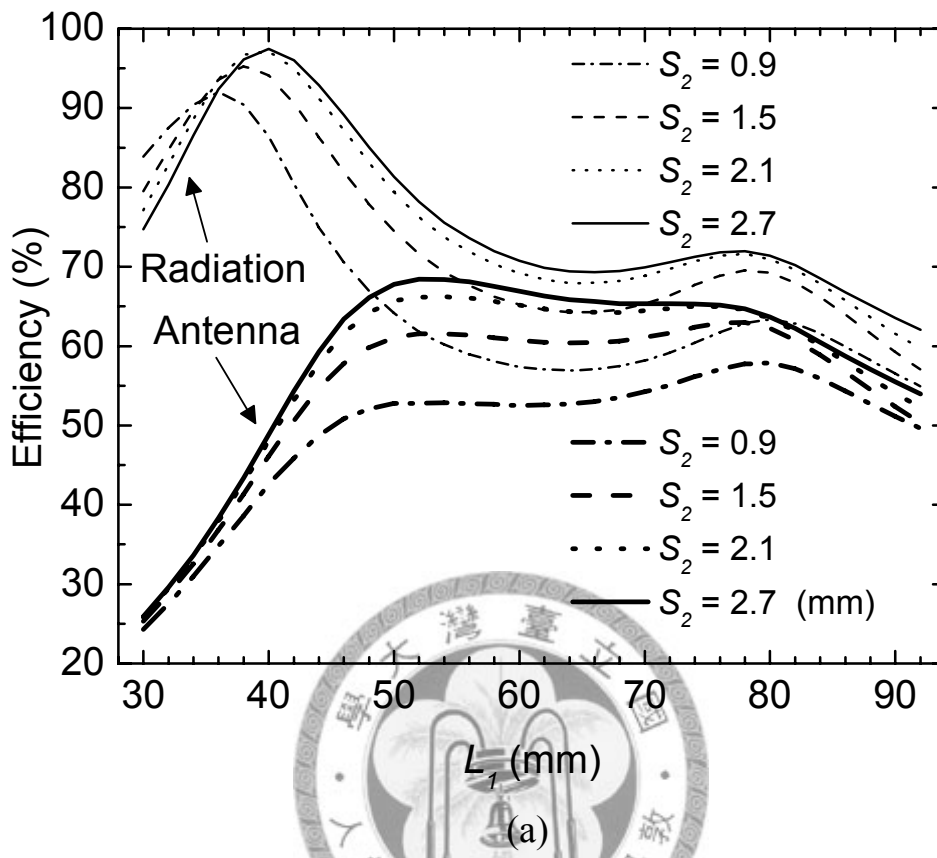


Fig. 2. 3 Simulated results for normalized  $L_2$  versus  $L_1$  with a broadside main beam at 5 GHz.  $S_1 = 1.5$  mm,  $L_f = 15$  mm,  $d = 13.1$  mm,  $W = 2.5$  mm,  $G = 0.8$  mm,  $h = 1.6$  mm,  $\epsilon_r = 4.2$ , and  $\tan\delta = 0.02$ .





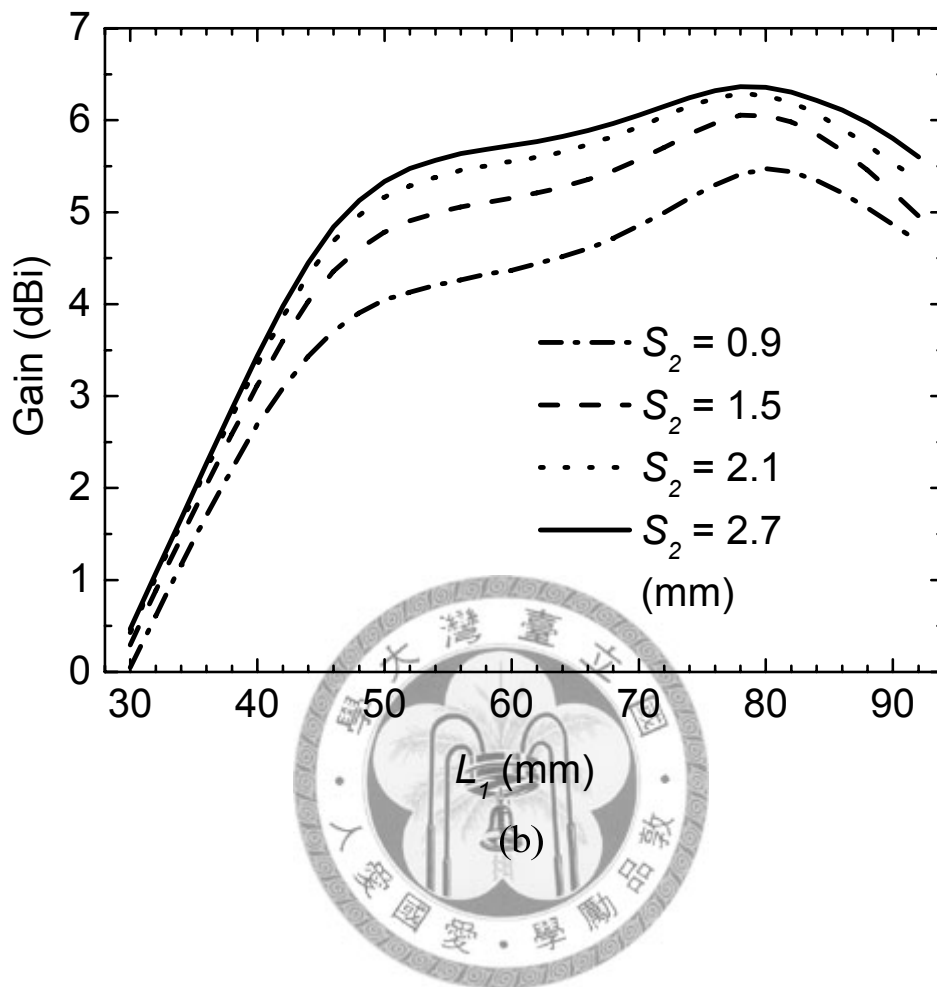


Fig. 2. 4 Simulated (a) radiation and antenna efficiencies and (b) antenna gain versus  $L_1$  at 5 GHz.  $S_1 = 1.5$  mm,  $L_f = 15$  mm,  $d = 13.1$  mm,  $W = 2.5$  mm,  $G = 0.8$  mm,  $h = 1.6$  mm,  $\epsilon_r = 4.2$ , and  $\tan\delta = 0.02$ .

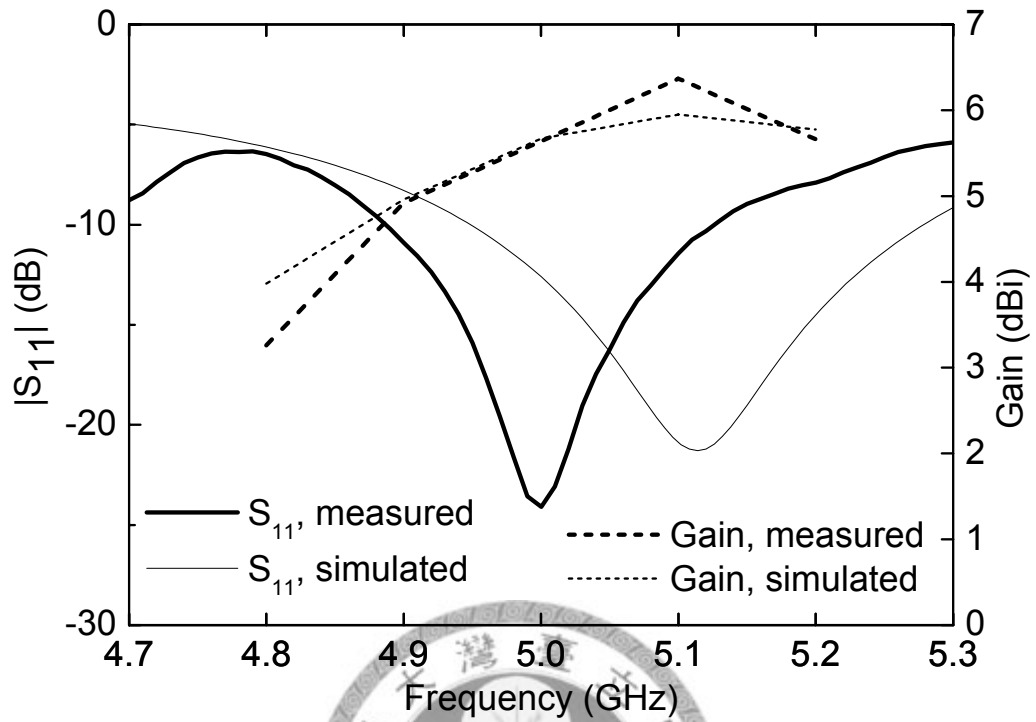
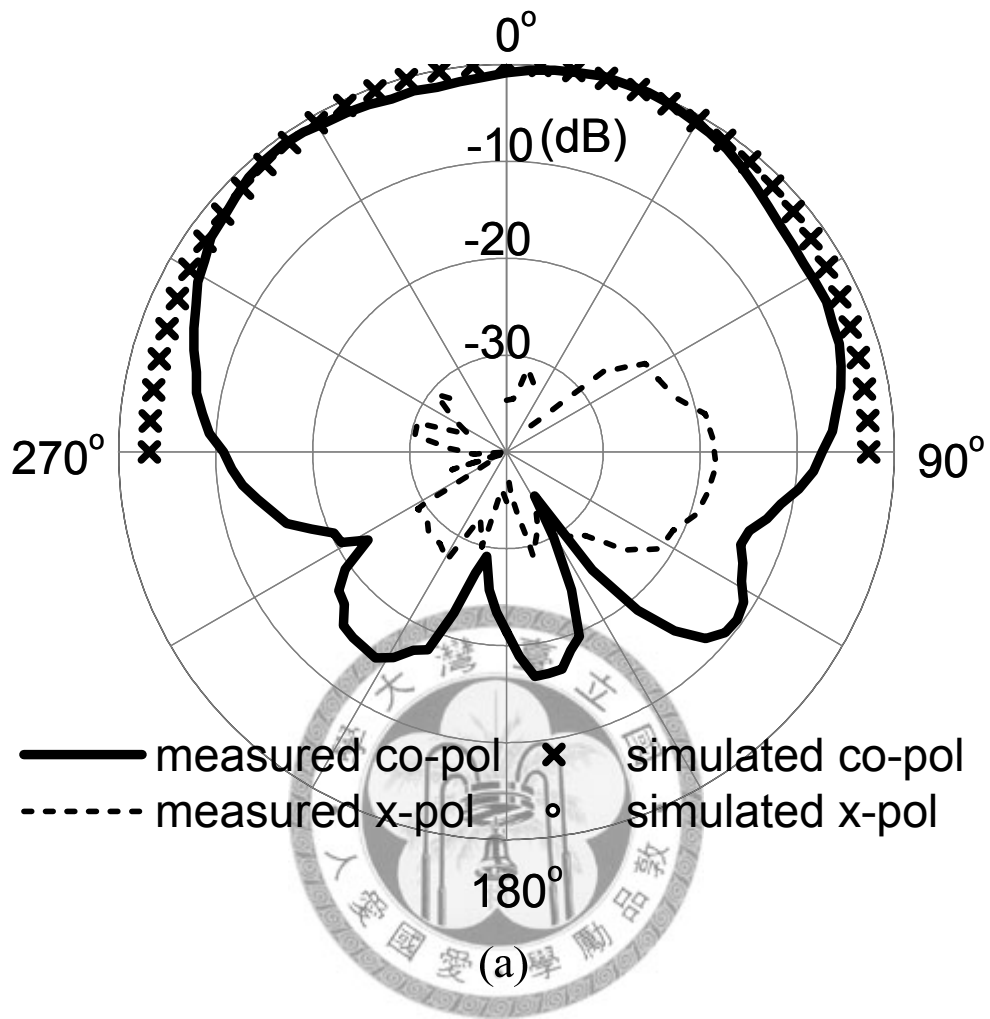


Fig. 2. 5 Simulated and measured input return losses and gains of the proposed antenna with  $L_1 = 60$  mm,  $L_2 = 59$  mm,  $S_1 = 1.5$  mm,  $S_2 = 2.7$  mm,  $d = 13.1$  mm,  $L_f = 15$  mm,  $W = 2.5$  mm,  $G = 0.8$  mm,  $h = 1.6$  mm,  $\epsilon_r = 4.2$ , and  $\tan\delta = 0.02$ .



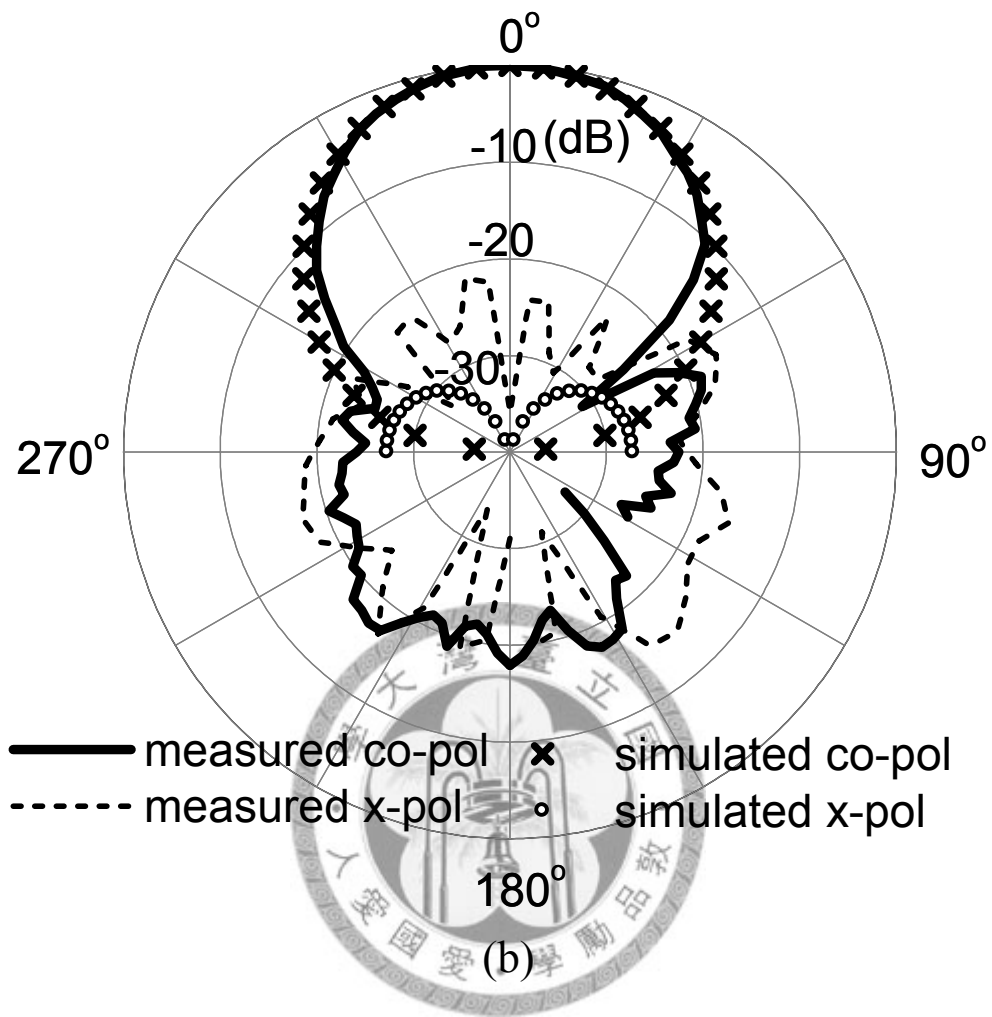
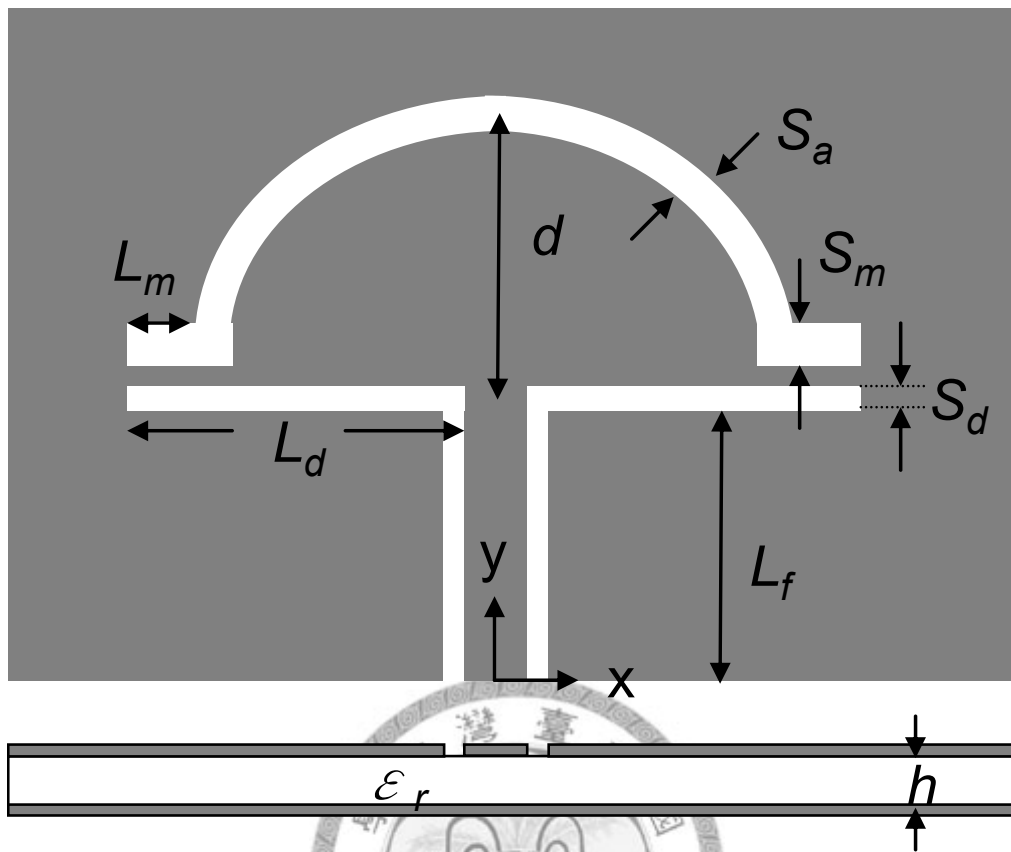
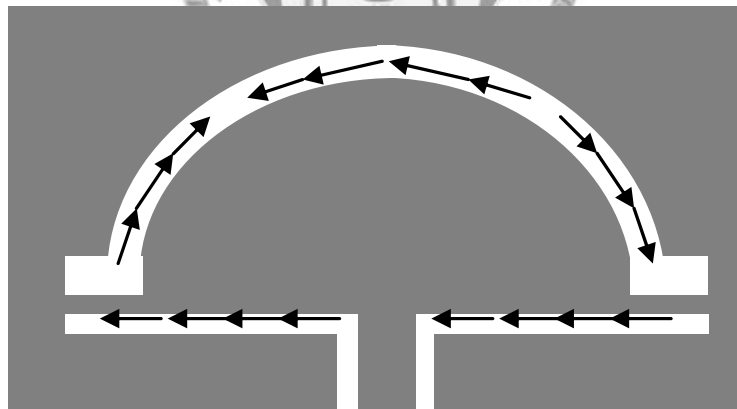


Fig. 2. 6 Simulated and measured radiation patterns of the proposed antenna at 5 GHz.

(a) E-plane (y-z plane). (b) H-plane (x-z plane).



(a)



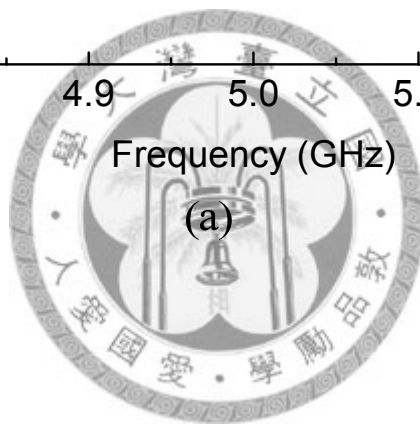
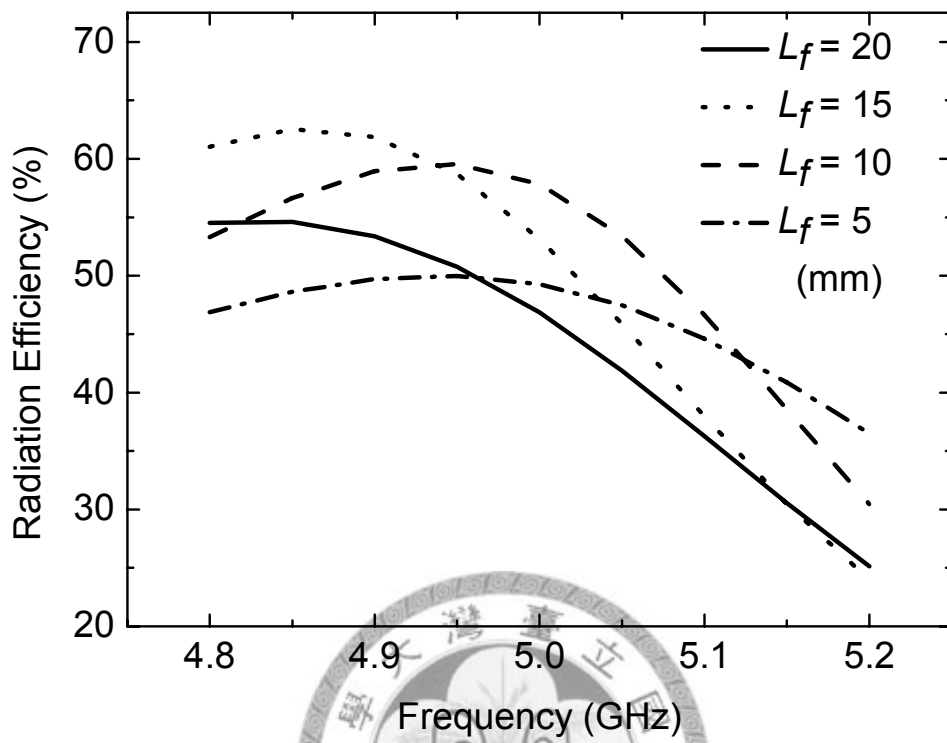
(b)



(c)

Fig. 2. 7 (a) Geometry of the proposed CBCPW-fed slot dipole coupled with an arc-slot. (b) Equivalent magnetic current on the radiating slots. (c) Photograph.





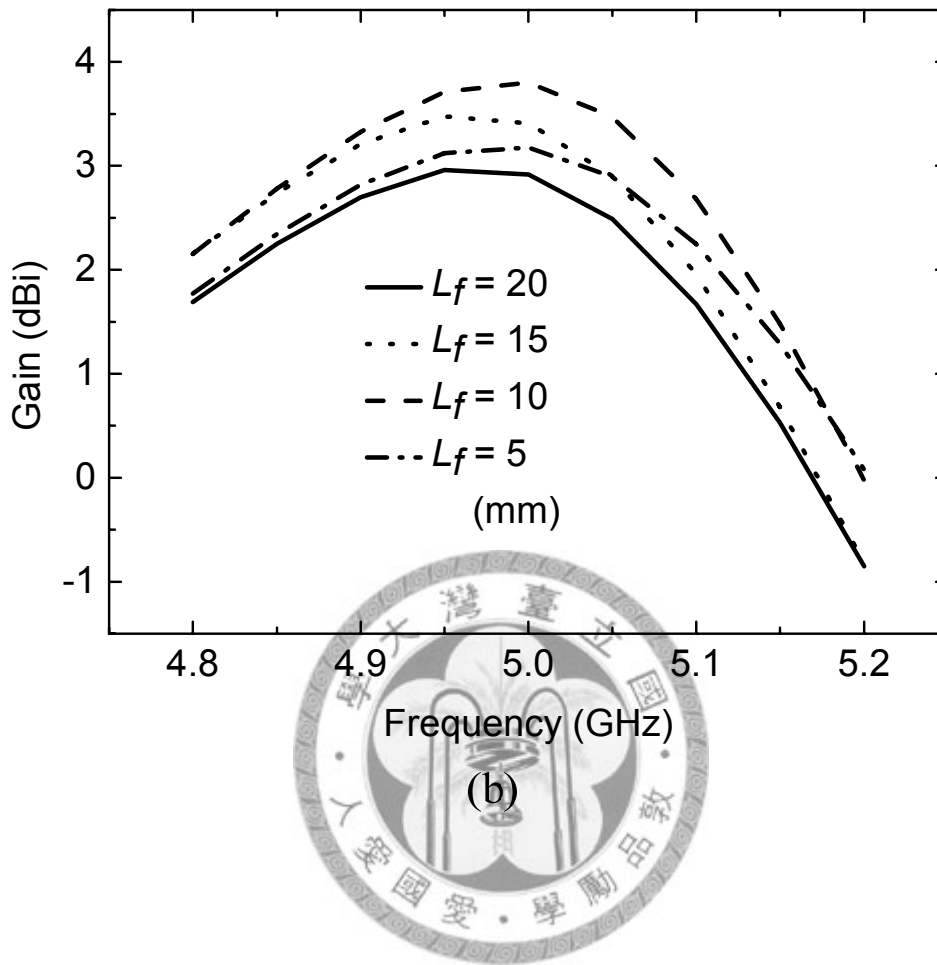


Fig. 2. 8 Simulations of (a) radiation efficiency and (b) antenna gain.  $S_d = 1$  mm,  $S_a = 1.5$  mm,  $S_m = 1$  mm,  $L_d = 18.5$  mm,  $L_m = 4$  mm, and  $d = 15.65$  mm.



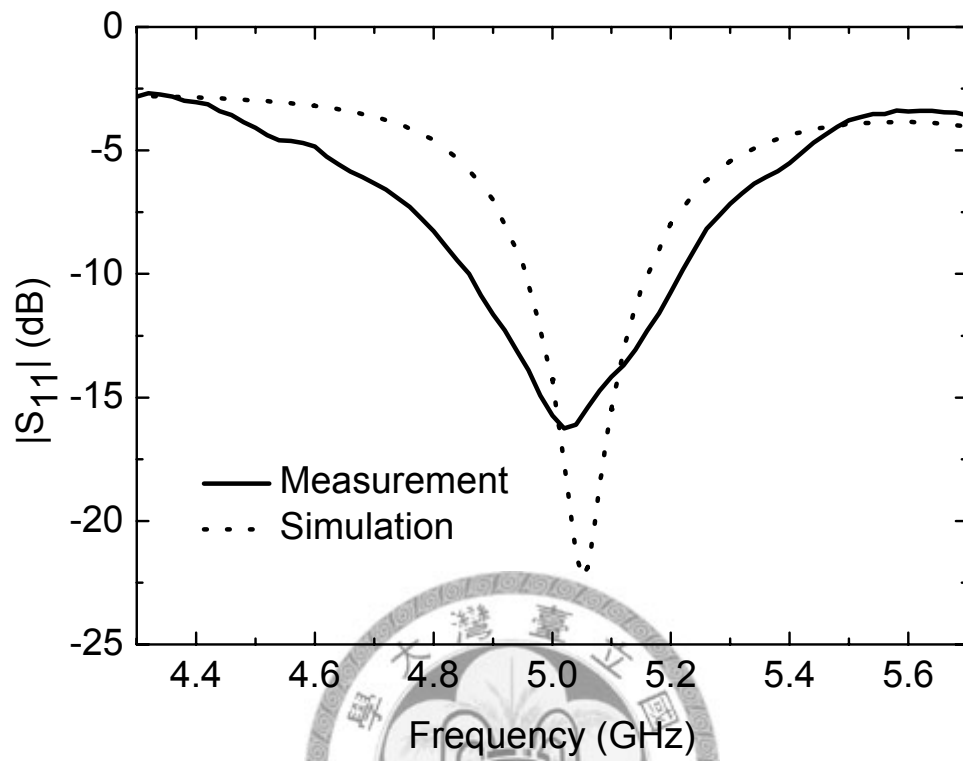


Fig. 2. 9 Simulated and measured input return losses.

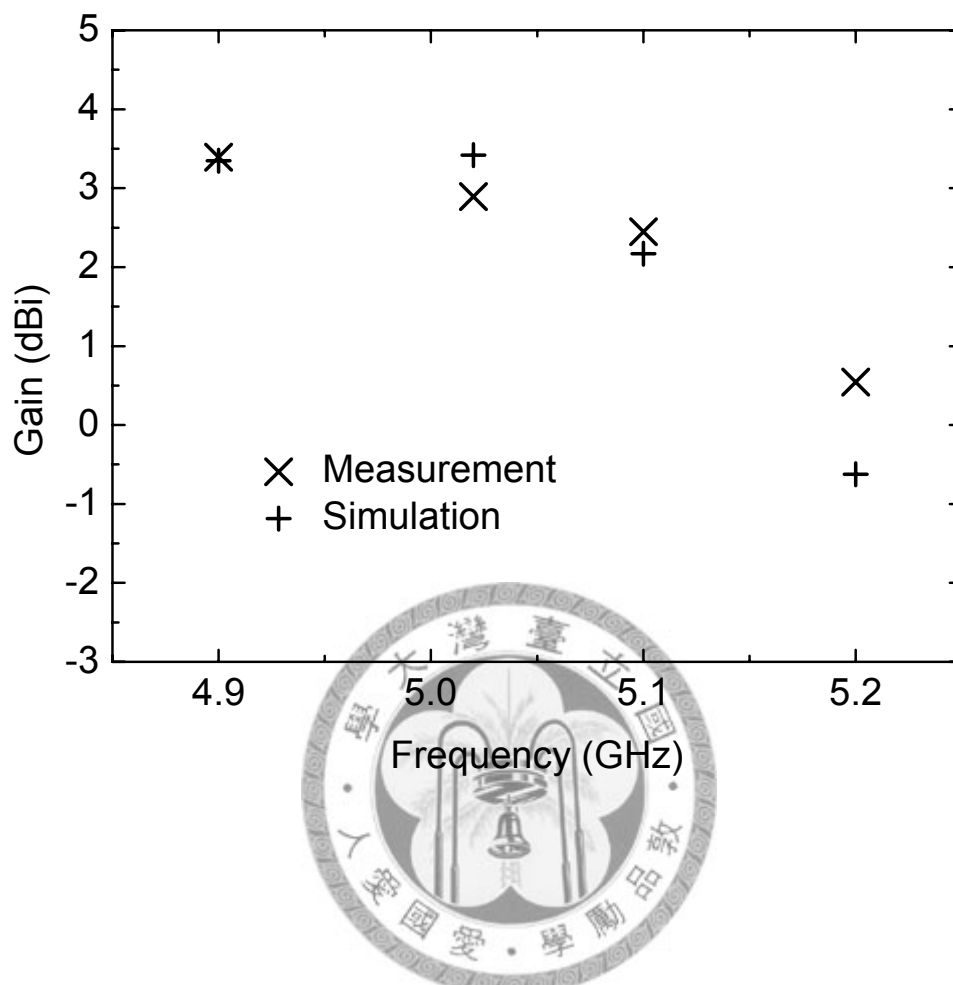
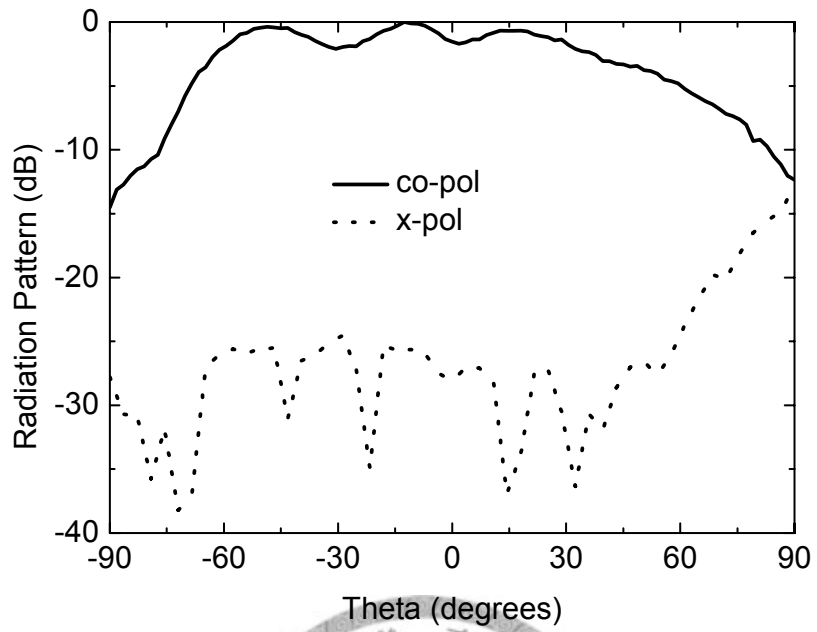
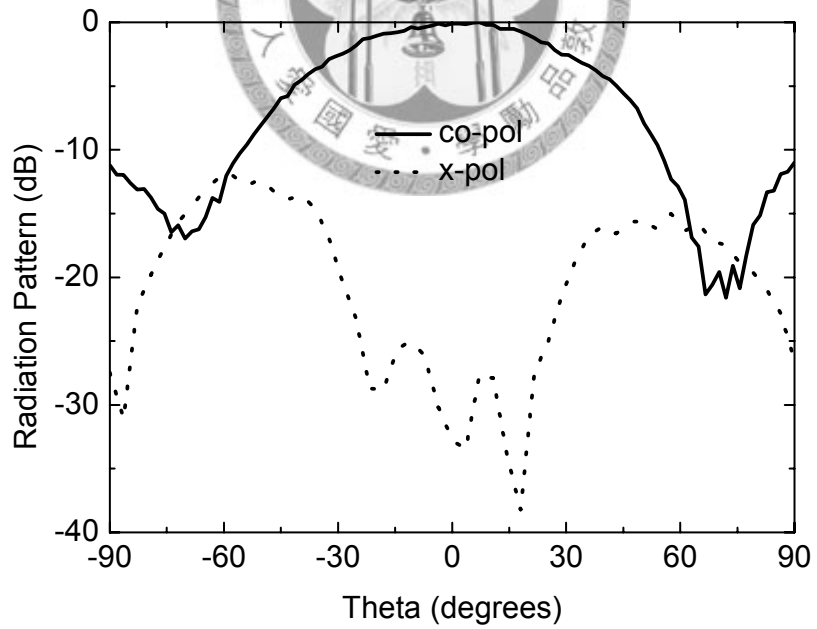


Fig. 2. 10 Simulated and measured antenna gains.

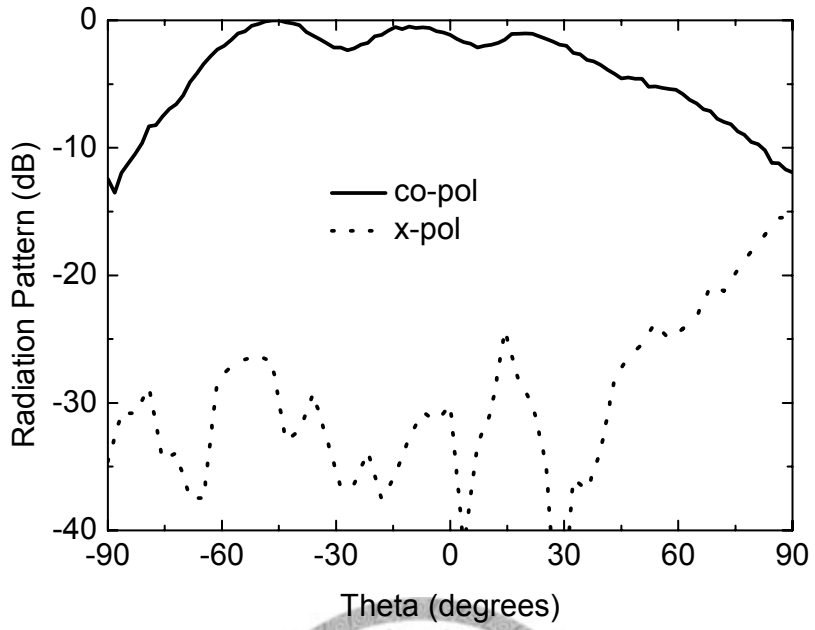


(a)

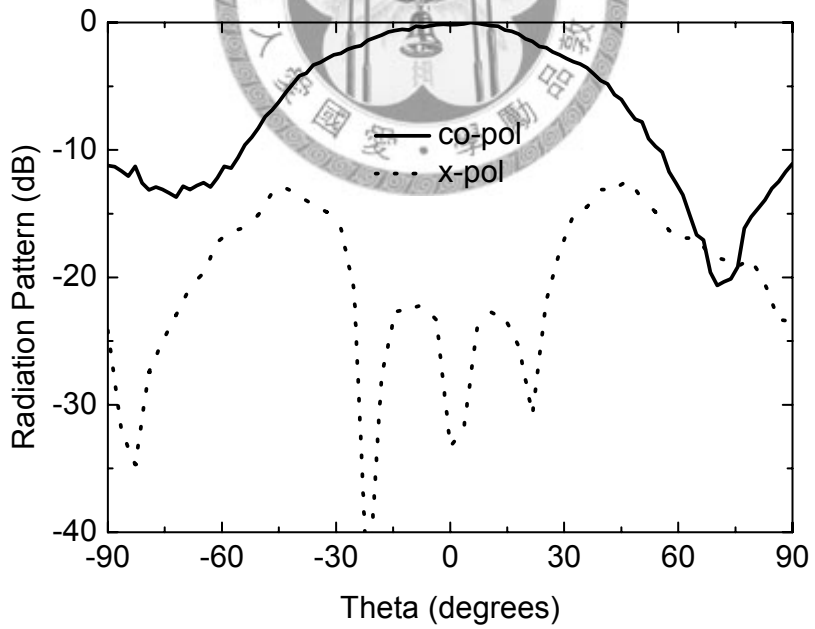


(b)

Fig. 2. 11 Measured radiation patterns at 5.02 GHz. (a) E-plane; (b) H-plane.

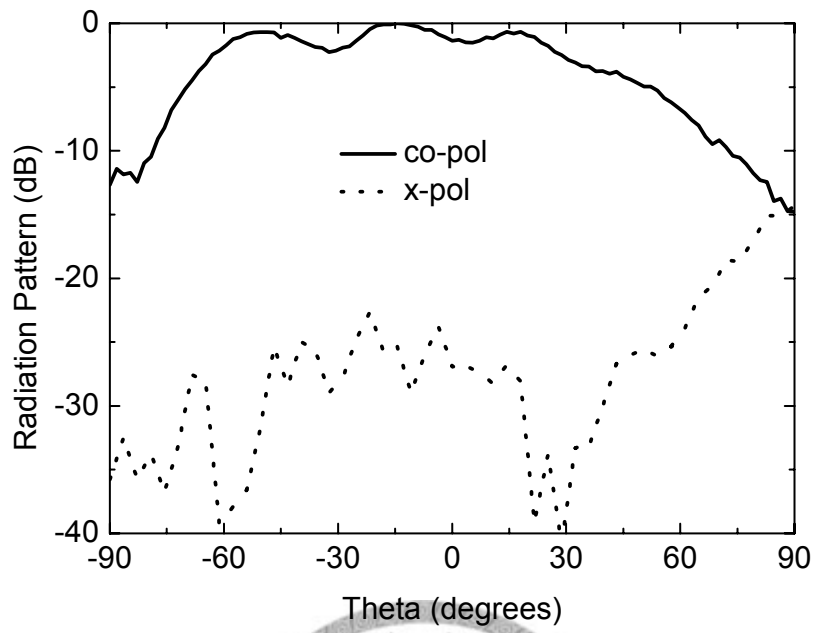


(a)

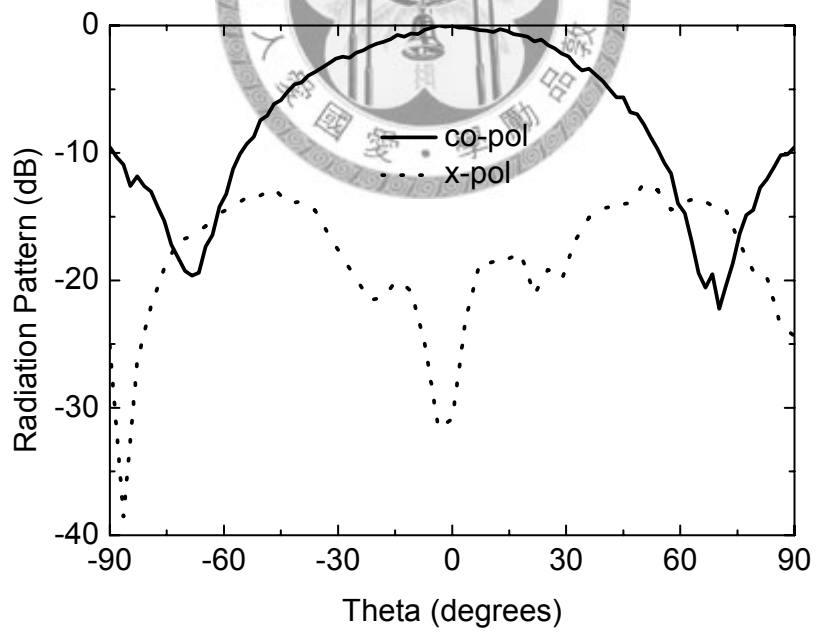


(b)

Fig. 2. 12 Measured radiation patterns at 4.9 GHz. (a) E-plane; (b) H-plane.



(a)



(b)

Fig. 2. 13 Measured radiation patterns at 5.2 GHz. (a) E-plane; (b) H-plane.

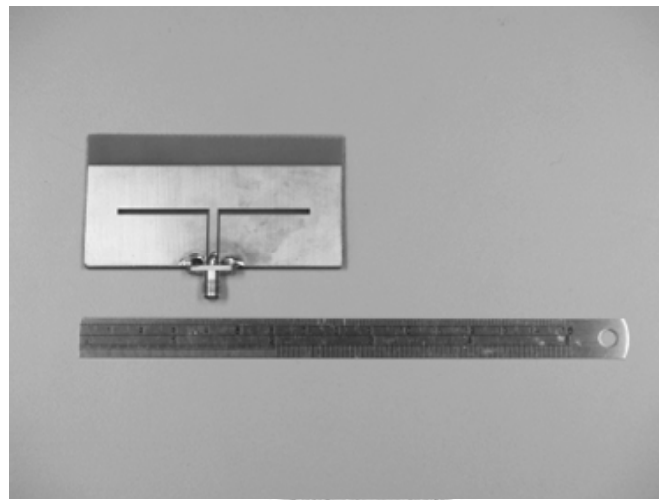
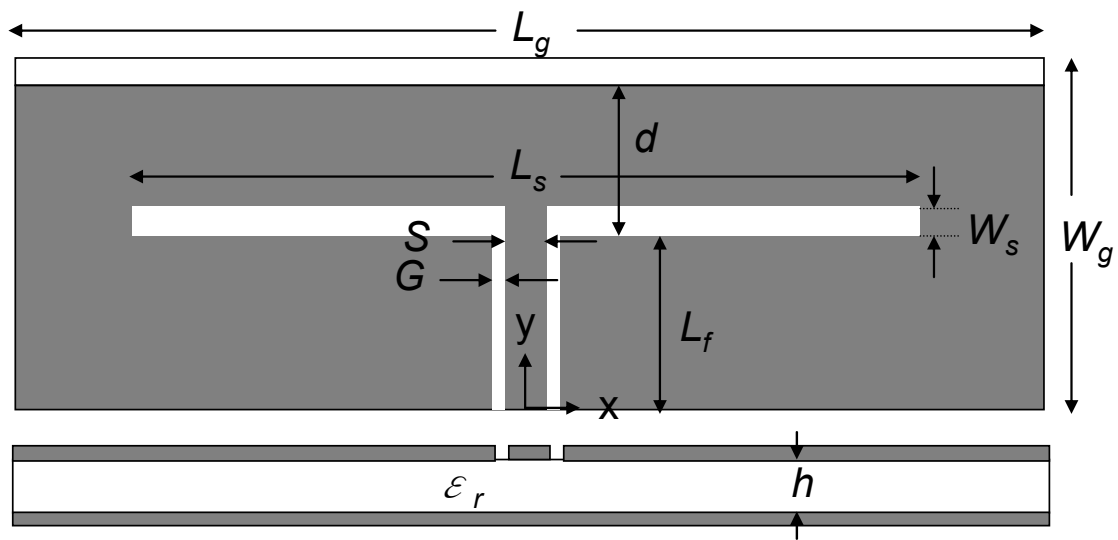


Fig. 2. 14 Geometry and photograph of the proposed CBCPW-fed finite ground slot dipole antenna.

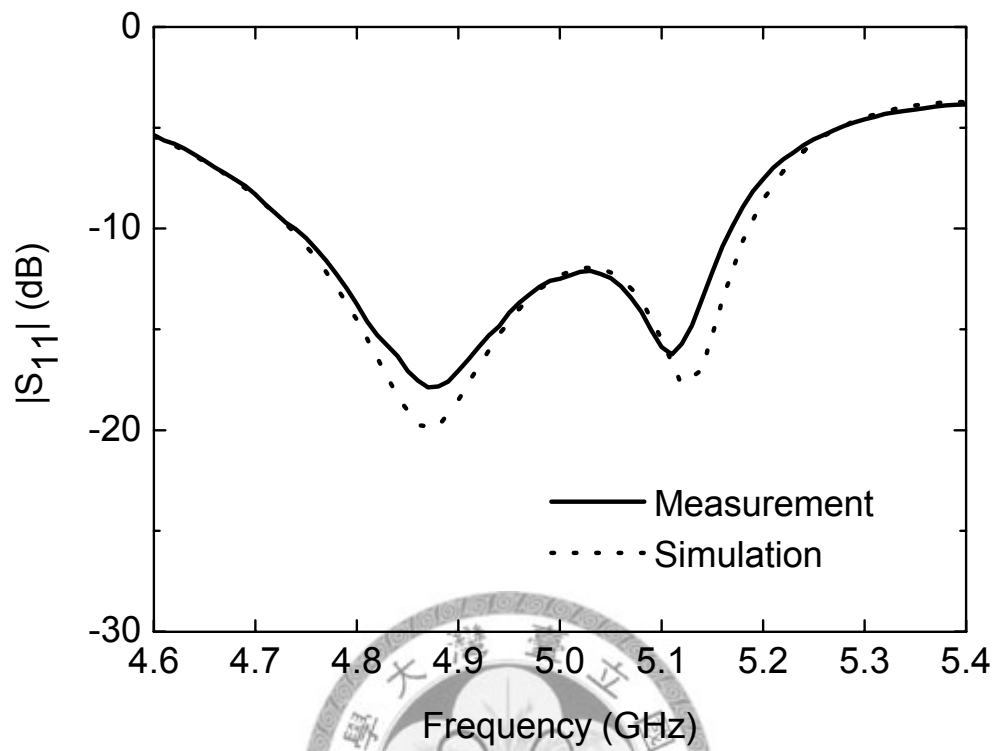


Fig. 2. 15 Measured and simulated input return losses of the proposed antenna.

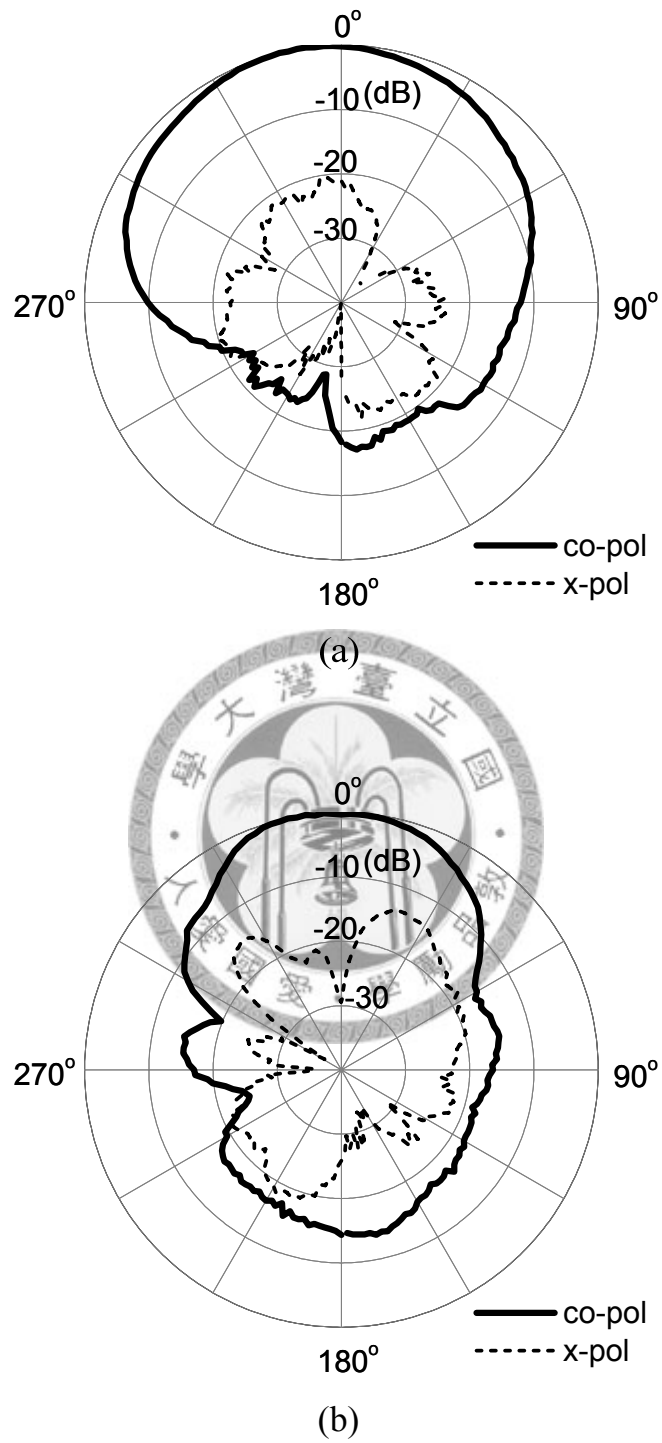
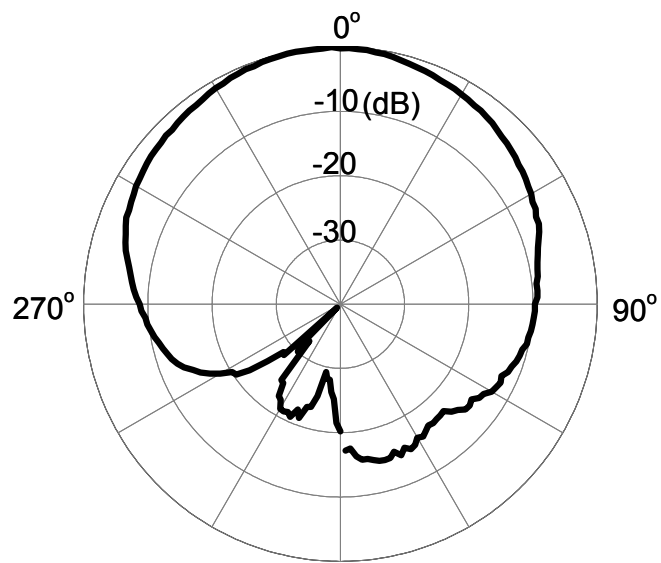


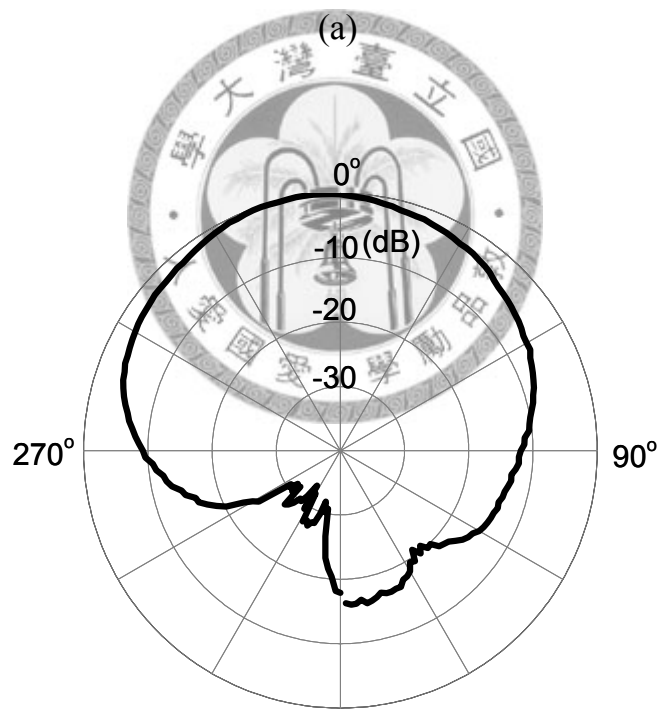
Fig. 2. 16 Normalized measured (a) E-plane and (b) H-plane radiation patterns at 5.0 GHz.





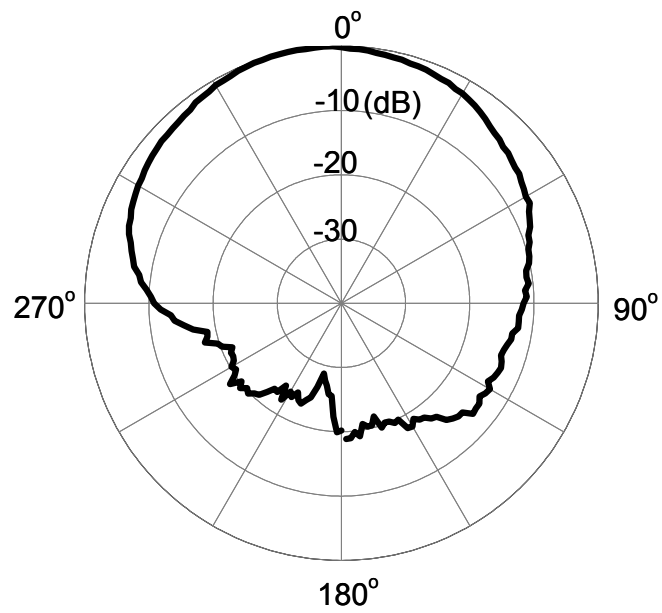
180°

(a)



180°

(b)



(c)

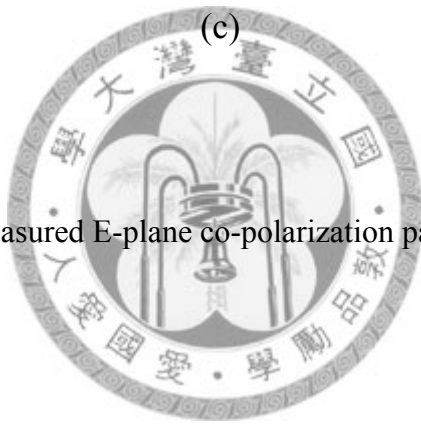


Fig. 2. 17 Normalized measured E-plane co-polarization patterns at (a) 4.8 GHz, (b) 4.9 GHz, and (c) 5.1 GHz.

TABLE I  
SUMMARY OF THE MEASUREMENT RESULTS OF THE THREE DESIGNS OF THE COUPLED  
TWIN SLOTS

	Straight slot case	Arc-slot case	Miniaturized case
Center frequency (GHz)	5.00	5.02	5.00
10-dB return loss bandwidth (%)	5	7.2	8.6
In-band peak gains (dBi)	4.92 – 6.37	0.55 – 3.40	3.8 – 6.4
Peak gain at the center frequency (dBi)	5.64	2.89	6.40 <sup>*2</sup>
Antenna efficiency at the center frequency (%)	69.8	50.6	84.4 <sup>*2</sup>
Total area of antenna plus ground plane <sup>*1</sup> (width * length, mm)	150 * 86	150 * 104	82 * 42.5

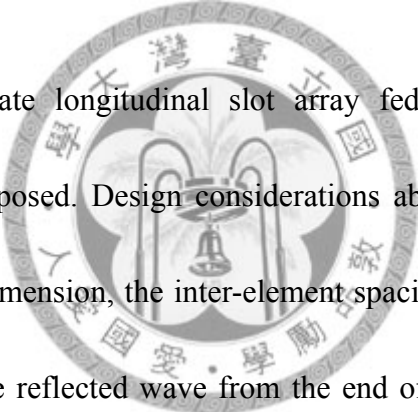
※1: In the first and the second cases, the ground plane size may be adjusted if needed, whereas in the third case, the listed value delivers the optimum performance.

※2: The anechoic chamber at NTU Electromagnet Wave Group had been rebuilt during the summer of 2007, which was before the experiments of the miniaturized case were undertaken. Hence while the first two cases were measured in the old chamber, the third case was measured in the new one. From the author's experience, the measured gain data of a same test piece in the old and the new chambers sometimes show variations of several decibels. So it is reasonable to assume there is some level of inaccuracy when directly comparing the gain and efficiency data of the first two cases to those of the third case.

# Chapter 3

## Parallel-Plate Slot Array Fed by Conductor-Backed Coplanar Waveguide

### 3.1 THE LONGITUDINAL CASE



The novel parallel-plate longitudinal slot array fed by the conductor-backed coplanar waveguide is proposed. Design considerations about the choices of the slot orientation, the feed-line dimension, the inter-element spacing, and the slot dimensions are explained in detail. The reflected wave from the end of the feed-line is also taken into consideration to compensate for the power tapering along the radiating apertures. To further increase the efficiency, additional columns of slots are needed to intercept more power for radiation. A 5 x 6 and two 5 x 2 arrays with and without the feed-line termination are fabricated and tested. The measured and simulated results agree well and thus verify the design concepts. The proposed design has a broadside unidirectional pattern and is capable of frequency-scanning in the H-plane.

### 3.1.1 INTRODUCTION

The coplanar waveguide (CPW) is an attractive feeding structure for planar printed antennas due to its uniplanar structure, low radiation loss, low dispersion, ease of fabrication, and the ability of being easily integrated with active and passive devices without the need of via holes [2]. In practical situations, however, there are often conducting planes backing the substrate to improve the mechanical strength and the heat-sinking capability. This turns the structure into the leaky conductor-backed coplanar waveguide (CBCPW). The originally bound CPW mode now leaks power in the form of the parallel-plate mode supported by the top and bottom conducting planes and along a particular angle relative to the main CPW line [75]. This phenomenon occurs at all frequencies and the CBCPW-fed antennas are hence inefficient radiators.

In this and the next sections, we propose a new type of slot array antenna based on the CBCPW structure that uses the parallel-plate mode leakage to radiate through the slot array etched on both sides of the ground plane of the CPW feed-line. The geometry is relatively simple and single-layered. The array design is flexible to achieve required radiation patterns. Besides, large array designs can easily be done without input-matching problems.

Compared to the transverse slot array that will be presented in the next section, the

performance of the longitudinal array in this section is further improved by addressing two additional problems that are not considered. First, the end reflection of the feed-line, which is crucial to the input return loss in small array designs, is taken into account. Second, the transverse slots are replaced by longitudinal ones for efficiency consideration. This is because when the slots are in the transverse direction and a broadside main beam is required, the inter-element spacing of the slots in the longitudinal direction will be close to a guided wavelength of the dominant parallel-plate mode. This, along with the in-phase excitations of the slots, performs exactly the opposite of the phase cancellation technique. The power leaked into the dielectric region is enhanced and therefore the efficiency as well as the pattern deteriorates. On the other hand, when the slots are placed longitudinally, the above dilemma no longer exists. The control of the main beam position and the placement of the additional columns of longitudinal slots for efficiency improvement can now be separated into designs in the longitudinal and transverse directions, respectively.

### **3.1.2 ANTENNA STRUCTURE**

The structure of the proposed antenna is shown in Fig. 3.1. The gray area represents the metal whereas the white ones are the etched slots and the feed-line. Only

one layer of dielectric substrate is used. As soon as the wave is launched at the input, it travels down the CBCPW and at the same time leaks power to the side ground planes and excites the nearby slots. The angle  $\theta_l$  between the directions of the leakage power and the CBCPW line, as shown in Fig. 3.2, is similar to that of the conductor-backed slot line [27], and can be expressed as

$$\theta_l = \cos^{-1} \frac{\beta_{CBCPW}}{\beta_{pp}}, \quad (3-1)$$

where  $\beta_{CBCPW}$  is the propagation constant of the dominant propagating mode of the CBCPW and  $\beta_{pp}$  is that of the parallel-plate TEM mode. At the end of the transmission line the wave reflects back if the line is not terminated. The backward traveling wave obeys the same mechanism as the forward one, with the slots excited in the reverse order. The dimensions of the CBCPW ( $S$  and  $G$ ) determine the leakage rate of the feed-line. The separation between the slots and the CBCPW ( $d_s$ ), and the slot length ( $l_s$ ) and width ( $w_s$ ) can be varied to control the amount of the radiated power from each slot. The parameter  $d$ , which represents the offset along the  $y$ -axis between the corresponding slots on the right- and left-hand sides of the CBCPW, will be adjusted to achieve the in-phase excitations of both sides of the slots. The distance between adjacent slots in the  $y$ -direction ( $d_y$ ) affects the relative phases of the excitations of the slots. The distance between the neighboring  $m^{\text{th}}$  and  $n^{\text{th}}$  columns of slots in the transverse direction,  $d_{xmn}$ , is about half a guided wavelength of the parallel-plate TEM

mode, whereas the offset between the neighboring  $m^{\text{th}}$  and  $n^{\text{th}}$  columns of slots in the longitudinal direction,  $d_{ymn}$ , is tuned to assist in the phase cancellation. If the dimension of the array in the y-direction is large, or if the leakage rate of the CBCPW is high, the reflected wave from the end of the feed-line is negligible and  $d_t$  is somewhat arbitrary. But if the array size is small, or if the leakage rate of the CBCPW is low, the reflected wave contributes to the radiation and  $d_t$  must be carefully chosen accordingly. Moreover, reflections also occur at the periphery of the ground plane. In our design, we use the largest available area of the ground plane (150 mm by 250 mm) to mitigate this effect.

### 3.1.3 ANALYSIS



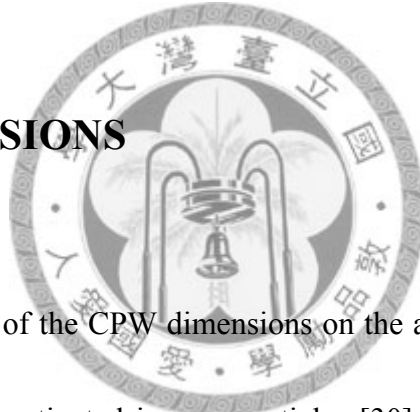
#### A. SLOT ORIENTATION

There are two possible ways to obtain the linearly-polarized radiation. In the next section the first method will be introduced, with the slots placed transverse to the feed-line direction and  $d = 0$ . Both slots in each slot pair that is symmetrical about the y-z plane are excited in-phase. The arrangement resembles the conventional CPW-fed slot array but with the radiating slots detached from the central CPW. Linear polarization can also be achieved by placing the slots in the longitudinal direction of the



feed-line, as Fig. 3.1 shows. In this case, for in-phase excitation of each slot pair formed by a slot on the right-hand side and its corresponding one on the left-hand side of the CBCPW,  $d$  should be changed to half of a guided wavelength of the dominant CBCPW mode to compensate for the out-of-phase leakage from different slotline of the CBCPW such that A and A' or B and B' in Fig. 3.2 are in-phase. The polarization differs by  $90^\circ$  from that in the transverse slot case. In this section, we shall concentrate on the second method, that is, the longitudinal slot arrays.

## B. CPW DIMENSIONS



Although the impacts of the CPW dimensions on the attenuation characteristics of the CBCPW have been investigated in many articles [30], [115], this is the first time that the effects on the array synthesis are presented. For this purpose, we first define the normalized leakage power in terms of the S-parameters:

$$P_L = 1 - |S_{11}|^2 - |S_{21}|^2 \quad (3-2)$$

The normalized leakage power for various combinations of the length and width of the transmission line is calculated at 5.5 GHz. The characteristic impedance of the CBCPW is fixed at  $50 \Omega$  in each case. The simulation setup is based on the FR4 substrate with dielectric constant  $\epsilon_r = 4.3$ , thickness  $h = 1.6$  mm, and loss tangent  $\tan\delta = 0.02$ . The

simulation is carried out using the package software IE3D v.10.0 from *Zeland*. The results are shown in Fig. 3.3(a). Next we use the data in Fig. 3.3(a) to calculate the normalized power leaked from each section (10-mm long) of the leaky transmission line. Since  $S_{11}$  is relatively small compared to  $S_{21}$ , the power to be found is approximated by the difference between each adjacent point along a curve in Fig. 3.3(a). Fig. 3.3(b) plots the results.

From Fig. 3.3(a) we can see that for a fixed characteristic impedance, the wider the central strip width of the line is, the larger the leakage rate will be. But how to choose the line configuration depends on the array size. In the next few paragraphs, we will show that the dimensions of the radiating slots can be adjusted to control the radiated power from each slot. But if the ratio of the power impinging on the first and the last pairs is too large, adjustments of the parameters of the slots may not be practical for the uniformly-excited array. Fig. 3.3(b) tells us that although the feed-line with wider strip width has higher leakage rate, if the array size is not small, the power delivered to the last pair of slots will be lower than the one with narrower strip width does. Therefore, depending on the array size, one should choose the suitable line width to deliver enough power to the end elements. On the other hand, although the narrower line has a flatter leakage rate along the line, the residual power at the end of the line is higher than those of the wider ones. Since we will not terminate the line, but instead let the residual power

reflect back and contribute to the radiation again to compensate for the power tapering originally existed on the slots, and since too large of the backward traveling wave will deteriorate the input matching performance, therefore we make a trade-off here and choose the feed-line with  $S = 2.5$  mm.

## C. INTER-ELEMENT SPACING

Fig. 3.2 also illustrates the phase relationship between two adjacent slots in the y-direction and the leakage from the CBCPW. Since  $d_x$  is invariant in our analysis and  $\theta_l$  is also a constant along the entire CBCPW, it is obvious that the distance traversed by the leakage wave between the CBCPW and the radiating slot is the same for each slot. Therefore the phase difference between any two adjacent slots in the y-direction is the distance the dominant CBCPW mode has to travel to cause the leakage that contributes to the corresponding portion of the slots. This is the distance AB or A'B' in Fig. 3.2. As can be seen, AB or A'B' simply equals  $d_y$ . Therefore, in order to achieve a broadside pattern,  $d_y$  is chosen to be close to one guided wavelength of the dominant CBCPW mode such that the field on each slot is in-phase.

## D. SLOT DIMENSIONS

The slot length and the spacing between the CBCPW and the first columns of slots  $d_s$  are adjusted to control the radiated power. We first determine the proper value of  $d_s$ . Please note that although the conductor-backed slots are excited by a propagating wave, the leakage wave from the conductor-backed slots makes the excitation more like a standing wave, so the distance  $d_s$  affects the radiated power. The normalized radiated power, self-normalized to the maximum, of a slot pair versus  $d_s$  at 5.5 GHz is plotted in Fig. 3.4. The slots are found to radiate most strongly when  $d_s$  equals approximately half a guided wavelength of the parallel-plate TEM mode, which is 13.2 mm at 5.5 GHz. Hence we choose  $d_s$  to be 13 mm. To facilitate the design, the slot width is fixed at 2 mm and we calculate the normalized radiated power for different lengths of the slots. Here the normalized radiated power is defined as the radiated power divided by the maximum among the simulation data, i.e. the radiated power of the first slot pair when  $l_s = 24$  mm. We simulate five pairs of slots with  $d_y = 31$  mm, a value slightly less than a guided wavelength of the dominant CBCPW mode at 5.5 GHz due to the slot coupling. The slots are simulated with one pair present at a time and the CBCPW is treated as a two-port device. The obtained data are thus the isolated radiated power due to the leakage from the forward traveling wave only. Fig. 3.5 plots these results. As can be seen, the slots radiate most strongly when the slot length is about 23 mm or 24 mm. We

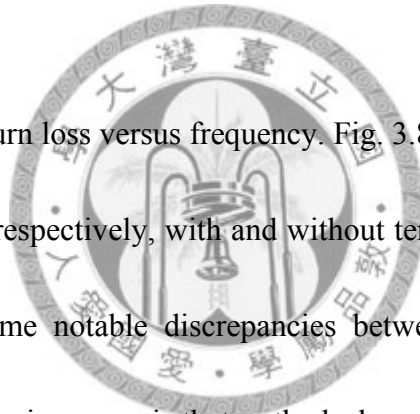
choose 23 mm for all of the slots for simplicity.

### 3.1.4 ARRAY DESIGN AND MEASUREMENT

An array with five pairs of slots is simulated with  $d_t$  varying. The results are shown in Fig. 3.6. Here the normalized radiated power is obtained by normalizing the radiated powers by the maximum among them, i.e. the one when  $d_t = 18$  mm. The normalized radiated power peaks when  $d_t$  is about 18 mm and oscillates with the periodicity of 16 mm, which is close to half of a guided wavelength of the dominant CBCPW mode at 5.5 GHz. The simulated H-plane ( $\varphi = 90^\circ$ ) radiation pattern with this value of  $d_t$  is plotted with the cross marks in Fig. 3.8. The figure also plots, with the circular marks, the same array but with the end of the transmission line terminated. When the line is terminated, the power tapering makes the pattern rather asymmetrical, with the first pair of the side lobes at -16.86 dB and -10.98 dB, respectively. When the forward traveling wave on the CBCPW is allowed to reflect back, its leakage also excites the side slots, but now it is the last (5<sup>th</sup>) pair that is excited most strongly and decays in the reverse order. This compensates for the original tapering and shapes the pattern much more symmetrical, so the levels of the first pair of the side lobes become -13.03 dB and -12.06 dB, which is comparable to that of a uniformly-excited array.

To check the validity of our design, the above array was fabricated on the FR4 substrate with dielectric constant  $\epsilon_r = 4.3$ , thickness  $h = 1.6$  mm, and loss tangent  $\tan\delta = 0.02$ . The remaining parameters are as follows:  $w_s = 2$  mm,  $l_s = 23$  mm,  $d_t = 18$  mm,  $d_y = 31$  mm,  $d = 15.5$  mm, and  $d_s = 13$  mm. The dimensions of the feed-line are  $G = 0.8$  mm and  $S = 2.5$  mm, which correspond to a 50- $\Omega$  characteristic impedance. The return loss is measured using the Agilent E8364B network analyzer. The E- and H-plane radiation patterns are measured in an anechoic chamber, using the Agilent 8722ES network analyzer.

Fig. 3.7 shows the return loss versus frequency. Fig. 3.8 and Fig. 3.9 are the H- and E-plane ( $\phi = 0^\circ$ ) patterns, respectively, with and without termination at 5.5 GHz. It can be seen that there are some notable discrepancies between the simulation and the measurement results. The main reason is that as the leakage wave impinges on the slots, it partly radiates, partly reflects back, and partly transmits to the side directions. In the simulation, because the infinitely large ground plane and substrate are assumed, these transmitted waves will never reflect back. However, in practice they radiate as well as reflect at the periphery of the structure and interfere with the antenna itself, thus resulting in the poor performance. We therefore design another larger array with three columns of slots on each side of the feed-line. The number of rows is still five. The offsets  $d_{x12} = 14$  mm,  $d_{x23} = 12$  mm,  $d_{y12} = 4$  mm, and  $d_{y23} = 10$  mm. The transverse



spacing  $d_{xmn}$  is chosen to be about  $\lambda_{\text{gpp}}/2$  according to the phase cancellation technique and the longitudinal spacing  $d_{ymn}$  is tuned to ensure the in-phase excitations of the columns of slots. Here  $\lambda_{\text{gpp}}$  denotes the guided wavelength of the parallel-plate TEM mode. The columns of slots are not at each other's exact broadside due to the longitudinal offset  $d_{ymn}$ , but the phase cancellation can still be achieved in the transverse (x-) direction as [116] indicates. It is expected that with the increasing number of slots on the side, more power will radiate through the slots instead of radiating and reflecting at the ground edge. The photograph of the 5 x 6 array is shown in Fig. 3.10. The input return loss, the H-plane pattern, and the E-plane pattern are shown in Figs. 3.11, 3.12, and 3.13, respectively. The cross-polarization level is below -20 dB in all directions and is omitted here for clarity. The accuracy of the simulation improves considerably, especially in the patterns. This also confirms the above discussions. The main beam points towards broadside and the backside radiation level is below -30 dB. The levels of the first pair of the side lobes are -13.6 dB and -12.8 dB, respectively. The measured antenna gain is 10.84 dBi, which corresponds to the antennas efficiency of 33.6 %. Note that doubling the substrate height will drastically increase the efficiency to more than 50 %.

The array is capable of frequency-scanning in the H-plane. Fig. 3.14 plots H-plane

patterns at various frequencies between 5 GHz and 6 GHz. The amount of the beam scanning and antenna gains are summarized in Table II.

### 3.1.5 DESIGN PROCEDURE

The design procedure can be summarized as follows.

1. Start the design by listing several possible feed-line dimensions for the predetermined characteristic impedance. The lower and upper bounds may be, for example, the fabrication process limit and the dimension that is mechanically not matched to the connector, respectively. Choose one that has the medium leakage rate
2. For the design with a broadside main beam, make  $d_x$  and  $d_y$  equal to  $0.5 * \lambda_{gCPCPW}$  and  $\lambda_{gCPCPW}$ , respectively.
3. Choose  $d_s$  to be about  $0.5 * \lambda_{gpp}$ .
4. Choose  $l_s$  and  $w_s$  such that the maximum radiated power is obtained.
5. Place one column of slots on either side of the feed-line. Vary  $d_t$  and choose the value that results in the maximum radiated power.
6. If the resulting H-plane radiation pattern is too asymmetrical, or if the input reflection is too strong, go back to Step 1 and choose another feed-line dimension accordingly.
7. Let  $d_{xmn}$  be about a half of the guided wavelength of the parallel-plate TEM mode.



Adjust  $d_{ymn}$  such that all slots are in-phase, or nearly so, and a maximum antenna gain is achieved.

### 3.1.6 SUMMARY

A novel design of a longitudinal slot array antenna fed by a CBCPW has been presented. By longitudinally placing the slots and offsetting, the array radiates pure linearly-polarized broadside main beam. The attenuation characteristic of the CBCPW has been studied for suitable choice of the feed-line configuration. The dimensions and the arrangement of the radiating slots and the effects of the reflected wave have been discussed. A small array was fabricated but the performance suffered from the reflection and the radiation from the waves at the periphery of the structure. A larger array was therefore designed and fabricated to overcome this problem. The array exhibits wide impedance bandwidth and a highly unidirectional pattern capable of frequency-scanning. This antenna, using only one layer of the dielectric substrate, can find applications where inexpensive frequency-scanning arrays on the CBCPW are demanded.

## 3.2 THE TRANSVERSE CASE

A novel type of antenna which combines the leakage nature of the conductor-backed coplanar waveguide (CBCPW) and the parallel-plate slot array is proposed. The structure is simple and uses only one layer of substrate without any via holes. The proposed antenna features wide impedance bandwidth, high front-to-back ratio of the radiation pattern, and is readily expandable into large planar arrays. Simulated and measured data are presented with good agreement.

### 3.2.1 INTRODUCTION



In this section, we propose a new type of antenna based on CBCPW that uses the parallel-plate mode leakage to radiate through the transverse slot array etched on both sides of the ground plane of the CPW feed-line. The geometry is relatively simple and single-layered. The array design is flexible to achieve required radiation patterns. Besides, large array designs can easily be done without input-matching problems.

### 3.2.2 ANTENNA STRUCTURE

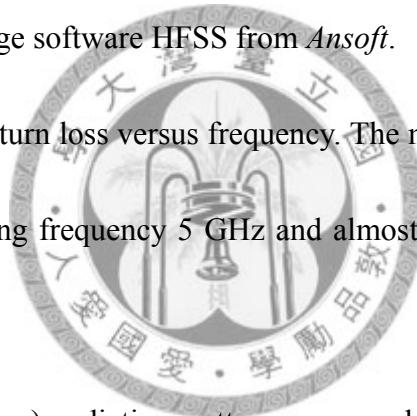
The proposed antenna structure and its photograph are shown in Fig. 3.15. The gray area represents the metal while the white ones are the etched slots and the feed-line. Only one layer of dielectric substrate is used. As soon as the wave is launched, it travels down the CBCPW and at the same time leaks power to the side ground planes and excites the nearby slots. By adjusting the parameters of the CBCPW and the slots, the leakage rate of the CBCPW and the radiated power per slot can be controlled in order to achieve a desired aperture excitation amplitude distribution. If the dimension of the array in the y-direction is large, the reflected wave from the short end of the CBCPW is negligible and  $L_t$  is somewhat arbitrary. But if the array size is small, the reflected wave contributes to the radiation and  $L_t$  must be carefully chosen accordingly. Moreover, reflections also occur at the periphery of the ground plane. In our design, we use the largest available area of the ground plane to mitigate this effect.

### 3.2.3 SIMULATION AND MEASUREMENT RESULTS

The design and fabrication of the prototype antenna are on an FR4 substrate with dielectric constant  $\epsilon_r = 4.3$ , thickness  $h = 1.6$  mm and loss tangent  $\tan\delta = 0.02$ . It should be mentioned that either the array size or the slot separation can be modified to accommodate the required radiation pattern. For example, if a broadside main beam and

hence the in-phase excitations along the y-axis are required,  $d_y$  should be set to one guided wavelength of the CBCPW mode. In the present case, we design a 8 x 4 array with the distance between adjacent slots in either x- or y- directions being about half a free space wavelength at the operating frequency 5 GHz. The remaining parameters are as follows:  $W_s = 3.3$  mm,  $L_s = 24.5$  mm,  $L_t = 7.25$  mm, and  $d_s = 2.75$  mm. The dimensions of the CBCPW feed-line are  $G = 0.5$  mm and  $S = 2$  mm, which correspond to a 50- $\Omega$  characteristic impedance. Throughout the design process, simulations are carried out using the package software HFSS from *Ansoft*.

Fig. 3.16 shows the return loss versus frequency. The measured return loss is 20.87 dB at the designed operating frequency 5 GHz and almost all below 10 dB within the entire band 4 - 6 GHz.



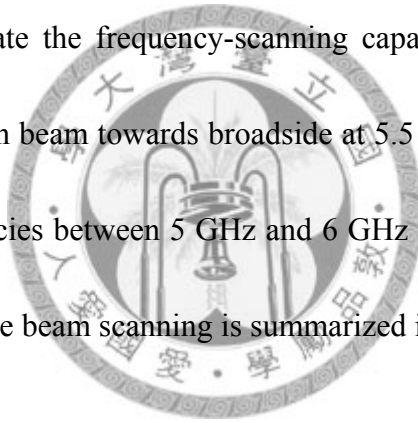
The E-plane (y-z plane) radiation pattern measured at the design frequency is shown in Fig. 3.17. The cross-polarization level is below -20 dB in all directions and is omitted here for clarity. As can be seen, the backside radiation level is low and stays below -20 dB. The main beam position can be estimated by the following equation [117]:

$$\theta_0 = \cos^{-1}\left[\left(\frac{\alpha}{2\pi}\right)\left(\frac{\lambda}{d}\right)\right] \quad (3-3)$$

where  $\theta_0$  is the angle of the main beam position measured from the array axis (y-axis) and  $\alpha$  is the *uniform progressive phase factor*. In this case,  $\alpha/2\pi$  is about -0.16 and  $\theta_0$  is

108.6° at 5 GHz, which correspond to 18.6° off broadside. This is close to the measured value of 20°. The secondary maximum lobe and the associated side lobes between 0° and 90° in Fig. 3.17 are mainly caused by the reflected wave from the short end of the CBCPW. These can be avoided in large arrays where the reflected wave is negligible, or by terminating the far end of the CBCPW. The measured antenna gain at 5 GHz is 9.35 dBi. All of the above-mentioned simulation and measurement results agree quite well.

In order to demonstrate the frequency-scanning capability, we designed another array which points the main beam towards broadside at 5.5 GHz. The E-plane radiation patterns at various frequencies between 5 GHz and 6 GHz are plotted and compared in Fig. 3.18. The amount of the beam scanning is summarized in Table III.



### 3.2.4 DESIGN PROCEDURE

The basic design procedures are similar to those described in the previous section.

So only the differences are listed here.

1. There is no offset distance  $d$  in the transverse array design.
2. The parameters  $d_s$  and  $d_x$  have minor effects in this case.

### 3.2.5 SUMMARY

A novel design of a slot array antenna fed by the CBCPW has been presented. With the utilization of the parallel-plate mode leakage, the proposed antenna, using only a single layer of substrate, exhibits wide impedance bandwidth, high front-to-back ratio and high expandability to large arrays. This antenna can find applications where large frequency-scanning arrays on CBCPW are demanded.



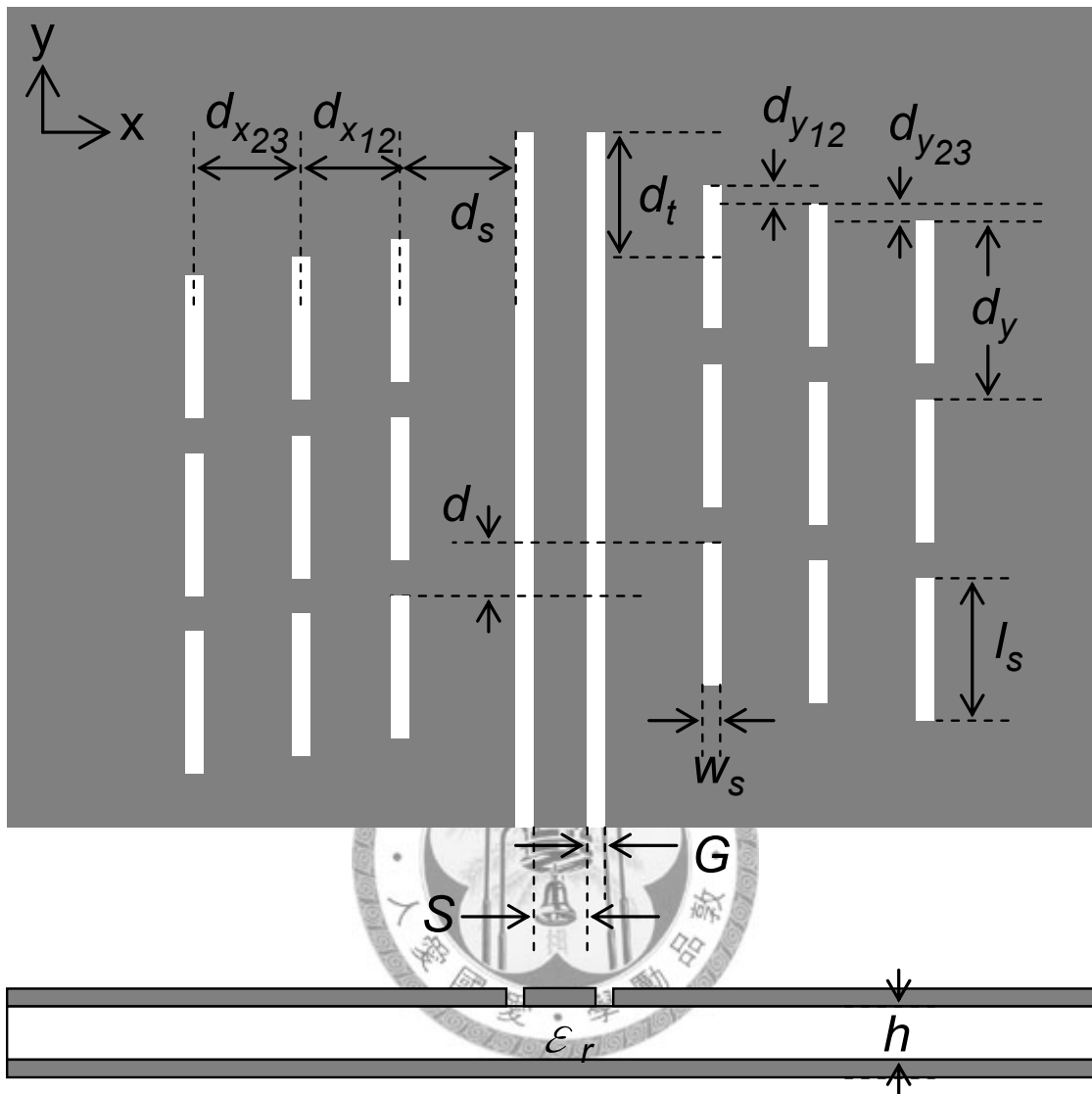


Fig. 3. 1 Geometry of the proposed antenna with a 3 x 6 longitudinal slot array.

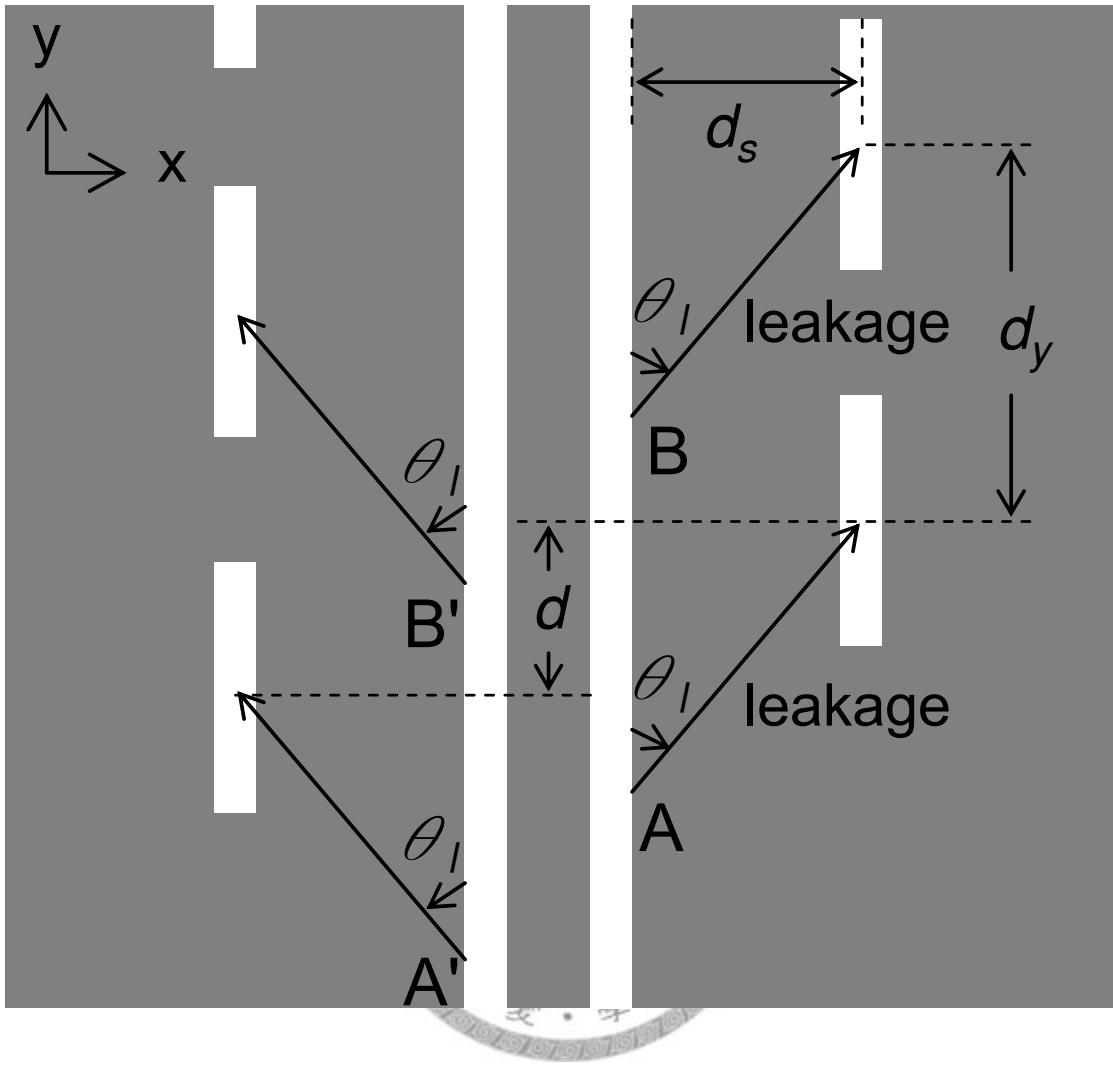
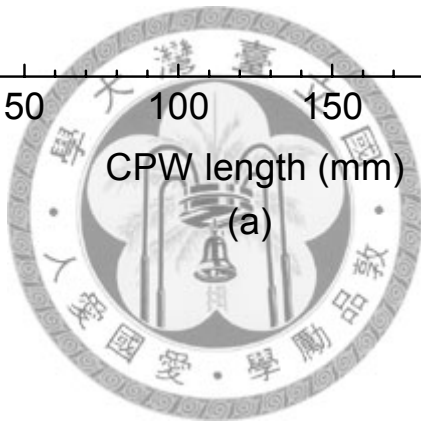
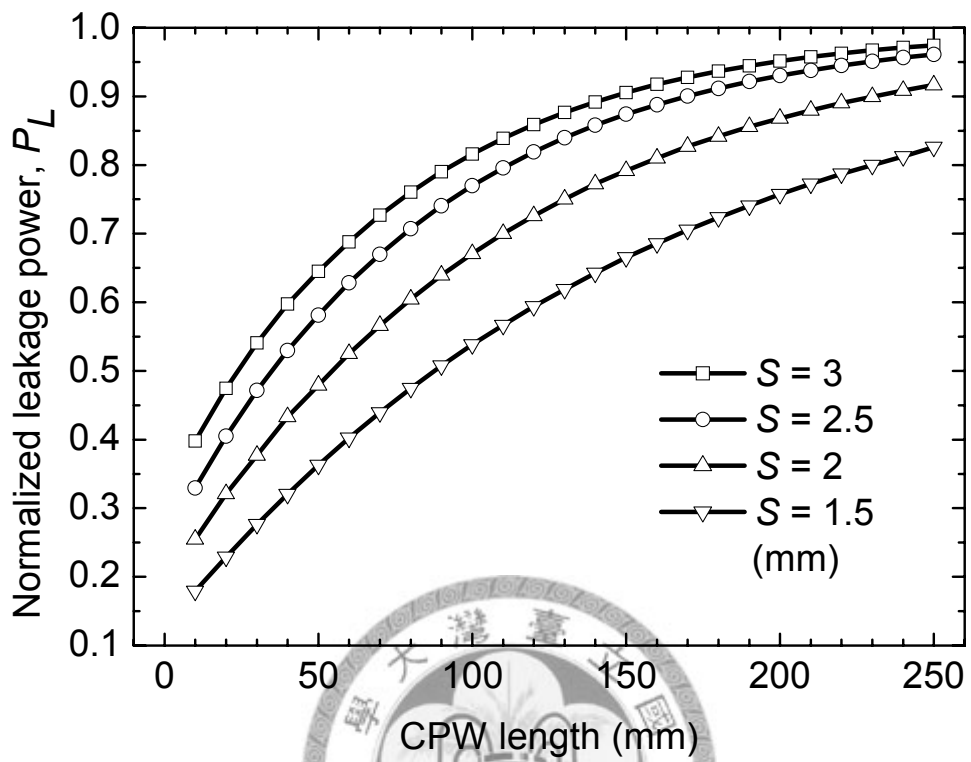


Fig. 3. 2 Relationship between the leakage wave and the relative phases of the fields on the slots.





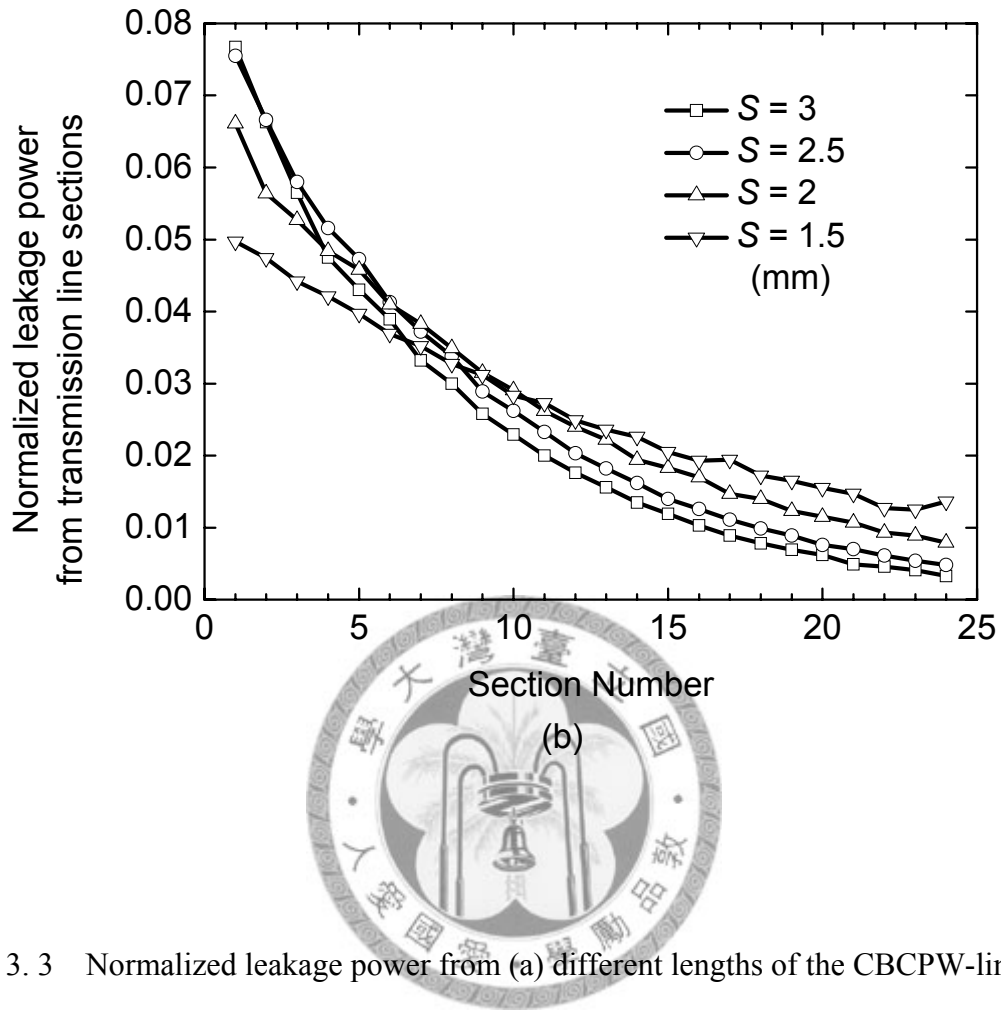


Fig. 3. 3 Normalized leakage power from (a) different lengths of the CBCPW-line and (b) different sections within a line with a total length of 250 mm.

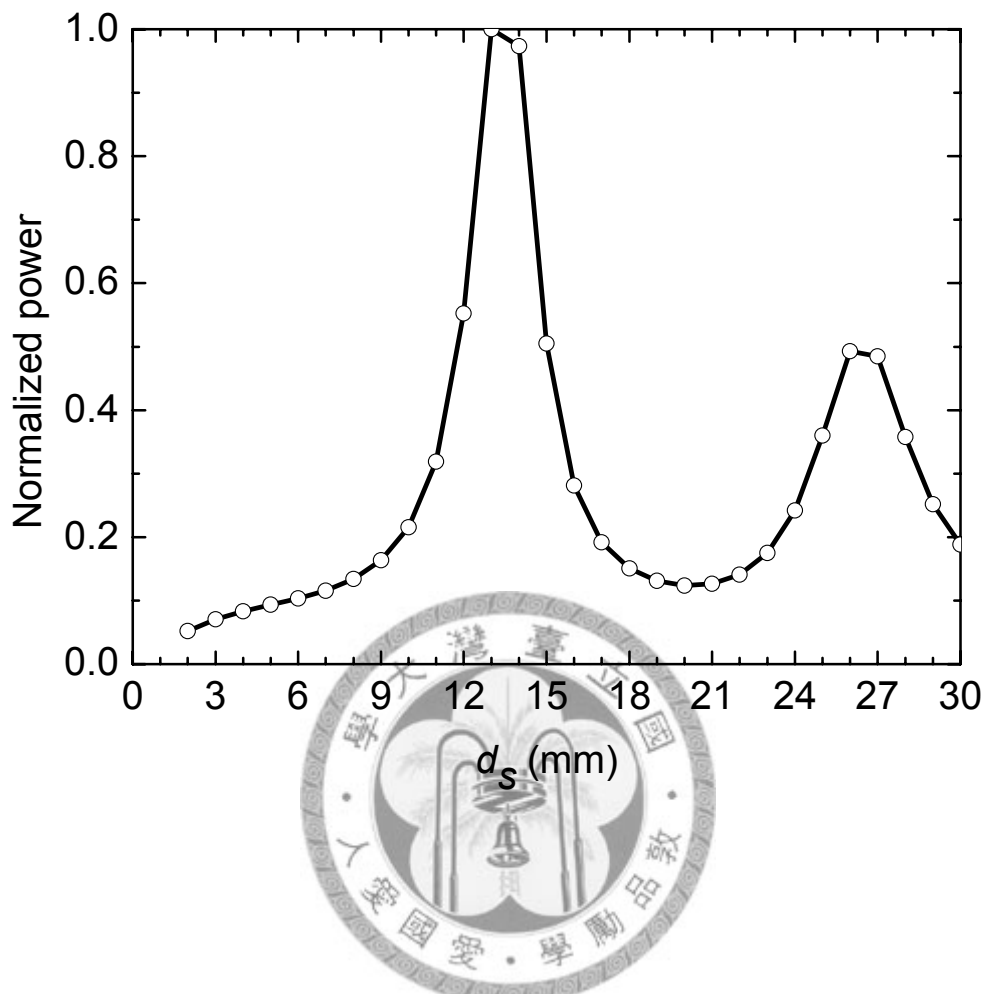


Fig. 3. 4 Normalized radiated power of a slot pair versus  $d_s$  at 5.5 GHz.  $l_s = 23$  mm and  $w_s = 2$  mm.

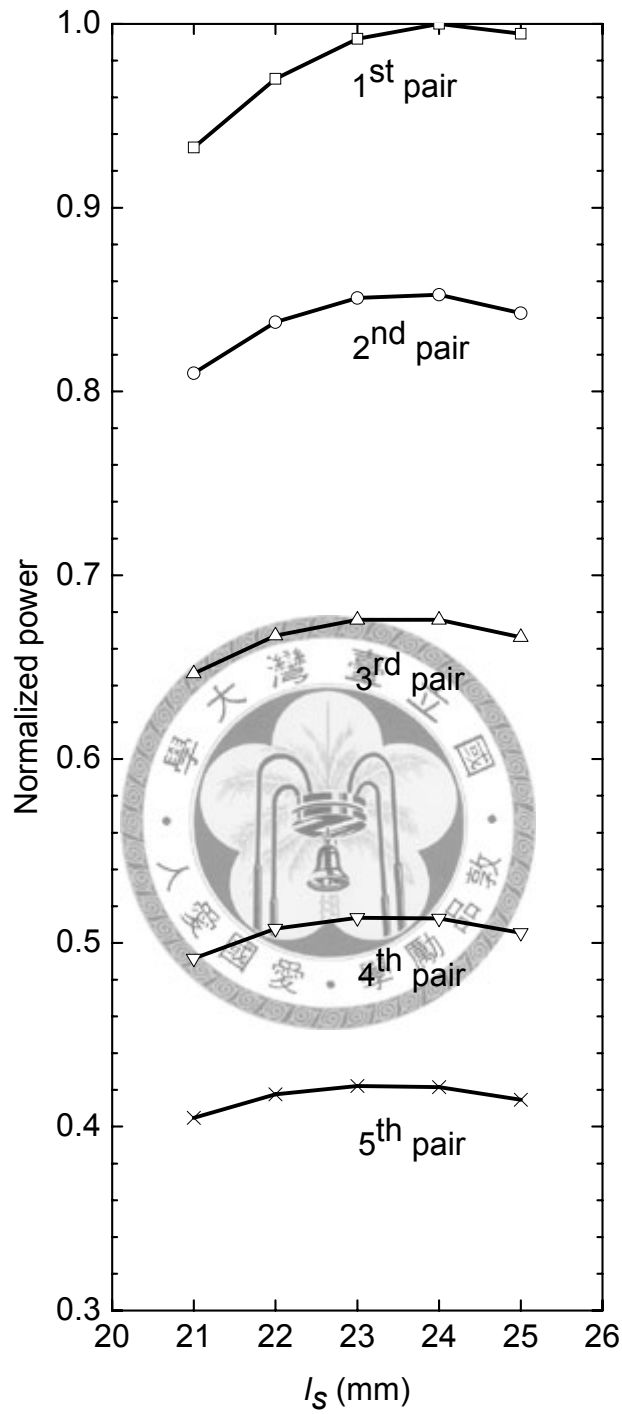


Fig. 3. 5 Normalized radiated power of a slot pair versus slot length.  $f = 5.5$  GHz,  $w_s = 2$  mm,  $d_s = 13$  mm, and  $d_y = 31$  mm.

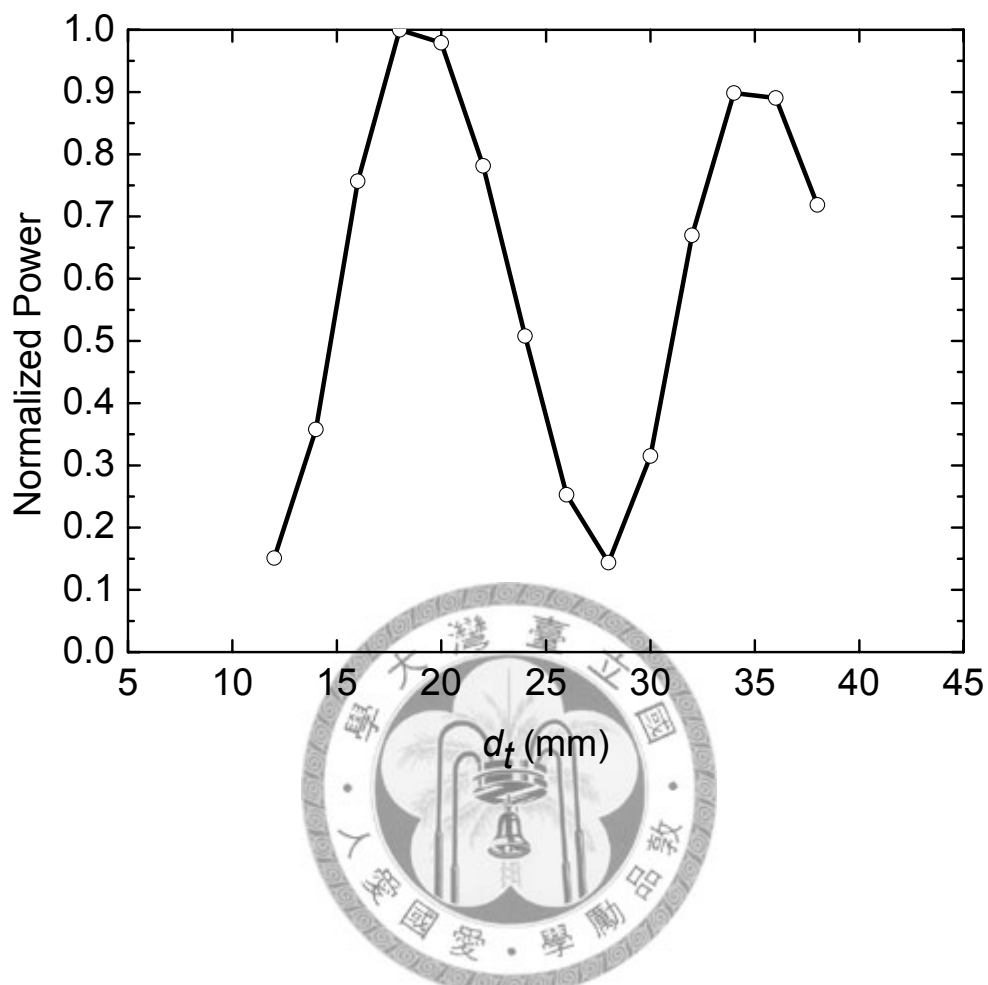


Fig. 3. 6 Normalized radiated power versus  $d_t$  for a 5 x 2 array at 5.5 GHz.

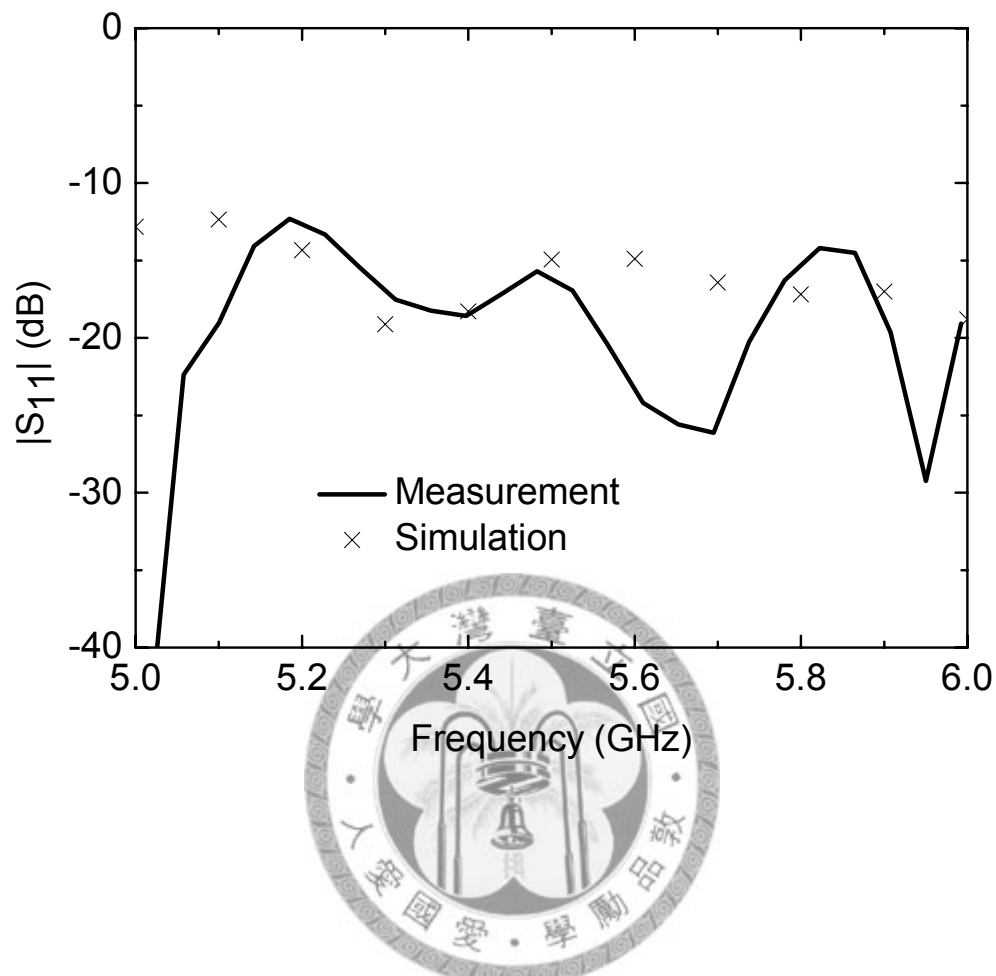


Fig. 3. 7 Measured and simulated input return losses of the 5 x 2 array without termination.

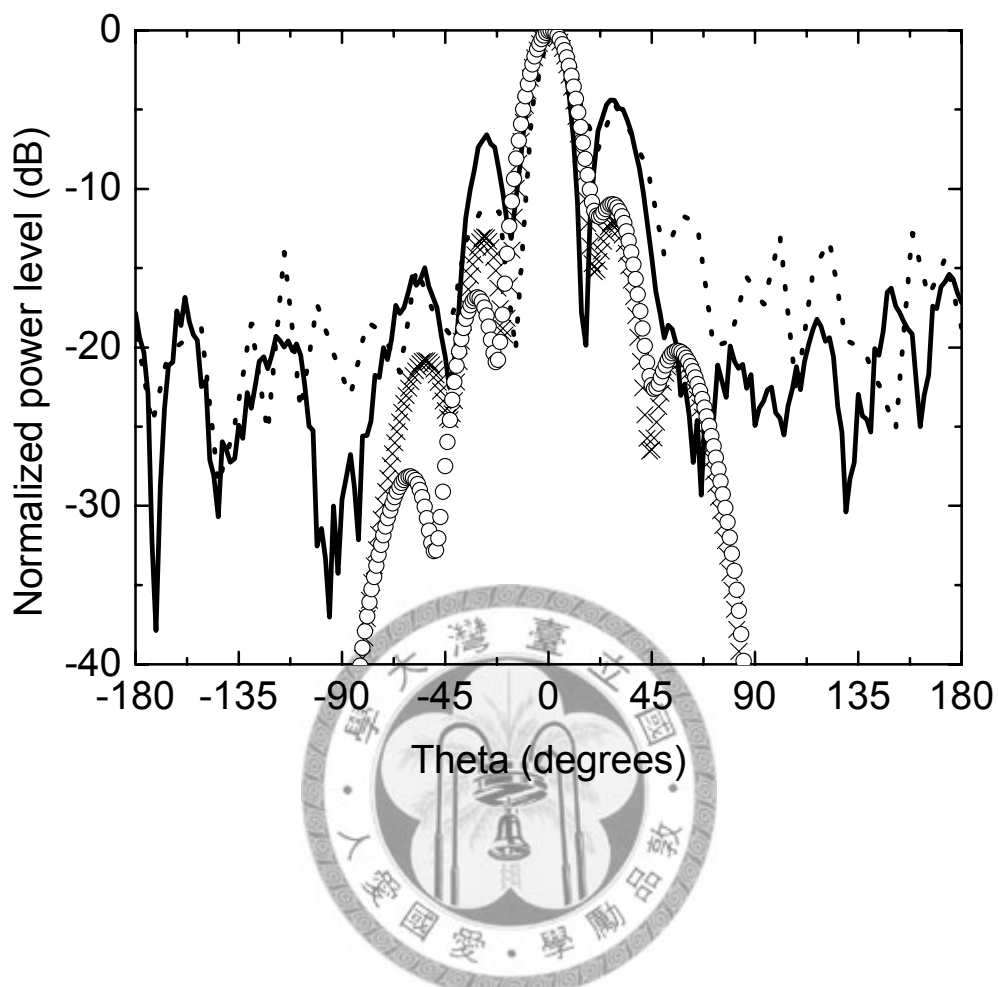


Fig. 3. 8 Measured and simulated H-plane patterns of the 5 x 2 array with and without termination at 5.5 GHz. Solid line: measurement without termination; dotted line: measurement with termination; cross: simulation without termination; circle: simulation with termination.

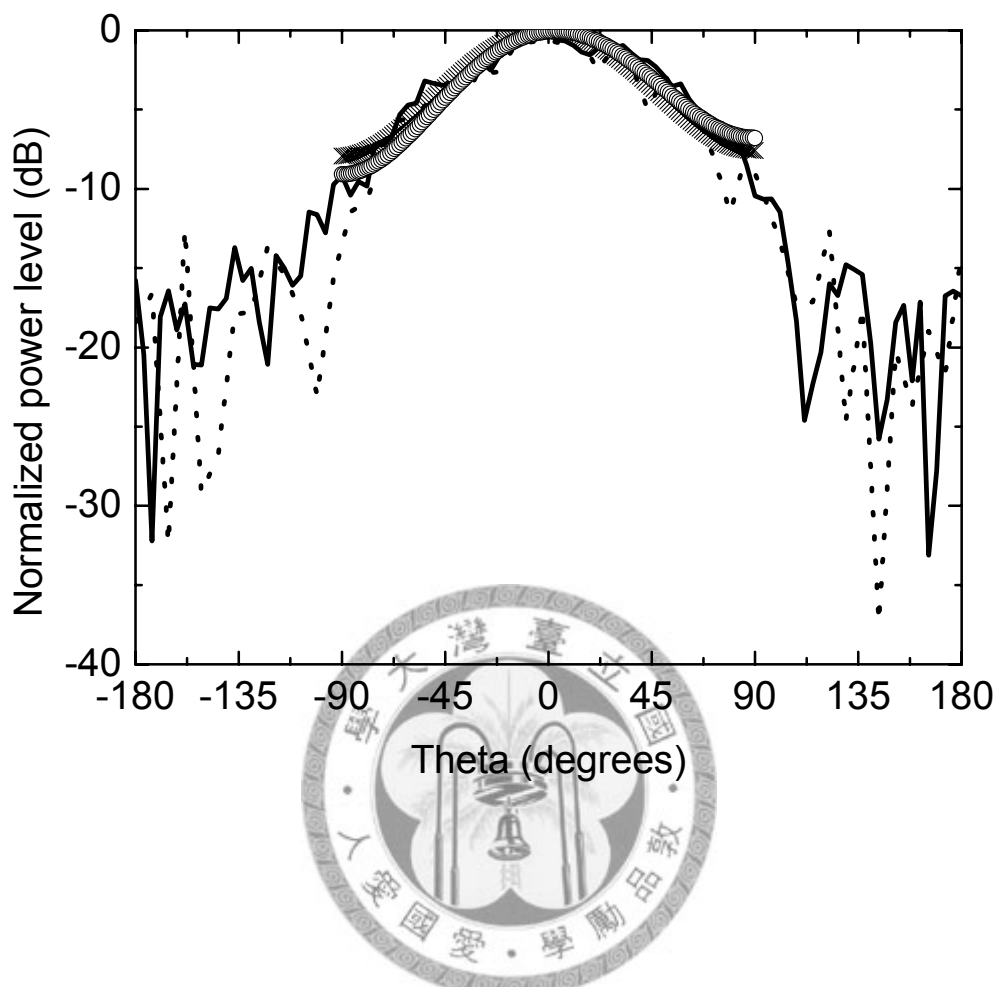


Fig. 3. 9 Measured and simulated E-plane patterns of the 5 x 2 array with and without termination at 5.5 GHz. Solid line: measurement without termination; dotted line: measurement with termination; cross: simulation without termination; circle: simulation with termination.





Fig. 3. 10 Photograph of the 5 x 6 array.

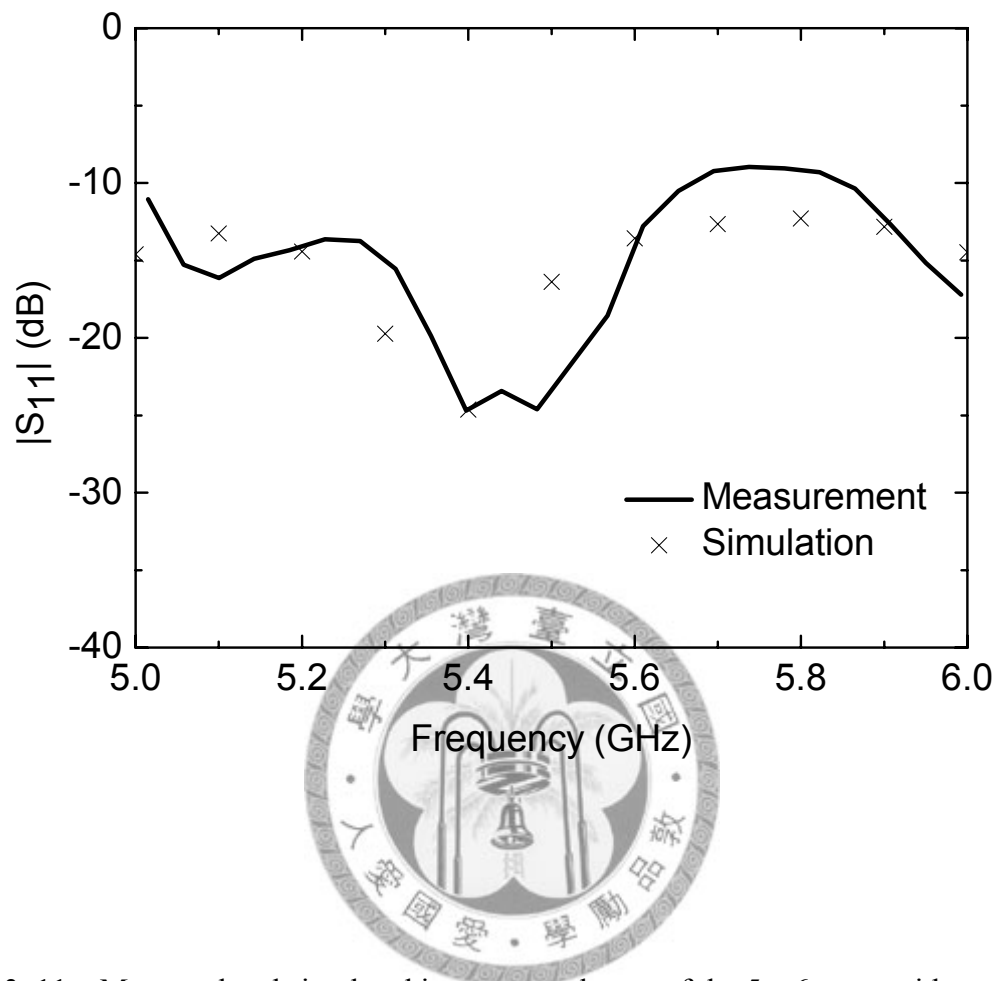


Fig. 3. 11 Measured and simulated input return losses of the 5 x 6 array without termination.

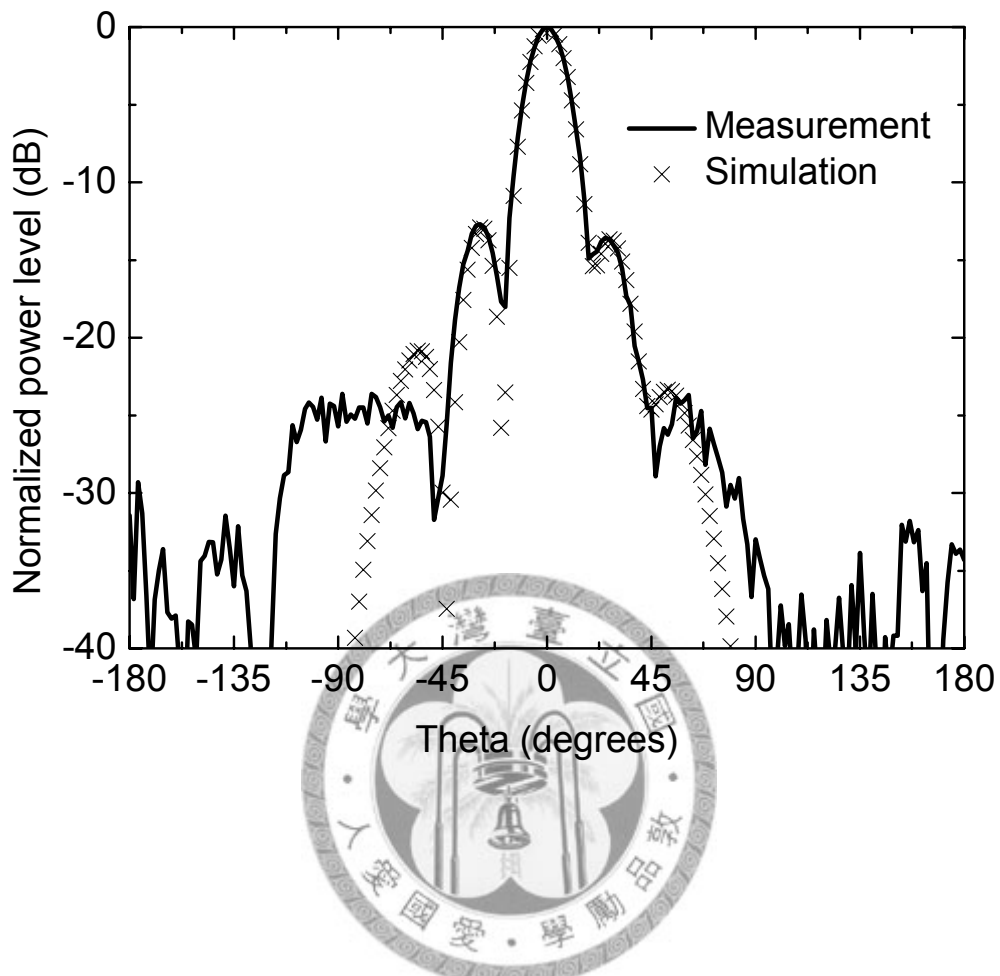


Fig. 3. 12 Measured and simulated H-plane patterns of the 5 x 6 array without termination at 5.5 GHz.

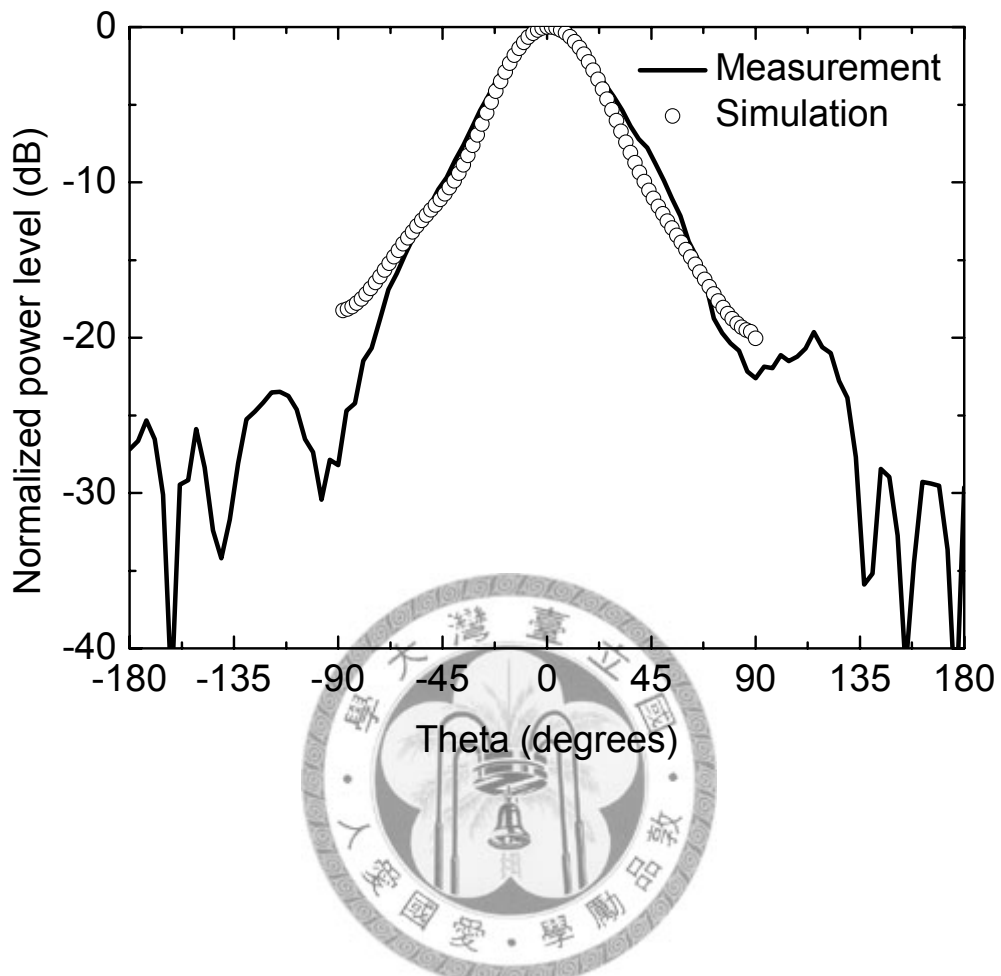
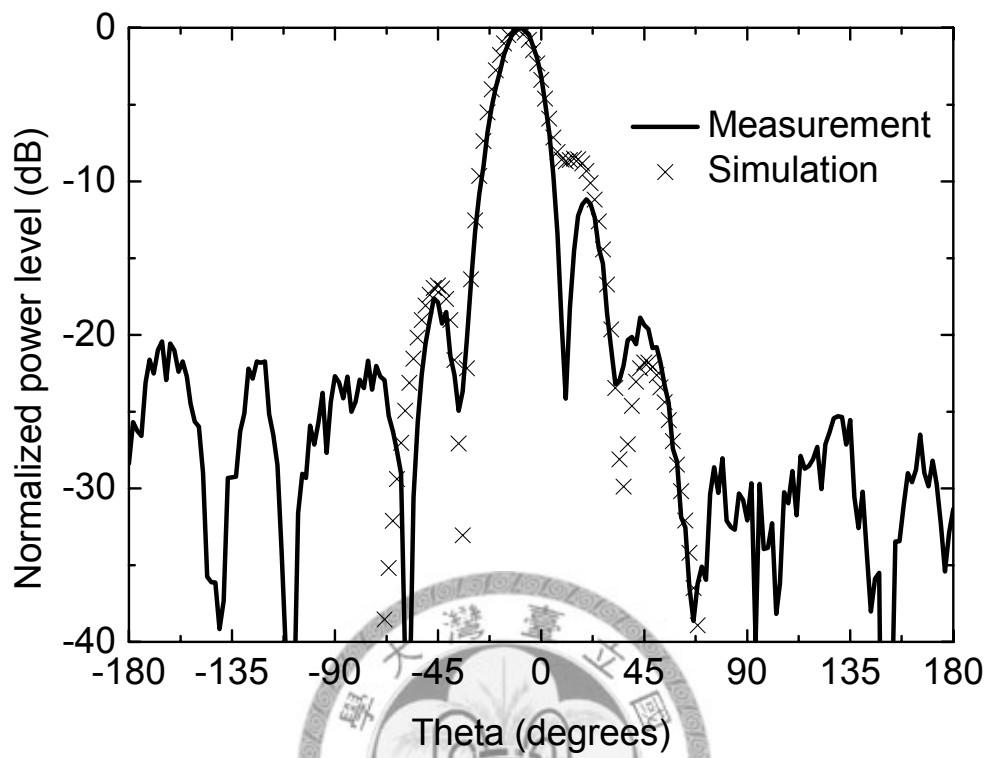
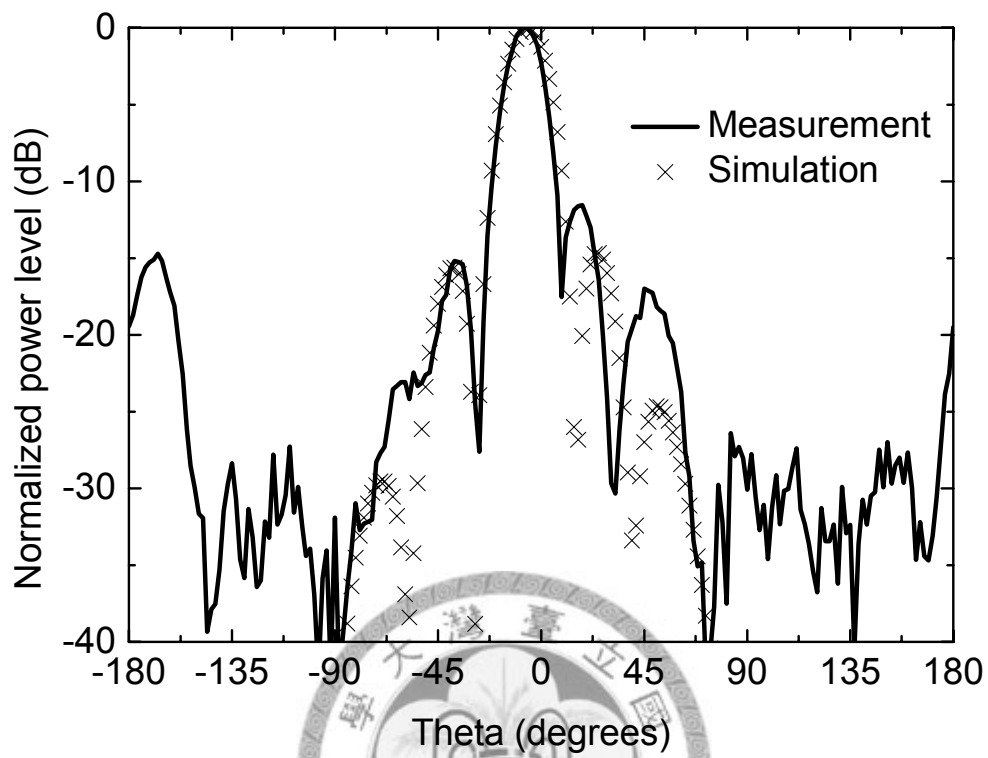


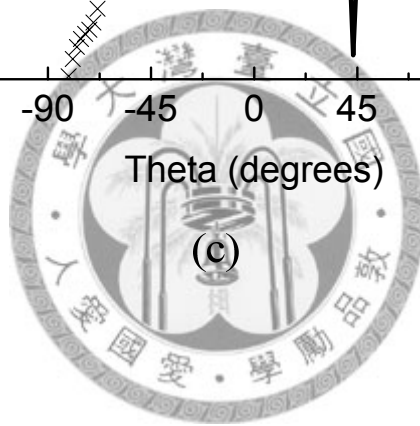
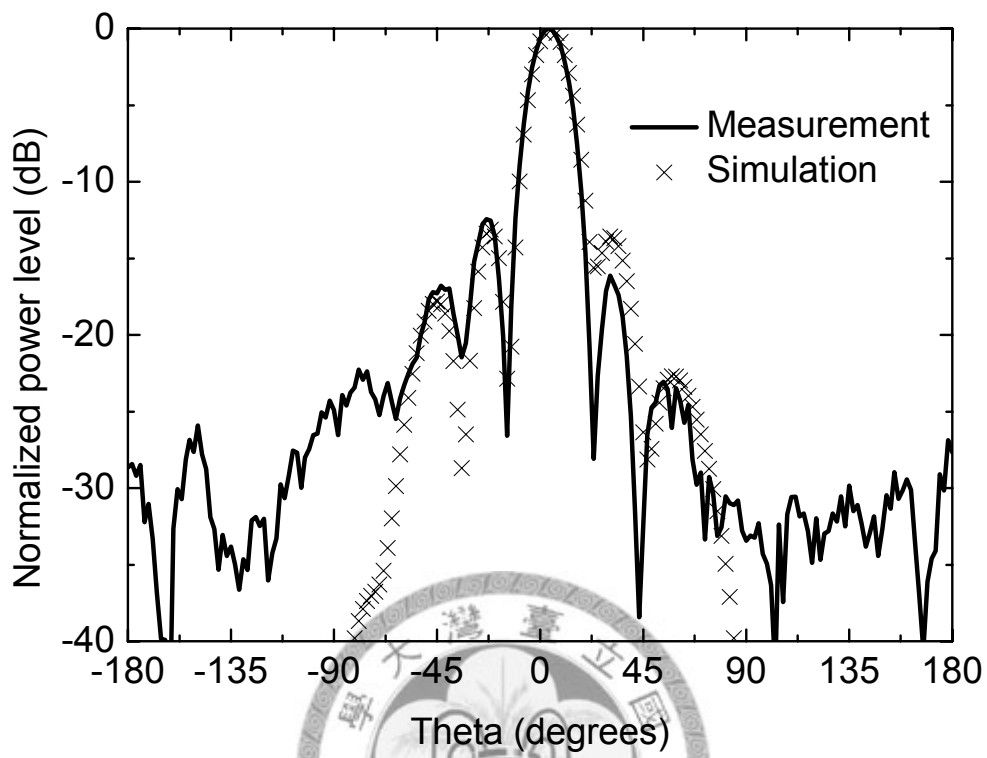
Fig. 3. 13 Measured and simulated E-plane patterns of the 5 x 6 array without termination at 5.5 GHz.



(a)



(b)



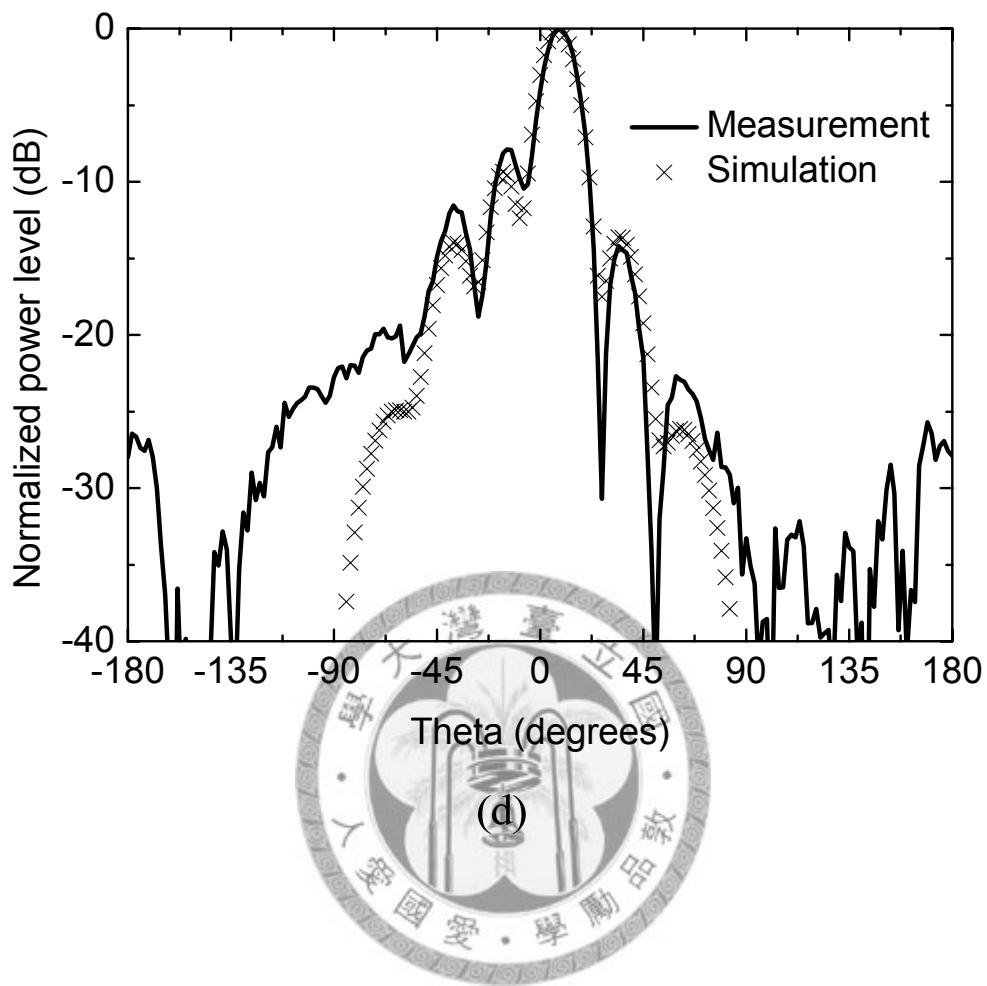


Fig. 3. 14 H-plane patterns of the 5 x 6 array without termination. (a) 5 GHz, (b) 5.25 GHz, (c) 5.75 GHz, and (d) 6 GHz.



TABLE II  
SUMMARY OF THE H-PLANE MAIN BEAM POSITIONS AND ANTENNA GAINS OF THE 5X6  
ARRAY WITHOUT TERMINATION

Frequency (GHz)	5	5.25	5.5	5.75	6
Angle (°)	-9.36	-6.48	0	4.32	8.64
Gain (dBi)	5.07	7.76	10.84	8.70	9.66



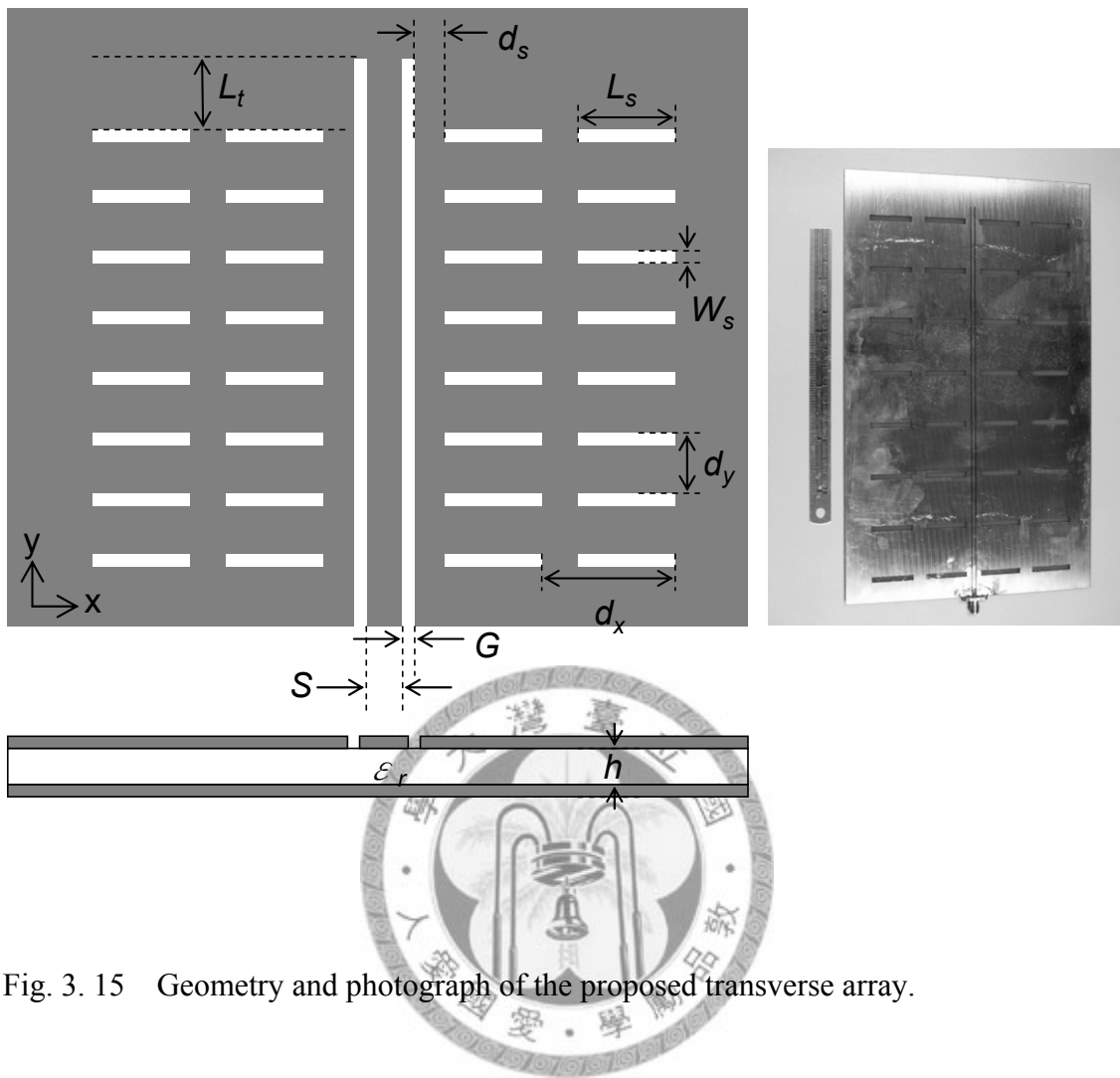


Fig. 3. 15 Geometry and photograph of the proposed transverse array.

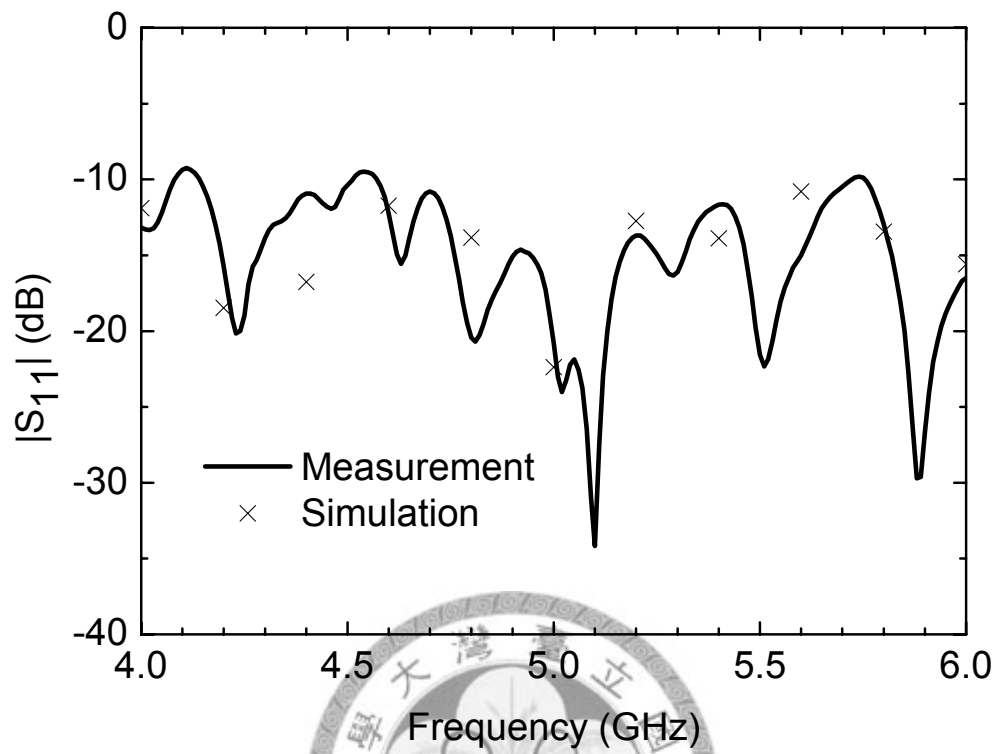


Fig. 3. 16 Measured and simulated input return losses.

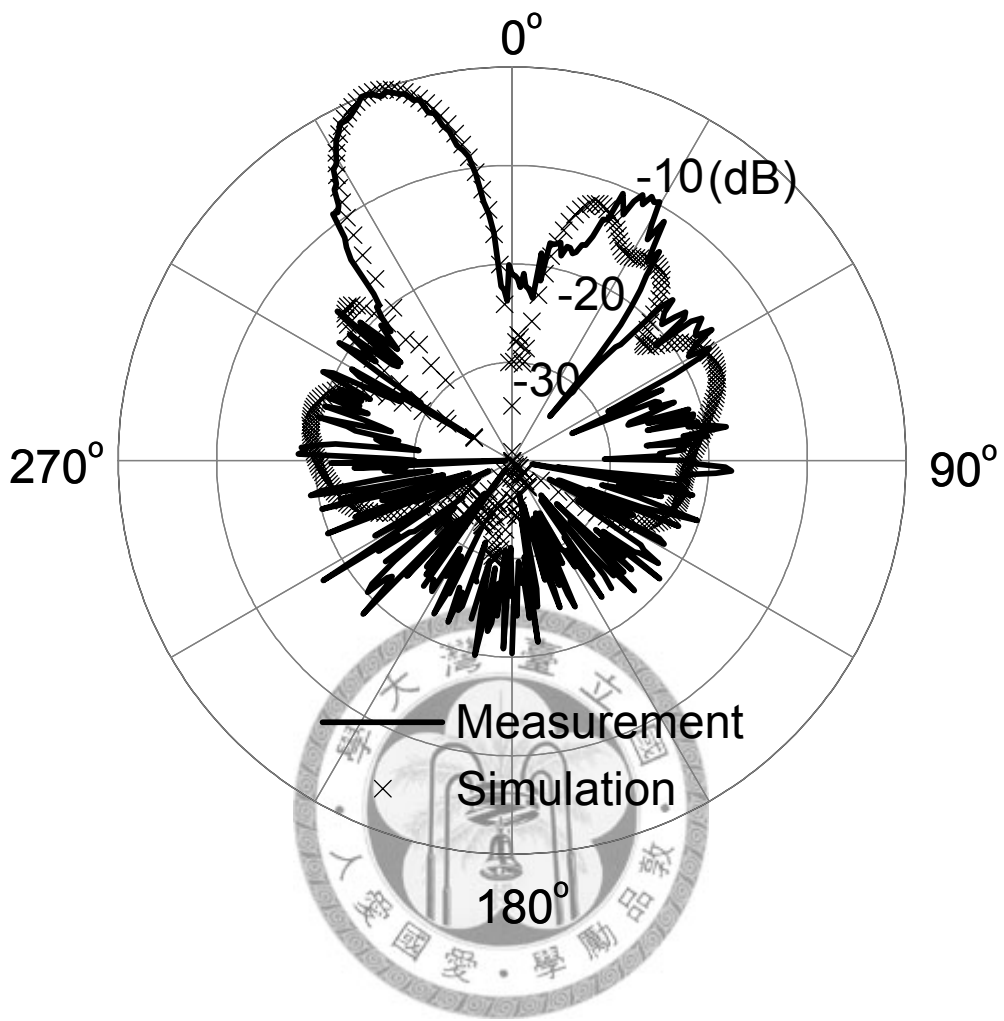


Fig. 3. 17 Measured and simulated radiation patterns in the y-z plane.

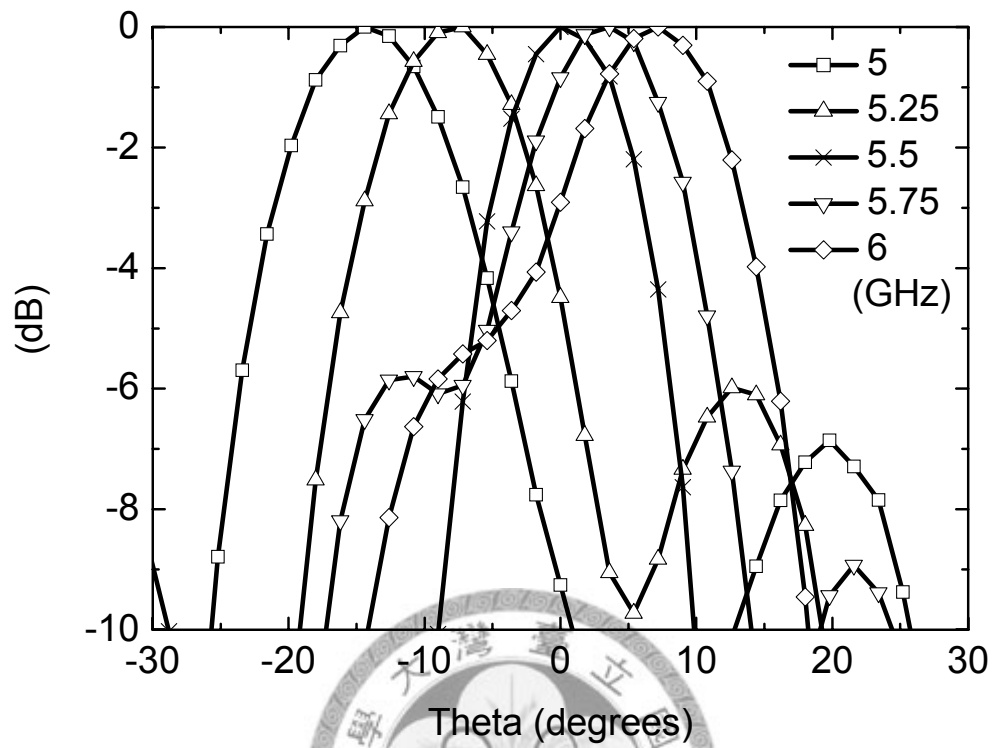


Fig. 3. 18 Radiation patterns in the E-plane at various frequencies.

TABLE III  
SUMMARY OF THE E-PLANE MAIN BEAM POSITIONS

Frequency (GHz)	5	5.25	5.5	5.75	6
Angle (°)	-14.4	-7.2	0	3.6	7.2



# Chapter 4

## Conclusion

A series of slot antennas fed by the conductor-backed coplanar waveguide have been presented in this dissertation. The first category includes the slot dipole coupled with a straight slot, the slot dipole coupled with an arc-slot, and the miniaturized case. The second group comprises the longitudinal and the transverse parallel-plate slot arrays. These antennas are all based on the simplest and the most original form of the conductor-backed coplanar waveguide that contains only one dielectric layer metal-plated on either side without any via holes. The back conductor is kept intact.

In Chapter 2, first the leakage phenomenon of the CBCPW-fed slot dipole has been illustrated visually. Then the coupling mechanism of the slot dipole coupled with a straight slot has been investigated. The coupled twin slots have been fabricated and tested, showing 10-dB return loss bandwidth of 5 %, antenna gain of 4.92 – 6.37 dBi, and antenna efficiency of 69.8 % at the center frequency. This structure serves as the basis of the following two designs.

In the second section of Chapter 2, the slot dipole coupled with an arc-slot has been proposed. This antenna, although inferior to the previous design in terms of antenna efficiency and gain, is more compact and wide-banded. The 10-dB return loss

bandwidth, the antenna gain, and the antenna efficiency at the center frequency have been found to be 7.2 %, 0.55 – 3.40 dBi, and 50.6 %, respectively.

In the third section of Chapter 2, the miniaturized design has been proposed. Using the fringing fields developed at the truncation of the ground plane and the dielectric substrate, this modification has been shown to provide similar performance to the original coupled twin slots, whereas the antennas size has much reduced. The antenna performance can be summarized as follows: 10-dB return loss bandwidth of 8.6 %, antenna gain of 3.8 – 6.4 dBi, and antenna efficiency at the center frequency of 84.4 %.

In Chapter 3, two versions of the parallel-plate slot arrays have been presented. First, for the longitudinal slot array, design considerations about the various aspects of the feed-line and the radiating slots have been discussed. The reflected wave from the end of the feed-line has been taken into consideration to compensate for the power tapering along the radiating apertures. A 5 x 6 and two 5 x 2 arrays with and without the feed-line termination have been fabricated and tested. The proposed array features wide impedance bandwidth, high front-to-back ratio, a broadside unidirectional pattern, and is capable of frequency-scanning in the H-plane.

In the bottom half of Chapter 3, the transverse array has been presented. The physical mechanism and the basic design principles are identical to the longitudinal case. An array with an off-broadside main beam has been designed to illustrate the basic



concept and the predictable main beam position. Then another array with a broadside main beam has been designed to demonstrate the frequency-scanning property.



# Appendix A

## Explanation of the Leakage Occurrence

Leakage effects can be observed in many types of printed-circuit waveguides, such as microstrip lines, slot lines, coplanar waveguides, and their variants [25]. Despite the different guiding structures and the manners in which the dominant mode power leaks, the basic physical idea is common. Below we describe this point.

Fig. A.1 shows the top view of a metal strip on an air-dielectric interface, where the strip may represent that of the various guiding structures mentioned above. As can be seen in this figure, the transverse wave number  $k_x$  is related to the other wave numbers

by

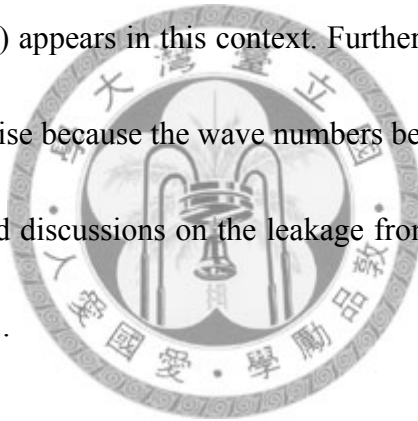
$$k_x^2 = k_s^2 - \beta^2 \quad (\text{A-1})$$

where  $\beta$  is the phase constant of the dominant mode guided along the  $z$ -direction and  $k_s$  is the propagation wave number of the relevant surface wave that can be supported on the substrate in the vicinity of the guiding strip. If  $\beta > k_s$ ,  $k_x$  is seen to be imaginary. The mode guided along the  $z$ -direction is then purely bound, and the field decays transversely in the  $x$ -direction away from the strip. On the other hand, if  $\beta < k_s$ ,  $k_x$  is seen to be real. Power now leaks away from the guided mode at an angle  $\theta$  in the form

of the surface wave on the surrounding dielectric substrate layer. The angle  $\theta$  is related to  $\beta$  and  $k_s$  by

$$\theta \cong \cos^{-1} \frac{\beta}{k_s} \quad (\text{A-2})$$

The approximation sign in (A.2) needs some explanations. When leakage occurs, the propagation wave number  $k_z$  of the guided mode becomes complex, with  $k_z = \beta - j\alpha$ . The transverse wave number  $k_x$  also becomes complex. Relation (A.1) is no longer exactly correct under these conditions, but it is still a very good approximation. The approximation sign in (A.2) appears in this context. Further topics on the modifications of the field behavior that arise because the wave numbers become complex can be found in [118] and [119]. Detailed discussions on the leakage from various types of dielectric waveguides appear in [120].



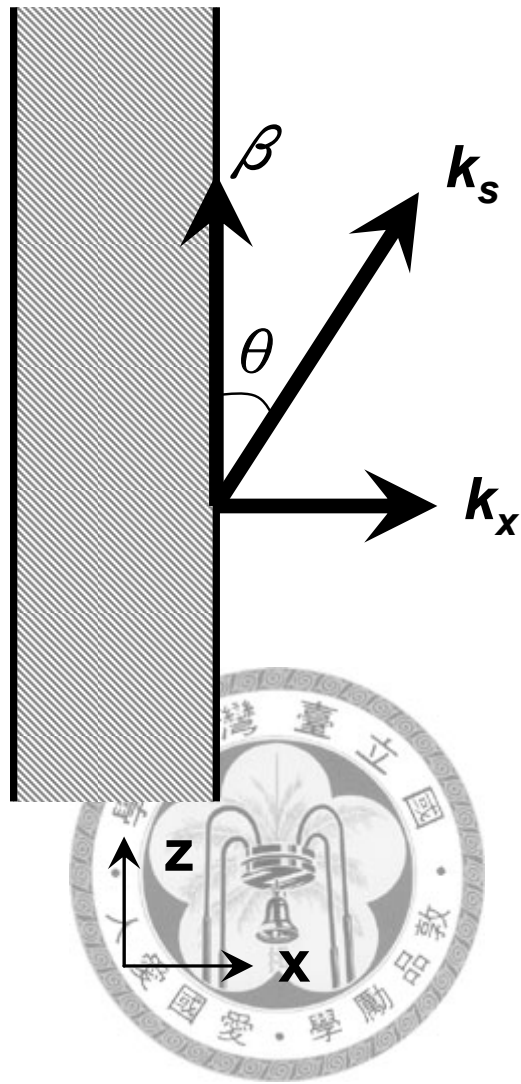


Fig. A. 1 Top view of a printed strip, showing the angle of leakage  $\theta$  into the surface wave of wave number  $k_s$  on the surrounding dielectric substrate layer.

# Reference

- [1] C. P. Wen, "Coplanar waveguide: a surface strip transmission line suitable for nonreciprocal gyromagnetic device applications," *IEEE Trans. Microw. Theory Tech.*, vol. 17, no. 12, pp. 1087-1090, Dec. 1969.
- [2] R. N. Simons, *Coplanar waveguide circuits, components, and systems*. New York: John Wiley & Sons, 2001.
- [3] Y. Liu and T. Itoh, "Four-layered coplanar waveguide with double side conductor backings," in *IEEE Topical Meeting on Electrical Performance of Electronic Packaging*, Portland, OR, 1995, pp. 188-190.
- [4] R. Q. Lee and R. N. Simons, "Slot-coupled patch antenna with coplanar waveguide feed," in *IEEE AP-S Int. Symp. Dig.*, Chicago, IL, 1992, pp. 1048-1051.
- [5] R. Q. Lee and R. N. Simons, "Coplanar waveguide aperture-coupled microstrip patch antenna," *IEEE Microwave Guided Wave Lett.*, vol. 2, no. 4, pp. 138-139, Apr. 1992.
- [6] R. N. Simons and R. Q. Lee, "Coplanar waveguide aperture coupled patch antennas with ground plane/substrate of finite extent," *Electron. Lett.*, vol. 28, no. 1, pp. 75-76, 2 Jan. 1992.

- [7] F. A. Miranda, K. B. Bhasin, K.-S. Kong, T. Itoh, and M. A. Stan, "Conductor-backed coplanar waveguide resonators of  $\text{YBa}_2\text{Cu}_3\text{O}_{7-\delta}$  on  $\text{LaAlO}_3$ ," *IEEE Microwave Guided Wave Lett.*, vol. 2, no.7, pp. 287-288, Jul. 1992.
- [8] P. K. Shumaker, C. H. Ho, K. B. Smith, D. Huang, R. Wang, and J. W. Liao, "A new GCPW resonant quadrifilar helix antenna for GPS land mobile applications," in *IEEE AP-S Int. Symp. Dig.*, Montreal, Que., 1997, pp. 1344-1347.
- [9] J. C. Beard and D. V. Arnold, "6 GHz range finder using pulse compression," in *IEEE International Geoscience and Remote Sensing Symposium*, Honolulu, HI, 2000, pp. 2310-2312.
- [10] P. Ulavapalli and M. A. Saed, "An active subharmonic retrodirective array using dual polarized microstrip antennas," in *IEEE AP-S Int. Symp. Dig.*, 2004, p. 3939.
- [11] S. M. N., S. K. Menon, P. V. Bijumon, M. T. Sebastian, and P. Mohanan, "Experimental investigation on rectangular dielectric resonator antenna excited by conductor backed coplanar waveguide," in *IEEE AP-S Int. Symp. Dig.*, 2005, pp. 238-241.
- [12] C. T. H. Lim, A. Ali, and J. S. Fu, "A broadband printed triangular monopole," in *Asia Pacific Microw. Conf.*, 2005.

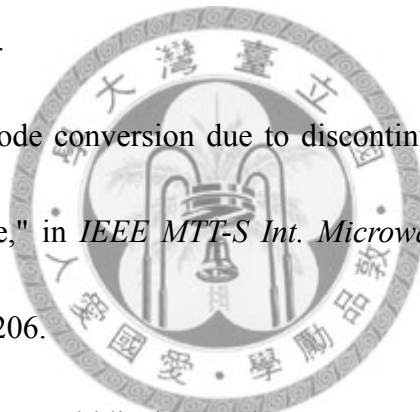
- [13] Y. Gao, A. P. Popov, B. L. Ooi, and M. S. Leong, "Experimental study of wideband hybrid dielectric resonator antenna on small ground plane," *Electron. Lett.*, vol. 42, no. 13, pp. 731-733, 22 Jun. 2006.
- [14] K. Ma, S. Xiao, J. Ma, K. T. Chan, K. S. Yeo, and M. A. Do, "Wide bandwidth stacked patch antenna on fourteen layers microwave board," in *IEEE MTT-S Int. Microwave Symp. Dig.*, San Francisco, CA, 2006, pp. 2031-2034.
- [15] K. M. K. H. Leong, Y. Qian, and T. Itoh, "First demonstration of a conductor backed coplanar waveguide fed quasi-Yagi antenna," in *IEEE AP-S Int. Symp. Dig.*, Salt Lake City, UT, 2000, pp. 1432-1435.
- [16] S.-G. Mao and S.-L. Chen, "Broadband series-fed printed dipole arrays with conductor-backed coplanar waveguide-to-coplanar stripline transitions," in *IEEE AP-S Int. Symp. Dig.*, 2005, pp. 565-568.
- [17] A. M. E. Safwat, K. A. Zaki, W. Johnson, and C. H. Lee, "Novel transition between different configurations of planar transmission lines," *IEEE Microwave Wireless Components Lett.*, vol. 12, no. 4, pp. 128-130, Apr. 2002.
- [18] D.-H. Kwon, "A wideband balun and vertical transition between conductor-backed CPW and parallel-strip transmission line," *IEEE Microwave Wireless Components Lett.*, vol. 16, no. 4, pp. 152-154, Apr. 2006.
- [19] N. Dib and A. Omar, "Analysis of grounded coplanar waveguide fed patches and

- waveguides," in *IEEE AP-S Int. Symp. Dig.*, Montreal, Que., 1997, pp. 2530-2533.
- [20] B. Kang, J. Cho, C. Cheon, and Y. Kwon, "Nondestructive measurement of complex permittivity and permeability using multilayered coplanar waveguide structures," *IEEE Microwave Wireless Components Lett.*, vol. 15, no. 5, pp. 381-383, May 2005.
- [21] J. Hu, A. Sligar, C.-H. Chang, S.-L. Lu, and R. K. Settaluri, "A grounded coplanar waveguide technique for microwave measurement of complex permittivity and permeability," *IEEE Trans. Magn.*, vol. 42, no. 7, pp. 1929-1931, Jul. 2006.
- [22] C. E. Bassey and G. R. Simpson, "A comparison of the coplanar waveguide (CPW) and conductor-backed coplanar waveguide (CBCPW) for use as aircraft ice sensors," in *IEEE AP-S Int. Symp. Dig.*, 2006, pp. 821-824.
- [23] L.-M. Chou, R. G. Rojas, and P. H. Pathak, "A WH/GSMT based full-wave analysis of the power leakage from conductor-backed coplanar waveguides," in *IEEE MTT-S Int. Microwave Symp. Dig.*, Albuquerque, NM, 1992, pp. 219-222.
- [24] K. Beilenhoff and W. Heinrich, "Excitation of the parasitic parallel-plate line mode at coplanar discontinuities," in *IEEE MTT-S Int. Microwave Symp. Dig.*, Denver, CO, 1997, pp. 1789-1792.



- [25] H. Shigesawa, M. Tsuji, and A. A. Oliner, "Dominant mode power leakage from printed-circuit waveguides," *Radio Science*, vol. 26, no. 2, pp. 559-564, March-April 1991.
- [26] Y.-C. Shih and T. Itoh, "Analysis of conductor-backed coplanar waveguide," *Electron. Lett.*, vol. 18, no.12, pp. 538-540, 10 Jun. 1982.
- [27] H. Shigesawa, M. Tsuji, and A. A. Oliner, "Conductor-backed slot line and coplanar waveguide: dangers and full-wave analyses," in *IEEE MTT-S Int. Microwave Symp. Dig.*, New York, NY, 1988, pp. 199-202.
- [28] G. Ghione and C. Naldi, "Parameters of coplanar waveguides with lower ground plane," *Electron. Lett.*, vol. 19, no.18, pp. 734-735, 26 Jul. 1983.
- [29] T. Krems, A. Tessmann, W. H. Haydl, C. Schmelz, and P. Heide, "Avoiding cross talk and feed back effects in packaging coplanar millimeter-wave circuits," in *IEEE MTT-S Int. Microwave Symp. Dig.*, Baltimore, MD, 1998, pp. 1901-1904.
- [30] W. E. McKinzie and N. G. Alexopoulos, "Leakage losses for the dominant mode of conductor-backed coplanar waveguide," *IEEE Microwave Guided Wave Lett.*, vol. 2, no. 2, pp. 65-66, Feb. 1992.
- [31] R. W. Jackson, "Mode conversion at discontinuities in finite-width conductor-backed coplanar waveguide," *IEEE Trans. Microw. Theory Tech.*, vol. 37, no. 10, pp. 1582-1589, Oct. 1989.

- [32] R. R. Kumar, S. Aditya, and D. Chadha, "Modes of a shielded conductor-backed coplanar waveguide," *Electron. Lett.*, vol. 30, no. 2, pp. 146-148, 20 Jan. 1994.
- [33] S.-P. Liu and C.-K. C. Tzuang, "Scattering analyses of asymmetric conductor-backed CPW open-end discontinuity problem," *IEEE Microwave Guided Wave Lett.*, vol. 7, no. 5, pp. 130-132, May 1997.
- [34] S.-J. Fang and B.-S. Wang, "Analysis of asymmetric coplanar waveguide with conductor backing," *IEEE Trans. Microw. Theory Tech.*, vol. 47, no.2, pp. 238-240, Feb. 1999.
- [35] R. W. Jackson, "Mode conversion due to discontinuities in modified grounded coplanar waveguide," in *IEEE MTT-S Int. Microwave Symp. Dig.*, New York, NY, 1988, pp. 203-206.
- [36] J. Hesselbarth and R. Vahldieck, "Leakage suppression in coplanar waveguide circuits by patterned backside metallization," in *IEEE MTT-S Int. Microwave Symp. Dig.*, Anaheim, CA, 1999, pp. 871-874.
- [37] T. Hirota and T. Itoh, "Coupling between slotlines through a conductor backing," *IEEE Microwave Guided Wave Lett.*, vol. 3, no. 2, pp. 40-41, Feb. 1993.
- [38] W.-T. Lo, C.-K. C. Tzuang, S.-T. Peng, C.-C. Chang, J.-W. Huang, and C.-C. Tien, "Resonant phenomena in conductor-backed coplanar waveguide (CBCPW)," in *IEEE MTT-S Int. Microwave Symp. Dig.*, Atlanta, GA, 1993, pp.



- 1199-1202.
- [39] W.-T. Lo, C.-K. C. Tzuang, S.-T. Peng, C.-C. Tien, C.-C. Chang, and J.-W. Huang, "Resonant phenomena in conductor-backed coplanar waveguides (CBCPW's)," *IEEE Trans. Microw. Theory Tech.*, vol. 41, no. 12, pp. 2099-2108, Dec. 1993.
- [40] W. H. Haydl, "Resonance phenomena and power loss in conductor-backed coplanar structures," *IEEE Microwave Guided Wave Lett.*, vol. 10, no. 12, pp. 514-516, Dec. 2000.
- [41] W. Heinrich, F. Schnieder, and T. Tischler, "Dispersion and radiation characteristics of conductor-backed CPW with finite ground width," in *IEEE MTT-S Int. Microwave Symp. Dig.*, Boston, MA, 2000, pp. 1663-1666.
- [42] B. Hou and R. W. Jackson, "Preserving isolation in grounded coplanar waveguide circuits without via holes," in *IEEE Conference on Electrical Performance of Electronic Packaging*, Scottsdale, AZ, 2000, pp. 265-268.
- [43] S.-J. Kim, H.-S. Yoon, and H.-Y. Lee, "Suppression of leakage resonance in coplanar MMIC packages using a Si sub-mount layer," *IEEE Trans. Microw. Theory Tech.*, vol. 48, no. 12, pp. 2664-2669, Dec. 2000.
- [44] W. H. Haydl, "On the use of vias in conductor-backed coplanar circuits," *IEEE Trans. Microw. Theory Tech.*, vol. 50, no. 6, pp. 1571-1577, Jun. 2002.

- [45] S. Bokhari and H. Ali, "On grounded co-planar waveguides as interconnects for 10Gb/s signals," in *IEEE International Symposium on Electromagnetic Compatibility*, 2003, pp. 607-609.
- [46] S.-N. Lee, J.-I. Lee, Y.-J. Kim, and J.-G. Yook, "Miniaturized CBCPW bandpass filter based on thin film polyimide on lossy silicon," *IEEE Microwave Wireless Components Lett.*, vol. 16, no. 10, pp. 546-548, Oct. 2006.
- [47] J. H. Lim and S. W. Hwang, "Analysis of microwave resonances in a wirebond transition between conductor-backed coplanar waveguides (CBCPWs)," in *European Microwave Conf.*, Manchester, 2006, pp. 437-440.
- [48] Y.-C. Shih and M. Maher, "Characterization of conductor-backed coplanar waveguide using accurate on-wafer measurement techniques," in *IEEE MTT-S Int. Microwave Symp. Dig.*, Dallas, TX, 1990, pp. 1129-1132.
- [49] T. Murata and M. Fujita, "An electromagnetically coupled active flat panel antenna for DBS reception," in *European Microwave Conf.*, Stuttgart, Germany, 1991, pp. 1167-1172.
- [50] M. Yu, R. Vahldieck, and J. Huang, "Comparing coax launcher and wafer probe excitation for 10 mil conductor backed CPW with via holes and airbridges," in *IEEE MTT-S Int. Microwave Symp. Dig.*, Atlanta, GA, USA, 1993, pp. 705-708.
- [51] E. T. Rahardjo, S. Kitao, and M. Haneishi, "Planar antenna excited by

- electromagnetically coupled coplanar waveguide," *Electron. Lett.*, vol. 29, pp. 870-872, 13 May 1993.
- [52] T. Murata and M. Fujita, "A self-steering planar array antenna for satellite broadcast reception," *IEEE Trans. Broadcast.*, vol. 40, no. 1, pp. 1-6, Mar. 1994.
- [53] J. M. Johnson and Y. Rahmat-Samii, "The tab monopole," *IEEE Trans. Antennas Propag.*, vol. 45, no. 1, pp. 187-188, Jan. 1997.
- [54] S. Hudson and D. M. Pozar, "Grounded coplanar waveguide-fed aperture-coupled cavity-backed microstrip antenna," *Electron. Lett.*, vol. 36, no. 12, pp. 1003-1005, 8 Jun. 2000.
- [55] J.-M. Kim and J.-G. Yook, "A parallel-plate-mode suppressed meander slot antenna with plated-through-holes," *IEEE Antennas Wireless Propagat. Lett.*, vol. 4, pp. 118-120, 2005.
- [56] H. S. Noh and I. S. Kim, "Dielectric resonator oscillator using the coupling between a coplanar waveguide( CPW ) and a  $TE_{01\delta}$  mode dielectric resonator," in *IEEE International Frequency Control Symposium and Exposition*, Miami, FL, 2006, pp. 875-877.
- [57] H. S. Noh, J. Kwon, and I. S. Kim, "S-parameter extraction on coupling between DR and GCPW," *IEEE Microwave Wireless Components Lett.*, vol. 17, no. 3, pp. 166-168, Mar. 2007.

- [58] N. K. Das, "Two conductor-backed configurations of slotline or coplanar waveguide for elimination or suppression of the power-leakage problem," in *IEEE MTT-S Int. Microwave Symp. Dig.*, San Diego, CA, 1994, pp. 153-156.
- [59] C.-C. Huang and H.-C. Lin, "A Novel Calibration Algorithm With Unknown Line-Series-Shunt Standards for Broadband S-Parameter Measurements," *IEEE Trans. Instrumentation and Measurement*, vol. 57, no. 5, pp. 891-896, May 2008.
- [60] J. H. Choi and P. Russer, "The picosecond pulse transmission on the conductor-backed coplanar waveguide with via holes," *IEEE Microwave Wireless Components Lett.*, vol. 16, no. 7, pp. 419-421, Jul. 2006.
- [61] C.-C. Tien, C.-K. C. Tzuang, and J. Monroe, "Effect of lateral walls on the propagation characteristics of finite-width conductor-backed coplanar waveguides," *Electron. Lett.*, vol. 29, no. 15, pp. 1357-1358, 22 Jul. 1993.
- [62] Y. Liu, K. Cha, and T. Itoh, "Non-leaky coplanar (NLC) waveguides with conductor backing," *IEEE Trans. Microw. Theory Tech.*, vol. 43, no. 5, pp. 1067-1072, May 1995.
- [63] H.-C. Liu, T.-S. Horng, and N. G. Alexopoulos, "Radiation from aperture antennas with a coplanar waveguide feed," in *IEEE AP-S Int. Symp. Dig.*, Chicago, IL, 1992, pp. 1820-1823.

- [64] M. A. Magerko, L. Fan, and K. Chang, "Multiple dielectric structures to eliminate moding problems in conductor-backed coplanar waveguide MIC's," *IEEE Microwave Guided Wave Lett.*, vol. 2, no. 6, pp. 257-259, Jun. 1992.
- [65] J.-W. Huang and C.-K. C. Tzuang, "Mode-coupling-avoidance of shielded conductor-backed coplanar waveguide (CBCPW) using dielectric lines compensation," in *IEEE MTT-S Int. Microwave Symp. Dig.*, San Diego, CA, 1994, pp. 149-152.
- [66] H.-C. Liu, T.-S. Horng, and N. G. Alexopoulos, "Radiation of printed antennas with a coplanar waveguide feed," *IEEE Trans. Antennas Propag.*, vol. 43, no. 10, pp. 1143-1148, Oct. 1995.
- [67] Y. Liu and T. Itoh, "Leakage phenomena in multilayered conductor-backed coplanar waveguides," *IEEE Microwave Guided Wave Lett.*, vol. 3, no. 11, pp. 426-427, Nov. 1993.
- [68] C.-Y. Lee, Y. Liu, and T. Itoh, "Leakage control in conductor-backed uniplanar structures," in *IEEE Topical Meeting on Electrical Performance of Electronic Packaging*, Monterey, CA, 1994, pp. 145-147.
- [69] K. Cha, Y. Liu, C.-Y. Lee, and T. Itoh, "Non-leaky coplanar waveguide active antenna," in *IEEE MTT-S Int. Microwave Symp. Dig.*, Orlando, FL, 1995, pp. 765-767.

- [70] Y. Liu, C.-Y. Lee, and T. Itoh, "Slotline antenna with non-leaky coplanar (NLC) waveguide feed," in *IEEE AP-S Int. Symp. Dig.*, Newport Beach, CA, 1995, pp. 366-369.
- [71] L. Giauffret and J. M. Laheurte, "Microstrip antennas fed by conductor backed coplanar waveguides," *Electron. Lett.*, vol. 32, no. 13, pp. 1149-1150, 20 Jun. 1996.
- [72] D. R. Jahagirdar and R. D. Stewart, "Non-leaky conductor-backed coplanar waveguide-fed microstrip patch antenna," in *High Frequency Postgraduate Student Colloquium*, Leeds, 1997, pp. 94-99.
- [73] Y. Qian and T. Itoh, "Characterization and minimization of mutual coupling between NLC-FED slot antennas," in *IEEE MTT-S Int. Microwave Symp. Dig.*, Denver, CO, 1997, pp. 1623-1626.
- [74] L. Dussopt and J. M. Laheurte, "Parasitic effects of parallel-plate modes in planar antennas fed by conductor-backed coplanar waveguides," in *IEE National Conference on Antennas and Propagation*, York, 1999, pp. 363-366.
- [75] F.-R. Yang, K.-P. Ma, Y. Qian, and T. Itoh, "A uniplanar compact photonic-bandgap (UC-PBG) structure and its applications for microwave circuits," *IEEE Trans. Microw. Theory Tech.*, vol. 47, no. 8, pp. 1509-1514, Aug. 1999.



- [76] K.-H. Oh, H.-J. Song, S. Moon, T.-Y. Kim, G. Mudhana, D.-Y. Kim, and J.-I. Song, "Characterization of near-field patterns of a novel UC-PBG FW-CBCPW by using an electrooptic field-mapping technique," in *European Microwave Conf.*, Paris, 2005.
- [77] K.-H. Oh, T.-Y. Kim, S. Moon, H.-J. Song, W.-B. Kim, C.-S. Park, and J.-I. Song, "Characterization of uniplanar compact photonic-bandgap finite-width conductor-backed coplanar waveguide by using an electrooptic near-field mapping technique," *IEEE Trans. Microw. Theory Tech.*, vol. 54, no. 2, pp. 854-860, Feb. 2006.
- [78] M. Hotta, M. Kobayashi, T. Inoue, M. Hano, and T. Sakane, "Effects of backside grooving on leakage loss of conductor-backed coplanar waveguide," in *Asia Pacific Microw. Conf.*, Taipei, 2001, pp. 847-850.
- [79] D. M. Pozar, "Considerations for millimeter wave printed antennas," *IEEE Trans. Antennas Propag.*, vol. 31, no. 5, pp. 740-747, Sep. 1983.
- [80] R. L. Rogers and D. P. Neikirk, "Use of broadside twin element antennas to increase efficiency on electrically thick dielectric substrates," *Int. J. Infrared Millim. Waves*, vol. 9, no. 11, pp. 949-969, 1988.
- [81] R. L. Rogers and D. P. Neikirk, "Radiation properties of slot and dipole elements on layered substrates," *Int. J. Infrared Millim. Waves*, vol. 10, no. 6, pp. 697-728,

- 1989.
- [82] R. L. Rogers, S. M. Wentworth, D. P. Neikirk, and T. Itoh, "A twin slot antenna on a layered substrate coupled to a microstrip feed line," *Int. J. Infrared Millim. Waves*, vol. 11, no. 10, pp. 1225-1249, 1990.
- [83] S. M. Wentworth, R. L. Rogers, J. G. Heston, D. P. Neikirk, and T. Itoh, "Millimeter wave twin slot antennas on layered substrates," *Int. J. Infrared Millim. Waves*, vol. 11, no. 2, pp. 111-131, 1990.
- [84] J. G. Heston, S. M. Wentworth, R. L. Rogers, D. P. Neikirk, and T. Itoh, "MM wave/FIR twin slot antenna structures," in *IEEE AP-S Int. Symp. Dig.*, Dallas, TX, 1990, pp. 788-790.
- [85] M. Qiu, M. Simcoe, and G. V. Eleftheriades, "Radiation efficiency of printed slot antennas backed by a ground reflector," in *IEEE AP-S Int. Symp. Dig.*, Salt Lake City, UT, 2000, pp. 1612-1615.
- [86] M. Qiu, G. V. Eleftheriades, and M. Hickey, "A reduced surface-wave twin arc-slot antenna element on electrically thick substrates," in *IEEE AP-S Int. Symp. Dig.*, Boston, MA, 2001, pp. 268-271.
- [87] M. Qiu, M. Simcoe, and G. V. Eleftheriades, "High-gain meanderless slot arrays on electrically thick substrates at millimeter-wave frequencies," *IEEE Trans. Microw. Theory Tech.*, vol. 50, no. 2, pp. 517-528, Feb. 2002.

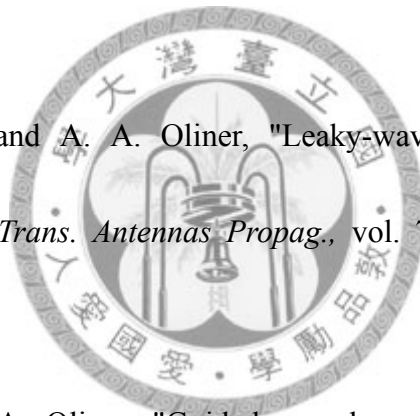
- [88] M. Qiu and G. V. Eleftheriades, "Highly efficient unidirectional twin arc-slot antennas on electrically thin substrates," *IEEE Trans. Antennas Propag.*, vol. 52, no. 1, pp. 53-58, Jan. 2004.
- [89] J. P. Jacobs, J. Joubert, and J. W. Odendaal, "Radiation efficiency of broadside conductor-backed CPW-fed twin slot antennas on two-layer dielectric substrate," in *IEEE Africon Conference in Africa*, 2002, pp. 531-533.
- [90] J. P. Jacobs, J. Joubert, and J. W. Odendaal, "Radiation efficiency and impedance bandwidth of conductor-backed CPW-fed broadside twin slot antennas on two-layer dielectric substrate," *IEEE Microwaves, Antennas and Propagation*, vol. 150, no. 4, pp. 185-190, 8 Aug. 2003.
- [91] K. Li, C. H. Cheng, T. Matsui, and M. Izutsu, "Simulation and experimental study on coplanar patch and array antennas," in *Asia Pacific Microw. Conf.*, Sydney, NSW, 2000, pp. 1411-1414.
- [92] K. Li, C. H. Cheng, T. Matsui, and M. Izutsu, "Coplanar patch antennas: principle, simulation and experiment," in *IEEE AP-S Int. Symp. Dig.*, Boston, MA, 2001, pp. 402-405.
- [93] K. Li and H. Izutsu, "Photodetection, photonic feeding coplanar patch antenna and transmitting experiment for radio-on-fiber system," in *IEEE MTT-S Int. Microwave Symp. Dig.*, Phoenix, AZ, 2001, pp. 73-76.

- [94] K. F. Tong, K. Li, T. Matsui, and M. Izutsu, "Wideband coplanar waveguide fed coplanar patch antenna," in *IEEE AP-S Int. Symp. Dig.*, Boston, MA, 2001, pp. 406-409.
- [95] K. Li, C. H. Cheng, K. F. Tong, and T. Matsui, "Broadband stacked coplanar patch antennas," in *European Microwave Conf.*, London, England, 2001, pp. 1-4.
- [96] C. H. Cheng, K. Li, and T. Matsui, "Stacked patch antenna fed by a coplanar waveguide," *Electron. Lett.*, vol. 38, no. 25, pp. 1630-1631, 5 Dec. 2002.
- [97] K. F. Tong, K. Li, T. Matsui, and M. Izutsu, "Broadband multi-layered coplanar patch antenna," in *IEEE AP-S Int. Symp. Dig.*, 2002, pp. 580-583.
- [98] P. L. Chin, A. Z. Elsherbeni, and C. E. Smith, "Characteristics of coplanar bow-tie patch antennas," in *IEEE AP-S Int. Symp. Dig.*, 2002, pp. 398-401.
- [99] A. Z. Elsherbeni, A. A. Eldek, B. N. Baker, C. E. Smith, and K. F. Lee, "Wideband coplanar patch-slot antennas for radar applications," in *IEEE AP-S Int. Symp. Dig.*, 2002, pp. 436-439.
- [100] A. A. Eldek, A. Z. Elsherbeni, C. E. Smith, and K. F. Lee, "Wideband rectangular slot antenna for personal wireless communication systems," in *IEEE Antennas and Propagation Magazine*. vol. 44, no. 5, 2002, pp. 146-155.
- [101] A. A. Eldek, A. Z. Elsherbeni, C. E. Smith, and K. F. Lee, "Wideband slot

- antennas for radar applications," in *IEEE Radar Conf.*, 2003, pp. 79-84.
- [102] K. F. Tong, K. Li, T. Matsui, and M. Izutsu, "Broad-band double-layered coplanar patch antennas with adjustable CPW feeding structure," *IEEE Trans. Antennas Propag.*, vol. 52, no. 11, pp. 3153-3156, Nov. 2004.
- [103] K. Li, C. P. Chen, T. Anada, and T. Matsui, "Electric field in coplanar patch antenna (CPA) - simulation and measurement," in *Asia Pacific Microw. Conf.*, 2005.
- [104] C.-H. K. Chin, Q. Xue, and C. H. Chan, "Design of a 5.8-GHz rectenna incorporating a new patch antenna," *IEEE Antennas Wireless Propagat. Lett.*, vol. 4, pp. 175-178, 2005.
- [105] T. Zwick, D. Liu, J. Grzyb, and B. Gaucher, "A coplanar patch antenna for integration with mmWave SiGe transceiver," in *IEEE International Workshop on Antenna Technology Small Antennas and Novel Metamaterials*, 2006, pp. 416-419.
- [106] S. Zhu and R. Langley, "Dual-band wearable antennas over EBG substrate," *Electron. Lett.*, vol. 43, no. 3, pp. 141-142, 1 Feb. 2007.
- [107] M. A. Hickey, M. Qiu, and G. V. Eleftheriades, "A reduced surface-wave twin arc-slot antenna for millimeter-wave applications," *IEEE Microwave Wireless Components Lett.*, vol. 11, no. 11, pp. 459-461, Nov. 2001.

- [108] W. L. Stutzman, "Estimating directivity and gain of antennas," in *IEEE Antennas and Propagation Magazine*, vol. 40, no. 4, 1998, pp. 7-11.
- [109] C. A. Balanis, "Pattern distortion due to edge diffractions," *IEEE Trans. Antennas Propag.*, vol. 18, no. 4, pp. 561-563, Jul. 1970.
- [110] B. Stockbroeckx, I. Huynen, and A. V. Vorst, "Effect of surface wave diffraction on radiation pattern of slot antenna etched in finite ground plane," *Electron. Lett.*, vol. 36, no. 17, pp. 1444-1446, 17 Aug. 2000.
- [111] J. Huang, "The finite ground plane effect on the microstrip antenna radiation patterns," *IEEE Trans. Antennas Propag.*, vol. 31, no. 4, pp. 649-653, Jul. 1983.
- [112] M. J. Vaughan, K. Y. Hur, and R. C. Compton, "Improvement of microstrip patch antenna radiation patterns," *IEEE Trans. Antennas Propag.*, vol. 42, no. 6, pp. 882-885, Jun. 1994.
- [113] S. Noghianian and L. Shafai, "Control of microstrip antenna radiation characteristics by ground plane size and shape," *Proc. Inst. Elect. Eng. Microwaves, Antennas Propagat.*, vol. 145, no. 3, pp. 207-212, Jun. 1998.
- [114] T. Namiki, Y. Murayama, and K. Ito, "Improving radiation-pattern distortion of a patch antenna having a finite ground plane," *IEEE Trans. Antennas Propag.*, vol. 51, no. 3, pp. 478-482, Mar. 2003.
- [115] J.-F. Huang and C.-W. Kuo, "More investigations of leakage and nonleakage

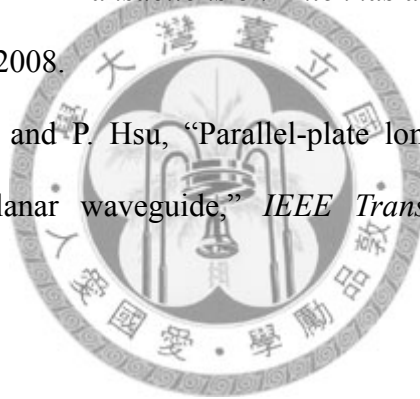
- conductor-backed coplanar waveguide," *IEEE Trans. Electromagn. Compat.*, vol. 40, no. 3, pp. 257-261, Aug. 1998.
- [116] G. V. Eleftheriades and M. Qiu, "Efficiency and gain of slot antennas and arrays on thick dielectric substrates for millimeter-wave applications: a unified approach," *IEEE Trans. Antennas Propag.*, vol. 50, no. 8, pp. 1088-1098, Aug. 2002.
- [117] R. S. Elliott, *Antenna theory and design*, 2<sup>nd</sup> ed. New York: John Wiley & Sons, 2003.
- [118] L. O. Goldstone and A. A. Oliner, "Leaky-wave antennas I: Rectangular waveguides," *IRE Trans. Antennas Propag.*, vol. 7, no. 4, pp. 307-319, Oct. 1959.
- [119] T. Tamir and A. A. Oliner, "Guided complex waves, part I, Fields at an interface," in *Proc. Inst. Electr. Eng.*, 1963, pp. 310-324.
- [120] A. A. Oliner, S. T. Peng, T. I. Hsu, and A. Sanchez, "Guidance and leakage properties of a class of open dielectric waveguides: Part II - New physical effects," *IEEE Trans. Microw. Theory Tech.*, vol. 29, no. 9, pp. 855-869, Sep. 1981.



# Publication List of I-Ching Lan

## Journal Paper

- [1] S.-Y. Chen, I-C. Lan, and P. Hsu, "In-line series-feed collinear slot array fed by a coplanar waveguide," *IEEE Transactions on Antennas and Propagation*, vol. 55, no. 6, pp. 1739-1744, Jun. 2007.
- [2] I-C. Lan, S.-Y. Chen, and P. Hsu, "Coupled twin slots fed by conductor-backed coplanar waveguide," *IEEE Transactions on Antennas and Propagation*, vol. 56, no. 6, pp. 1784-1786, Jun. 2008.
- [3] I-C. Lan, S.-Y. Chen, and P. Hsu, "Parallel-plate longitudinal slot array fed by conductor-backed coplanar waveguide," *IEEE Transactions on Antennas and Propagation* (revised).



## International Conference Paper

- [1] I-C. Lan and P. Hsu, "Parallel-plate slot array fed by conductor-backed coplanar waveguide," in *Proceedings of 35<sup>th</sup> European Microwave Conference (EuMC 2005)*, pp. 473-476, Paris, France, Oct. 2005.
- [2] I-C. Lan and P. Hsu, "Gain-enhanced slot antenna fed by conductor-backed coplanar waveguide," in *Proceedings of 2006 Asia-Pacific Microwave Conference (APMC 2006)*, pp. 73-76, Yokohama, Japan, Dec. 2006.
- [3] J.-H. Chen, J.-P. Chen, I-C. Lan, P. Hsu, and S.-Y. Chen, "Simplified GTEM cell for RFID tag antenna measurement," *URSI/SRS 2007 Radio Science Conference and*



*Taiwan-Japan Joint Meeting on Antennas and Propagation*, UD1, Yuan Ze Univ., Chung-Li, Taiwan, Mar. 2007.

- [4] I-C. Lan, S.-Y. Chen, and P. Hsu, "Pattern smoothness and gain enhancement of finite ground slot dipole antenna fed by conductor-backed coplanar waveguide," accepted by *2008 IEEE Antennas and Propagation Society International Symposium*, San Diego, USA, Jul. 2008.
- [5] C.-H. Lee, I-C. Lan, S.-Y. Chen, and P. Hsu, "Coplanar waveguide-fed twin slot antenna with and without back conductor," accepted by *2008 IEEE Antennas and Propagation Society International Symposium*, San Diego, USA, Jul. 2008.
- [6] Y.-J. Lu, I-C. Lan, S.-Y. Chen, and P. Hsu, "Finite-width conductor-backed coplanar waveguide-fed side-plane antenna," accepted by *2008 IEEE Antennas and Propagation Society International Symposium*, San Diego, USA, Jul. 2008.

